

**Estimation of the mechanical
loading
of the shoulder joint
in daily conditions**

ISBN / EAN: 978-90-9029177-2

Copyright ©2015	Wiebe de Vries. All rights reserved
Cover design:	Familie Six Dijkstra
Cover photography:	Martin Garnier, Enschede
Lay-out:	Wiebe de Vries
Printed by:	Gildeprint Drukkerijen, Enschede

Estimation of the mechanical loading of the shoulder joint in daily conditions

Proefschrift

ter verkrijging van de graad van Doctor
aan de Technische Universiteit Delft,
op gezag van de Rector Magnificus Prof. Ir. K.Ch.A.M. Luyben,
voorzitter van het College voor Promoties,
in het openbaar te verdedigen op
woensdag 16 september 2015 om 12u30
door

Wiebe Hein Klaas de VRIES

Doctorandus in de Bewegingswetenschappen
geboren te Apeldoorn, Nederland

DIT PROEFSCHRIFT IS GOEDGEKEURD DOOR DE PROMOTOREN:

Prof. dr. F.C.T. van der Helm

Prof. dr. H.E.J. Veeger

SAMENSTELLING PROMOTIECOMMISSIE:

Rector magnificus voorzitter

Prof. dr. F.C.T. van der Helm Technische Universiteit Delft, promotor

Prof. dr. H.E.J. Veeger Technische Universiteit Delft, promotor

ONAFHANKELIJKE LEDEN:

Prof. dr. J.H. van Dieën Vrije Universiteit Amsterdam

Prof. dr. R.G.H.H. Nelissen Leids Universitair Medisch Centrum

Prof. dr. ir. E.R. Valstar Technische Universiteit Delft

Dr. R.W. Selles Erasmus Medisch Centrum Rotterdam

OVERIGE LEDEN:

C.T.M. Baten, Msc Roessingh Research & Development
Enschede

RESERVELEDID

Prof. dr. J. Dankelman Technische Universiteit Delft

Dit proefschrift is tot stand gekomen binnen de context van de projecten
Freemotion en Fusion, beiden gesubsidieerd door Senter (als afgevaardigde
van het Ministerie van Economische Zaken)

Contents

1 General Introduction	3
2 Magnetic distortion in motion labs, implications for validating inertial magnetic sensors	13
3 Functionally interpretable local coordinate systems for the upper extremity using inertial & magnetic measurement systems.....	35
4 Determining a long term ambulatory load profile of the shoulder joint: Neural networks predicting input for a musculoskeletal model.....	59
5 Can shoulder joint reaction forces be estimated by neural networks?	77
6 General Discussion.....	97
References.....	117
Summary	125
Samenvatting.....	131
Curriculum Vitae.....	137
Publications by W.H.K. de Vries	139
Dankwoord.....	141

1

General Introduction

In the Netherlands the prevalence of shoulder complaints is estimated at 31% (Winters, 2008). One of the suspected factors involved in the development of shoulder complaints or joint wear is the mechanical loading of the shoulder joint. When the mechanical loading is exceeding biological limits (in the case of a healthy shoulder) or design limits (in the case of a shoulder endo-prosthesis) this will lead to joint wear and the gradual degradation of the shoulder or endo-prosthesis. Neither these biological limits in shoulder joint loading are known, nor are the load profiles on the joint under daily conditions. To gain more insight into the underlying mechanisms of the development of joint damage, and to enable the future development of enhanced endo-protheses, a long term load profile of the shoulder joint in daily living conditions is desired.

Such a mechanical load profile of the shoulder joint in daily conditions has not been established yet. The only way to estimate shoulder joint load in the healthy shoulder is by applying a musculoskeletal model; any invasive method to measure joint reaction forces directly with an instrumented prosthesis is at the level of patient data. Existing laboratory based methods for the estimation of shoulder joint reaction forces cannot be applied since the variables needed as input for these methods cannot be measured in daily conditions, or only with great difficulty.

Goal of the thesis

The goal of this thesis is to assemble a method to estimate shoulder joint reaction forces, in daily conditions, based on long term collection of ambulatory measurable variables, to obtain the desired long term mechanical load profile of the shoulder.

Background

The human shoulder combines two inherently conflicting characteristics, namely a large range of motion over several degrees of freedom, and a stable joint. For standardized Activities of Daily Living humeral elevation reaches approximately 140° internal and external rotation 60° and -89° respectively (van Andel et al., 2008). The glenohumeral joint is unstable by structure, and stability is mainly controlled by the rotator cuff muscles; only if the resultant (the summed force vector) from muscular activity is directed towards the glenoid surface of the scapula dislocation can be prevented (van der Helm, 1994a). Due to trauma, a variety of pathologies or mechanical loading of the joint, stability can be compromised, and in the end, lead to severe shoulder dysfunction. In cases where the joint is damaged due to severe wear or degeneration, joint replacement using a shoulder endo-prosthesis is often indicated.

Although survival time of shoulder endo-prostheses in the human body is comparable to other joint implants nowadays, shoulder endo-prostheses start loosening, or show severe wearing of joint surface over time (Torchia et al., 1997). Several studies have been performed that quantify the load on the shoulder during (standardized) Activities of Daily Living (Westerhoff et al., 2009a; Anglin et al., 2000), others have limited this to a description of the Range of Motion as an indicator for shoulder load (Magermans et al., 2005). These studies were laboratory based, and focused on a small, specific set of movements. These results form a too small base to be extrapolated to a long term mechanical load profile of the shoulder.

The shoulder

As stated, the human shoulder combines two inherently conflicting characteristics. This challenge is accomplished by an interaction of the existing structure and dynamic stabilization. The human shoulder consists of three bones, the clavicle, the scapula and the humerus. The clavicle is attached to the sternum and scapula; the scapula is pulled to the gliding plane of the thorax, and closing the mechanical chain. The humeral head can be described as a sphere, and the glenoid surface is acting as a smaller supporting base for this sphere; it is this structure that allows for a large range of motion. The scapula is, within constraints, dynamically positioned for optimal support of the humerus. A cuff of muscles surrounding the glenohumeral joint provide dynamic stability to keep the humeral head in close contact with its supporting base, and counteracting any dislocating forces.

Estimation of Shoulder joint load

The only way to estimate the load on the shoulder is using a musculoskeletal model. When using instrumented prostheses the measured output is at the level of patient data. A musculoskeletal model is a mathematical description of the functional elements of the shoulder and upper extremity, describing and modeling force generating (active) elements such as muscles, and passive elements ligaments, geometry of bones and joint surfaces.

Such a model should comprise the full shoulder structure, as well as some of the constraints within the system; more specifically, the gleno humeral joint integrity, i.e. its resistance to subluxation. The Delft Shoulder and Elbow Model (DSeM) is such a model. This model, based on extensive cadaver studies (van der Helm, 1994b), has been developed in the '90's to gain more insight in the working mechanism of the shoulder. It has been since regularly used for a series of applications to estimate load on the shoulder complex (see (Bolsterlee et al.,

2013) for a recent overview) or simulation of the effect of rotator cuff tears or tendon transfers (Magermans et al., 2004). The musculoskeletal model is defined as a Multi Body Model and consists of rigid bodies representing the bones of the shoulder, active elements which can deliver forces and are representing the muscles from thorax to humerus and forearm, and passive elements representing the various ligaments crossing the joints. With the model a variety of output can be estimated, for example net moments around the joints incorporated, muscle length, muscle moment arms, individual muscle forces and their resultant summing up into joint reaction forces. For the estimation of shoulder joint load, the musculoskeletal model uses two types of input; kinematics of thorax and upper extremity, and external force as exerted by the hand in manipulating the environment. These variables can be measured under controlled laboratory conditions without difficulty.

Requirements for ambulatory estimation of joint load

However, to estimate a long term shoulder joint load profile in daily conditions, upper extremity kinematics and external force have to be measured ambulatory, long term, and outside the laboratory. The standard instruments used for the measurement of these variables are designed to be used in fixed, laboratory settings, are usually not wearable or easily transported, or have a limited measurement volume. The standard instruments are therefore not suitable, nor practical to be used for ambulatory measurements, and the standard method cannot be applied.

To obtain the desired joint load profile, a method that can estimate joint reaction forces based on long term measurement of ambulatory obtainable variables is needed. Ambulatory variables should yield information about upper extremity kinematics, and external force, or more general stated, the musculoskeletal response of the upper extremity while manipulating objects in daily conditions.

Ambulatory measurement of kinematics

For the ambulatory measurement of segment kinematics, Inertial Measurement Units (IMU's) have become a popular and suitable candidate system. These sensors are lightweight, low on power consumption, and a dynamic accuracy of better than 2° is claimed by the manufacturers (for instance, among others, MTx sensors, Xsens, Enschede, Netherlands). IMU's are small boxes containing three types of sensors which measure acceleration, angular velocity and the earth magnetic field, all in 3D. In static conditions, gravity and Magnetic north form a natural frame of reference, while integration of angular velocity delivers change of orientation over time. With a proper fusion algorithm that can correct for integration drift the orientation of the sensor can be estimated over prolonged periods of time. For the sensors used in the experiments of this thesis, this fusion algorithm is implemented as a Kalman filter (Roetenberg et al., 2005). Orientation estimation is under the assumption of an average acceleration of zero over ten seconds, and a homogeneous earth magnetic field; small violations of these assumptions can be corrected for by the filter. Several experiments have been conducted to show the usability of these kind of sensors for the ambulatory measurement of human 3D kinematics for several types of motion (Cutti et al., 2008; van den Noort et al., 2013; Picerno et al., 2008).

Inertial Sensors: Assumptions & Threats

As stated, small violations of the assumption of a homogeneous earth magnetic field can be corrected for by the filter. For instance, the near presence of ferro containing material causes a distortion of the earth magnetic field, changing the direction of the magnetic vector, which can influence the orientation estimation of the sensor at that position. Rule of thumb is that at a distance of twice the depth (or width) of the object the earth magnetic field is homogeneous. Despite some

ferro containing constructions at the sides of our laboratory, the magnetic field was assumed to be homogeneous.

Preliminary results from a pilot study showed otherwise.

In fact, since several series of experiments were to be conducted in this specific laboratory, it forced us to conduct a separate experiment to examine the homogeneity of the earth magnetic field in our own laboratory, to be sure circumstances were within operating limits of the equipment used. Chapter 2 describes the procedure followed to obtain a mapping of the earth magnetic field within our standard gait analysis laboratory and its effect on the equipment and algorithms used, with surprising, but very useful results.

From wearable sensors to segment kinematics

IMU's deliver an estimation of sensor orientation around three axes, with respect to the earth frame of reference (the vertical axis aligned with the earth gravitational vector, and a heading along the earth magnetic field, up north to the magnetic north pole). Besides orientation estimation, calibrated sensor data like acceleration, angular velocity, and the vector of the earth magnetic field becomes available, all in 3D, in the sensor's frame of reference. For the measurement of segmental kinematics, the sensors relative orientation to the segment's frame of reference has to be determined. Standard laboratory experiments describe segmental frames of reference by the measurement of 3D positions of bony landmarks, conform guidelines as proposed by (Wu et al., 2005). Since IMU's do not deliver position data, but orientation only, these guidelines cannot be followed directly. Besides that, for ambulatory purposes, a sensor to segment calibration should preferably be carried out with the IMU's equipment, independent of other means. Several options exist in the definition of segment frames of reference using IMU's only. The manufacturer of the equipment proposed a static posture of the subject, a so-called T-pose, in which the frames of reference of all segments

are thought to be aligned with each other. Others used dedicated pointers equipped with IMU's to indicate the theoretical axis between two BLM (Picerno et al., 2008). An alternative to BLM based frames of reference is the use of anatomical axes, or functional axes of rotation of a segment (Luinge et al., 2007). It implies the performance of a series of well defined movements, from a subject equipped with IMU's in the same configuration as the intended following measurements. Chapter 3 describes the method to obtain these functional axes, the repeatability of the procedure, the construction of anatomical interpretable coordinate systems, and its relation with the standard method in obtaining segmental frames of reference following the mentioned ISB proposal.

Ambulatory measure of external force

Besides kinematics, external force is a required input for the musculoskeletal model used. In a laboratory setting external force can be measured with instrumented grips or force sensors. In daily conditions it is undoable to measure the forces exerted in every manipulation of objects by the subject directly, continuously and in 3D. Ideally subjects should wear a kind of instrumented glove, measuring all forces exerted by the hand in 3 dimensions. Such an instrument is not available yet, the development of such a device was not in the scope of this thesis. Since external force, which is one of the required inputs for musculoskeletal models to calculate shoulder joint load, is not obtainable in ambulatory measurements, these models can practically not be applied. An alternative method has to be sought after. During manipulation of an object the musculoskeletal response, recordable as surface EMG, can be recorded for longer periods of time with ease, and contains information on external force. The use of surface EMG is noninvasive, portable, and can comprise the measurement of the activation level of multiple muscles over time (Ochia and Cavanagh, 2007).

Linking kinematics and EMG to joint reaction force

From a biomechanical point of view all the information needed for the estimation of joint load (kinematics and a measure of external force) can be measured ambulatory, in daily conditions, but it still cannot be used directly in the standard estimation methods. To obtain the desired mechanical load profile of the shoulder in daily conditions a mapping is needed that links kinematics and EMG to net joint moments or joint reaction forces.

Neural Networks have been shown to be useful in the fusion of different data sources into a target variable (Song and Tong, 2005; Liu et al., 1999; Schollhorn, 2004). Neural Networks have good learning capabilities, and once trained, show a high processing speed of information, which is a clear advantage when analyzing large datasets. With these features Neural Networks appear to be a natural candidate method for the estimation of a long term shoulder joint load profile, using only kinematics and EMG as input. The emerging method has an appealing simplicity. The measurement of upper extremity kinematics and EMG with wearable equipment, and completing a minimal set of initial trials to collect data to train the neural network, enables the processing of several hours of measurements with the trained neural network into the desired variables of joint load. Chapter 4 describes an initial exploration of such a method in which a Neural Network, using 3D kinematics and relevant EMG from the upper extremity, is trained to predict a set of generalized forces and net moments around the shoulder. These generalized forces and net moments can concurrently be used as input for a musculoskeletal model to calculate full model output, like joint reaction forces, passive ligament forces, and estimates of individual muscle forces.

Direct prediction of joint reaction force

Joint reaction forces are the mathematical resultant of external force, individual muscle force, and passive forces like ligament strain. From that point of view, joint reaction forces combine information of all sources of mechanical loading of the shoulder in one single variable. A subsequent experiment was conducted in training Neural Networks predicting these joint reaction forces directly. Since several factors can influence the success of training a Neural Network, this experiment investigates in further detail the influence of these factors. For instance, the initial approach used, besides segmental kinematics, 13 channels of EMG as input for the Neural Networks, which is not a practical setup for long term ambulatory measurements. The effect of a reduction in the number of channels of EMG on Neural Network performance was examined. Chapter 5 examines these and other factors in a structured way, while comparing the neural network prediction of joint reaction force at the gleno humeral joint with corresponding output from a musculoskeletal model.

Chapter 6 integrates and discusses the findings of the preceding chapters, and proposes future directions for further development of the method.

2

Magnetic distortion in motion labs, implications for validating inertial magnetic sensors

W.H.K. de Vries^{a,b,*}, H.E.J. Veeger^{a,c}, C.T.M. Baten^b, F.C.T. van der Helm^a

Gait & Posture 29 (2009) 535–541

a Department of Biomechanical Engineering, Faculty of Mechanical, Maritime & Materials Engineering, Delft University of Technology, Delft, The Netherlands

b Roessingh Research & Development, Enschede, The Netherlands

c Research Institute MOVE, Department of Human Movement Sciences, VU University, Amsterdam, The Netherlands

Abstract

Background: Ambulatory 3D orientation estimation with Inertial Magnetic sensor Units (IMU's) use the earth magnetic field. The magnitude of distortion in orientation in a standard equipped motion lab and its effect on the accuracy of the orientation estimation with IMU's is addressed.

Methods: Orientations of the earth magnetic field vectors were expressed in the laboratory's reference frame. The effect of a distorted earth magnetic field on orientation estimation with IMU's (using both a quaternion and a Kalman fusing algorithm) was compared to orientations derived from an optical system.

Findings: The magnetic field varied considerably, with the strongest effects at 5 cm above floor level with a standard deviation in heading of 29°, decreasing to 3° at levels higher than 100 cm. Orientation estimation was poor with the quaternion filter, for the Kalman filter results were acceptable, despite a systematic deterioration over time (after 20-30 seconds).

Interpretation: Distortion of the earth magnetic field is depending on construction materials used in the building, and should be taken into account for calibration, alignment to a reference system, and further measurements. Mapping the measurement volume to determine its ferromagnetic characteristics in advance of planned experiments can be the rescue of the data set.

Conclusions: To obtain valid data, "mapping" of the laboratory is essential, although less critical with the Kalman filter and at larger distances (> 100 cm) from suspect materials. Measurements should start in a "safe" area and continue no longer than 20 – 30 seconds in a heavily distorted earth magnetic field.

Keywords: inertial magnetic sensing, magnetic distortion, orientation estimation, kalman filter.

Introduction

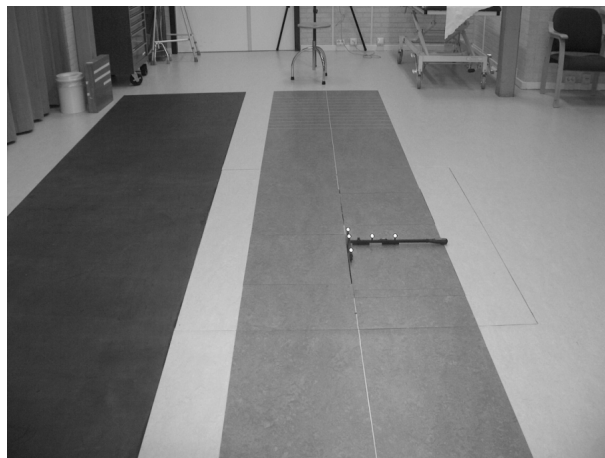
Over the last few years, a strongly increasing interest in ambulatory measurements during daily activities can be noticed, for instance to obtain a better insight in fall characteristics [1], activity level [2], functional behavior following arthroplasties [3] [4], or biomechanical loading of joints [5] in daily conditions.

Inertial Magnetic Units (IMU's) are a rather new motion capture technique. IMU's are lightweight, portable and low on energy usage (e.g. MT-X sensors, www.xsens.com). Data storage and transport have also become relatively easy. All these features have facilitated the opportunity to obtain long term, high quality, 3D kinematics outside dedicated motion laboratories.

IMU's are small boxes that combine several types of sensors like accelerometers, gyroscopes and magnetometers. The gyroscopes are used to track rapidly changing orientations in 3D and IMU heading is obtained from the earth magnetic field. This heading is obtained when acceleration of a sensor will be zero (apart from gravity) over a period of at least 10 seconds. This yields gravity as another vector for estimation of sensor-orientation. By a fusing algorithm these sensors data can be used to estimate IMU orientation.

To be able to use IMU's, validation is a clear necessity. Validation is usually performed in well equipped motion labs, by validating the new equipment against a reference system (e.g. Vicon, reflective markers, Oxford, UK; Optotrak, active markers, Northern Digital, Ontario, Canada). In IMU's, one of the assumptions in the fusing algorithms to estimate IMU orientation is the homogeneity of the earth magnetic field.

1A



1B



1C

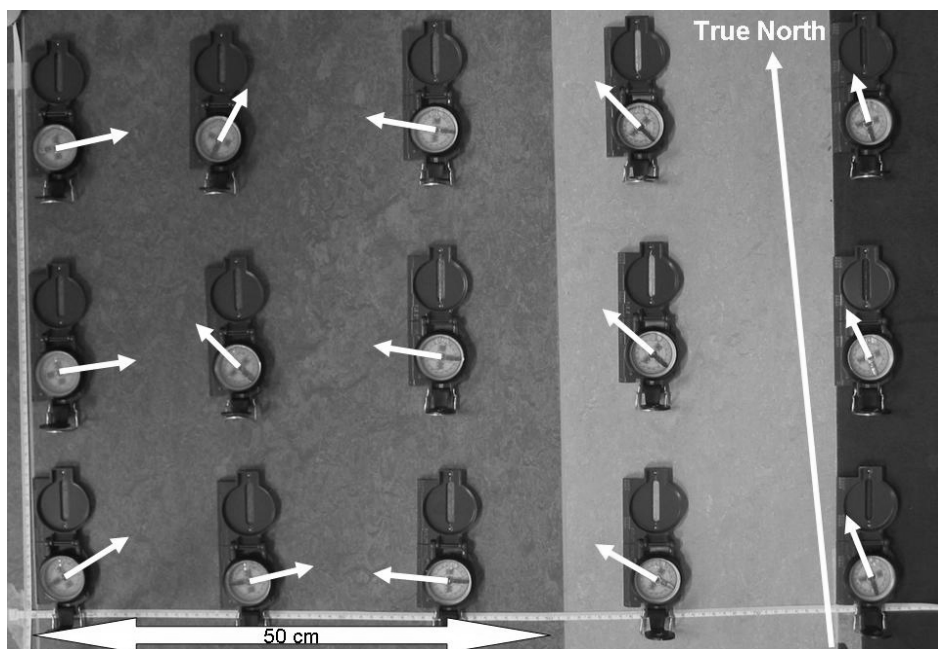


Figure 1a) The motion lab of RRD, current situation, and 1b) during construction, early '90's. Notice the amount of constructive iron forming a square, becoming a solid basis for the force plates, in figure 1a located under the Vicon calibration wand. Figure 1c shows a qualitative mapping, with 15 identical compasses, of an area with extremely high distortion.

Although not always obvious, it is not unusual that in the labs used for validation of this new equipment, the condition of the earth magnetic field is far from optimal, if not homogeneous at all. These irregularities can be caused by construction iron in floors, walls and ceilings (See figure 1a & b), or other equipment in the laboratory [6], and occur in both the horizontal and vertical plane. Distortion in the earth magnetic field was experienced in three different laboratories (Shoulder lab Delft University, Delft; Motion lab of Human Movement Sciences, Vrije Universiteit, Amsterdam; Motion lab of Roessingh Research & Development, Enschede, all in the Netherlands), and resulted in a more structured experiment on the homogeneity of the earth magnetic field, which took place at the gaitlab of Roessingh Research & Development, Enschede, Netherlands.

There can be seen some analogy with the Flock of Birds system, which makes use of an active generated magnetic field in 3 dimensions, to obtain 6 degrees of freedom per sensor. The generated magnetic field suffers from any constructive iron or iron containing equipment within the measurement volume, but when stationary, this measurement volume can be calibrated and mapped [7].

For IMU's, which use a fusing algorithm to estimate orientations, calibrating and mapping a lab for a distorted earth magnetic field is not trivial, since the fusing algorithm is designed to filter out disturbances to be able to determine the IMU orientation. The system is designed and developed to be used ambulatory, without prior knowledge of existence and location of disturbances. Besides that, IMU's do not produce position information (yet), only orientation information, so mapping of the measurement volume for possible disturbances needs additional equipment. However, there are a number of typical sources of error which threaten the assumptions in fusing algorithms. Although the fusing algorithms to

obtain 3D orientation are designed to filter disturbances in the earth magnetic field, there are implications for optimal starting locations of each measurement, as well as temporal aspects of the measurements, and output generated from it. In fact this accounts for all brands of sensors which make use of the earth magnetic field.

Another issue when validating against a gold standard, is the alignment of the different global frames of reference used by the measurement systems. IMU's use gravity and heading of the earth magnetic field, lab based measurement systems usually have one axis pointing vertically upwards, and one of the two other axes usually aligned with one of the walls of the lab, or the main direction of motion. The relationship between both global frames of reference should be known and corrected for, to enable a clean comparison between measurement systems.

This paper focuses on the validation process with IMU's in the light of the necessity to perform these using information from the magnetic field, in order to measure 3D kinematics. More specifically, we investigated:

1. The distortion of the earth magnetic field in a standard equipped motion lab (RRD, Enschede)
2. The effect of these disturbances on the accuracy of the orientation estimation with IMU's.

Using the above information, we subsequently determined the efficacy over time of two different orientation estimation algorithms, the standard, off the shelf, quaternion filter, and a newly developed Kalman filter (MT-Software V2.8.5, and MT-Software v2.9.5 XKF3-Beta release V084 resp., both from XSens) for validation measurements in the specified laboratory.

Methods

A Vicon six-camera opto-electronic system (Vicon MX, camera's MX13) was used as a reference system. The system was dynamically calibrated with a L-shaped wand. The origin of the lab coordinate system was defined with the same wand placed horizontally on a force plate, whereby the X-axis pointed along the long axis of the lab, and the Z-axis pointed vertically up. Marker data were stored at 100 Hz. Camera's and IMU's were electrically synchronized at 1000 Hz.

The IMU's used in this experiment were MTx sensors (XSens, static RMS-error $< 1^\circ$, dynamic RMS-error $< 2^\circ$), attached to a XBus-B system. Data were logged at 100 Hz with the standard MT software, which was supplied with the XBus system. Raw data as well as calibrated data and orientations from the sensor were stored, the latter estimated by the so called quaternion filter implemented in the standard MT-software. Since raw data were stored, the experimental Kalman filter could also be applied on the same data set.

Two algorithms were used for the estimation of IMU orientation:

- a quaternion filter, which can best be seen as a weighed average of orientation estimation of the three sources available (acceleration, angular velocity integrated to orientation, heading of the earth magnetic field).
- a Kalman filter: a mathematical error model of the sensors (all three types used in one IMU) characteristics is used to predict the error in orientation estimation, and corrects for this predicted error [8].

The Kalman filter uses two assumptions: Acceleration (apart from gravity) averaged over 10 seconds is zero; the Earth magnetic field is homogeneous, or distortion is temporary, and less than 10 seconds.

Five IMU sensors were manually aligned and taped on a wooden bar. Sensors were placed at 5, 40, 100, 140 and 180 cm from the base of the wooden bar (Figure 2). A local reference system was defined on this bar with five reflective markers (diameter 25 mm). The marker configuration on the objects and camera alignment in this experiment introduced a maximal uncertainty of $0.5^\circ \pm 0.6^\circ$ in the reference coordinate system definition due to marker positioning errors (Appendix 1).

To locally align the five IMU's an outlining measurement was conducted to obtain the sensor orientations with respect to the wooden bar in a mathematical way. In this measurement the bar and sensors were rotated several times around the three main axes of the bar (Appendix 2).

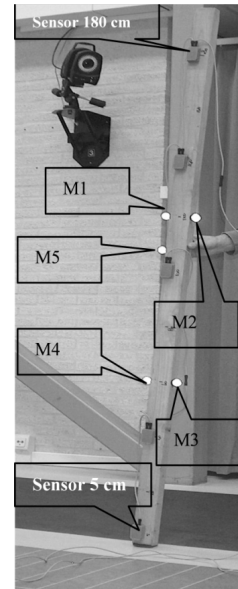


Figure 2. Equipment used, wooden bar with 5 MTx sensors, and 5 Vicon markers with diameter of 25 mm

The alignment between the IMU's frame of reference and reference system was obtained by estimation of gravity and the direction of the earth magnetic field during stand still (trial 1).

Gravity was measured with the accelerometers, subsequently expressed in the laboratory's coordinate system by pre-multiplying with the local alignment described in App. II, and the orientation of the bar, and then averaged over ten seconds. The angle between gravity and the laboratory vertical was estimated at less than 1° for all the five sensors.

Analogue to the measurement of the gravity vector, the earth magnetic field vector can be measured with the sensors magnetometers, and expressed in the laboratories coordinate system. Based on a pilot, a magnetic homogeneous area was selected as a safe start for the estimation of the direction of the magnetic

field vector, as well as an extremely disturbed area, which was labeled as “unsafe”. The safe area was in the middle of the lab at about 180 cm height. In the safe area the global heading of the earth magnetic field was measured and determined. The IMU magnetic earth vectors showed to be 7.5° relative to the laboratory X-axis, which was compatible to the estimated 7° for the geographical magnetic North following from the geographic coordinates for the laboratory (Roessingh Research & Development, coordinates $52^\circ 13'$, $55.35''\text{N}$, $6^\circ 52'$, $42.38''\text{E}$).

Based on the combination of the (separately obtained) direction of gravity and heading of the magnetic field vector, the global inertial reference system (and all data measured in this reference system) was aligned with the laboratory reference system. Subsequently, measurements were performed over the full surface of the laboratory, at 50 cm intervals, at normal to slow walking speed, to exclude any effects from acceleration and/or angular velocity on the orientation estimating algorithms. The bar was held upright (vertical), the lower part sliding on the floor, to enable simultaneous measurements at five different heights. The following trials were performed:

- 1) Standing still in safe area for 10 seconds, then rotating the bar with sensors around its three axes, five times each (further description in Appendix II).
- 2) Starting in “safe” area, scan the lab with normal to slow walking speed.
- 3) As Trial 2, but starting in “unsafe” area.

The orientation of the earth magnetic field was expressed in the global laboratory reference frame using the orientation and position from the reference system and thus independent from orientation estimation of the IMU themselves. The IMU global coordinate system orientation is based on the combination of the gravity vector and magnetic field vector. The reference coordinate system is based on the

optical vertical and a chosen horizontal direction, in this case the long axis of the laboratory. This implies that, when IMU magnetic vector data are expressed in the reference coordinate system, they can be visualized as direction vectors relative to the laboratory volume. The projection of the magnetic field vector to the horizontal plane, representing the direction of the magnetic field vector perpendicular to gravity, should ideally show a systematic, but stable, difference from the laboratory X- and Y-axes. If the magnetic field is variable, the IMU recordings would show this as a fluctuation over an, in principle, constant direction (being the magnetic North). This fluctuation can be expressed as the standard deviation of the angle of the individual direction vectors to the mean magnetic field vector:

$$\begin{aligned} {}^G \text{Mag}(i) &= {}^G R_{REF}(i) * {}^{REF} R_{sensor} * {}^{Sensor} \text{Mag}(i) \\ e_{mf} &= std({}^G \text{Mag}_{horizontal}) \end{aligned}$$

where:

${}^G R_{REF}(i)$ = the orientation of the reference coordinate system (the wooden bar) at time step (i)

${}^{REF} R_{sensor}$ = the outlining of the IMU to the reference coordinate system (the wooden bar);

${}^{Sensor} \text{Mag}(i)$ = Magnetic field vector in local sensor coordinate frame at time step (i)

${}^G \text{Mag}_{horizontal}$ = horizontal component of magnetic field vector in global (laboratory) coordinate system.

e_{mf} = standard deviation of the horizontal component of the magnetic vector over the ‘scanning’ part of the measurement.

When validating against a reference system the main source of error is that of the misalignment between the two systems, consisting of systematic differences as well as a variable error due to instabilities in the magnetic field (and / or gravity) as picked up by the IMU system. If the horizontal component of the magnetic

field vector is small, instabilities of this field can have extra large effects on this variable error. The variable error can be quantified as:

$$\begin{aligned}
 R\Delta(i) &= {}^G R_{REF}^T(i) \cdot {}^G R_{sensor}(i) \cdot {}^{REF} R_{sensor}^T \\
 \Delta_{error}(i) &= \arccos\left(\frac{\text{trace}(R\Delta(i))-1}{2}\right) \\
 e_{al} &= std(\Delta_{error})
 \end{aligned}$$

where:

${}^{REF} R_{sensor}^T$ = the transpose of the outlining of the IMU to the reference coordinate system (sensor with respect to the wooden bar);

${}^G R_{sensor}(i)$ = the orientation of the UMI at time step (i) (as measured with the sensor, expressed in the laboratory coordinate system);

${}^G R_{REF}^T(i)$ = the transpose of the reference coordinate system at time step (i) (as measured with the optoelectronic system).

Results

Recordings from the IMU's showed that the magnetic field varied considerably. Its orientation was strongly dependent on 3-D position in the lab, which clearly indicated that the magnetic field was not homogeneous. These effects were strongest five centimeter above the floor (Figure 3-B) where the standard deviation e_{mf} rose to 30°. At 180 cm above the floor, the homogeneity of the magnetic field was about 3° (Table 1, Figure 3-A).

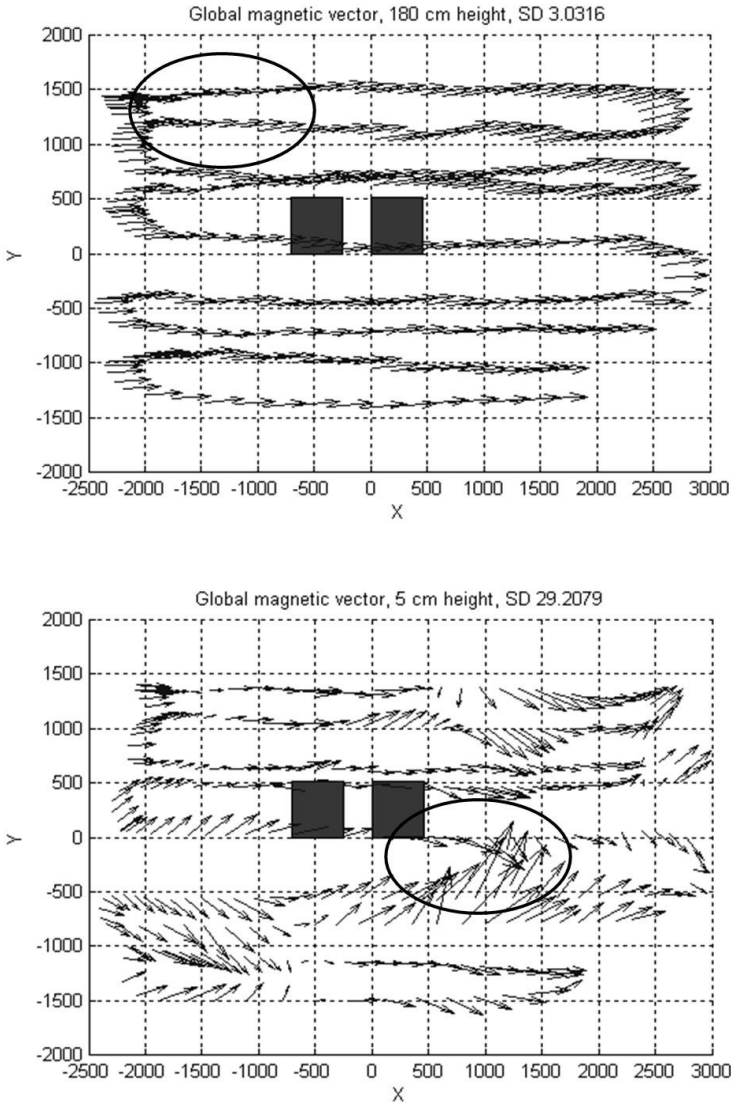


Figure 3. Heading of the earth magnetic field within the measurement volume of the Viconlab at Roessingh Research & Development (RRD), Enschede, at two heights. Figure 3A is at 180 cm, 3B is at 5 cm, both top view. Measurements started in the top left area of the graph (X=-2000, Y=1500), moving towards positive X, then roughly 50 cm towards negative Y, then towards negative X, etc. The two squares are the labs double AMTI force plates, which were, unexpectedly, not the main cause of distortion. The oval in figure B is definitely an “unsafe” area, at 5 cm height, the oval in figure A indicates a “safe” area at 180 cm height.

Errors in orientation estimation between the reference system and the IMU system were also estimated after starting IMU measurements in a “safe area”, where the magnetic field was known to have the correct direction (trial 2). Results proved to be bad for the standard filter, with a standard deviation e_{al} at 180 cm of 2° and 5 cm above floor level of 14° . For the Kalman filter results were better, especially for the 5 cm conditions where errors stayed lower (standard deviation e_{al} , Figure 4, Table 1) although a systematic deterioration over time could be discerned.

As expected, starting measurements in an “unsafe” area, where the magnetic field was known to be unstable, due to “constructive iron” and cable ducts, had no added effect on the orientation estimation with the standard quaternion filter, but did strongly affect results for the Kalman filter (compare Figure 4 and Figure 5). At 5 cm above the floor, the system showed high deviation for a period of approximately 50 seconds, after which results improved. However, the overall standard deviation e_{al} was still higher than in the previous condition (Table 1, Figure 5).

Table 1, variation in magnetic field e_{mf} , expressed in the laboratories frame of reference, and variable alignment error e_{al} for “safe” and “unsafe” starting conditions (all errors in degrees).

Height	Starting in “safe area”, trial 2			Starting in “unsafe area”, trial 3	
	e_{mf}	Quaternion filter error e_{al}	Kalman filter error e_{al}	Quaternion filter error e_{al}	Kalman filter error e_{al}
180 cm	3	2	2	2	2
140 cm	2	2	2	3	2
100 cm	3	2	2	3	2
40 cm	10	5	3	4	3
5 cm	30	14	4	12	8

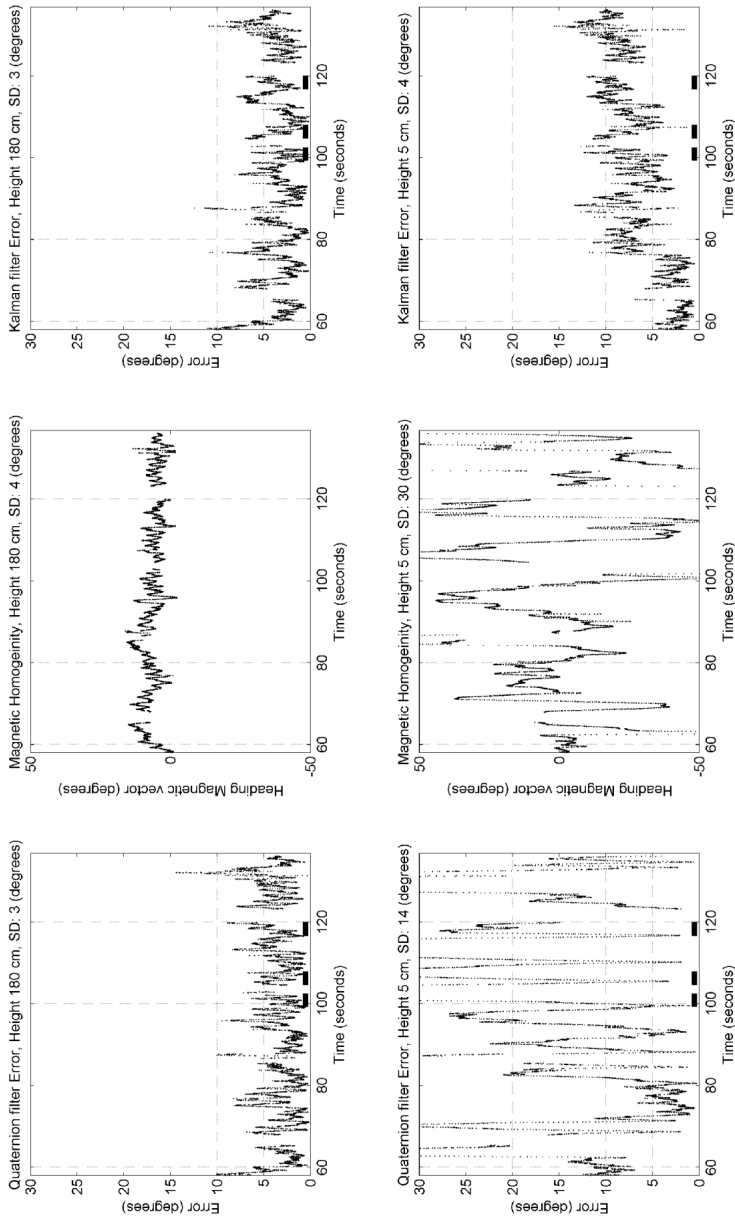


Figure 4, Temporal effect of distortion. Start in safe area, scan the lab with normal walking speed. Keep in mind the extremely distorted magnetic field of figure 3-B, for measurements at 5 cm height, which can also be noticed from the variation in the heading of the magnetic vector over time (middle lower graph). The thick markings at the base-line of the error graphs (left and right) indicate the time spent in the extremely distorted, “unsafe” area, as outlined in figure 3A.

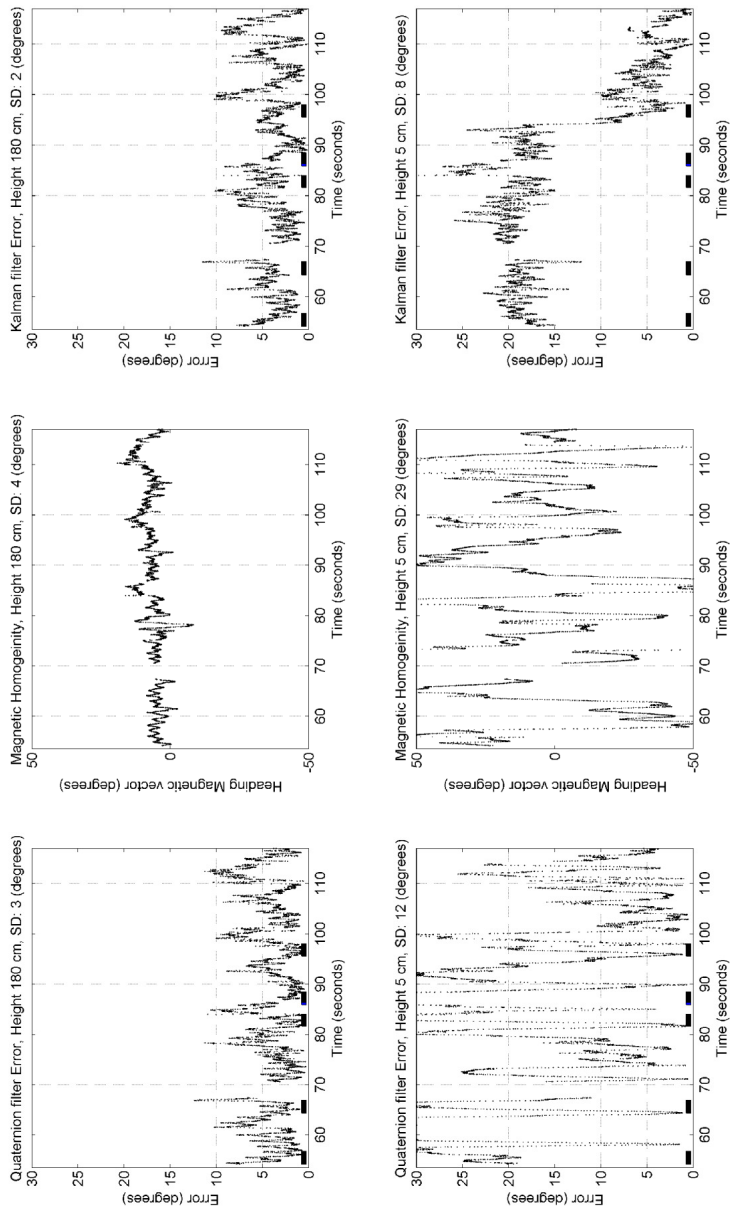


Figure 5, Temporal effect of distortion. Start in unsafe area, with a deviated magnetic heading at start of measurement, then scan the lab. Keep in mind the extremely distorted magnetic field of figure 3-B, for the measurement at 5 cm height, which can also be noticed from the variation in the heading of the magnetic vector over time (middle lower graph).

Discussion

The variation of the magnetic field in our lab was considerable, both in dip angle and in heading. Due to the use of heading of the magnetic field for the definition of the IMU X-axis, this factor is the strongest cause of estimation errors in the orientation of the IMU reference system. The quaternion filter can not correct for errors in the magnetic field direction (see Figures 3 and 4), but the kalman filter can, to some extent. The Kalman filter uses a mathematical error model of the sensors characteristics (all three types used in one IMU) to predict the possible error in orientation estimation when for instance deviations in the earth magnetic field are met, and corrects for this predicted error [8]. However, it should be determined to what extent the measurement volume complies to the assumptions used in Kalman filtering.

When starting in an “unsafe” area, the Kalman filter needs a considerable sampling time before data become more or less reliable. In our case, over more than 50 seconds. This effect also works the other way: disturbances of longer duration (20 – 30 seconds), or similar, staying in an area where the magnetic vector is uniform but deviating from the starting condition / location, will lead to an adaptation of the orientation estimation of the Kalman filter to the actual measured magnetic vector.

Results indicated a strong effect of height on the deviations of the magnetic field (figure 3). When only measuring with IMU's, with several sensors placed on different body segments, at different heights from floor level, and thus from constructive iron elements, there might arise a difference in heading of the local reference frames of the segments. Due to a different heading of the magnetic field at the heights of the IMU's, a single segment calibration will not reduce this difference in heading.

Based on the data of this experiment, it is recommended to perform measurements in this specific lab at least at 40 cm height. When using a Kalman filter, this recommendation is less strict, as long as there is the guarantee that sufficient time is spent in a “safe” area to allow the filter to settle (and vice versa, not to stay long in “unsafe” areas, to prevent the filter from setting to a distorted value).

Distortion of the earth magnetic field is depending on the distance of the IMU to ferro containing metal, and thus the construction materials used in the building. When calibrating an IMU (or a series of IMU's, as a system) to a reference system, e.g. video based like Vicon, this distortion should be taken into account for further measurements. A mapping of the measurement volume in advance of a series of experiments can be the rescue of the data set, so as to define “safe” and “unsafe” areas.

Stability of the Kalman algorithm is, in the end, also time limited in heavily disturbed environments, and depending on quality of gyroscopes. The better the gyroscope in terms of low drift, the longer it will take before integration drift in the form of random walk will increase to unacceptable levels. The current time limit with the equipment used is about 30 seconds. This means that a stay of up to 30 seconds in an disturbed magnetic field, the orientation can be estimated with an accuracy of about $3 - 5^\circ$ (Figures 4 and 5). When measuring in a disturbed, but mapped laboratory, this knowledge can be taken into account in the planning of measurements. When starting in a distorted area, it can take up to 50 to 60 seconds before orientation estimation error decreases to about 5 degrees (Figure 5).

Conclusions

- “Map” your laboratory on ferromagnetic characteristics before validating.
- Preferably use IMU’s well away from floors, walls and ceilings. In our experiment, a distance of at least 40 cm from the floor led to acceptable results;
- The Kalman filter is less sensitive to magnetic disturbances, especially when starting in a “safe” area, where the magnetic field has the correct heading. Downside is the relative unpredictability when staying in an “unsafe” area for longer periods;
- When calibrating against a reference system, every measurement should start at the same location in the measurement volume where calibration and alignment took place. This ensures a constant offset and offset correction.

Appendix 1: Estimation of coordinate system uncertainty

Vicon accuracy, which is dependent on camera resolution, but also on the setup of markers, and the definition of the local reference frame based on markers on a rigid body. The error measure for this procedure is calculated as follows:

1. The local reference frame for the Vicon-object and markers, and its initial orientation was calculated from a separate trial, according to:

$$\begin{aligned}
 X &= ((M3 + M4) / 2) - ((M1 + M2) / 2); X = \frac{X}{\|X\|} \\
 Y_{imp} &= ((M2 + M3) / 2) - ((M1 + M4) / 2); Y_{imp} = \frac{Y_{imp}}{\|Y_{imp}\|} \\
 Z &= \text{cross}(X, Y_{imp}); Z = \frac{Z}{\|Z\|} \\
 Y &= \text{cross}(Z, X); Y = \frac{Y}{\|Y\|} \\
 R_{Vicon_object_ini} &= [X, Y, Z]
 \end{aligned}$$

2. Subsequently the least squares method of Spoor & Veldpaus [9] was applied during tracking of the object to obtain the orientations.
3. Individual markers during the tracking are expressed in the local reference frame which orientation is calculated by the procedure of Spoor & Veldpaus.
4. The variation of these individual marker positions expressed in this local reference frame can be seen as the measurement error of Vicon.
5. When applying the formulas of step 1 in calculating orientation of the Vicon Object, on the markers expressed in its local reference frame (step 3 and 4), the difference in orientation can be expressed as the smallest angle between the calculated orientation and unity, by:

$$R\Delta_i = R_{BLM_local,i}$$

$$Vicon_{error,i} = \arccos\left(\frac{trace(R\Delta_i)-1}{2}\right)$$

In Table A1 for every trial the RMS, averaged and standard deviation of $Vicon_{error,i}$ is depicted (in degrees).

Table 1, variation in magnetic field e_{mf} , expressed in the laboratories frame of reference, and variable alignment error e_{al} for “safe” and “unsafe” starting conditions (all errors in degrees).

Height	Starting in “safe area”, trial 2			Starting in “unsafe area”, trial 3	
	e_{mf}	Quaternion filter error e_{al}	Kalman filter error e_{al}	Quaternion filter error e_{al}	Kalman filter error e_{al}
180 cm	3	2	2	2	2
140 cm	2	2	2	3	2
100 cm	3	2	2	3	2
40 cm	10	5	3	4	3
5 cm	30	14	4	12	8

Appendix 2: Local alignment of an inertial system with an optoelectronic system

The local alignment can be estimated by performing a number of rotations around the three axis of the object with markers and IMU's, and using the 3D angular velocity vectors of both systems to determine their relative orientation. Angular velocity is not critical, but should be well above noise level of the sensors. An arbitrary cutoff threshold of 0.2 rad/sec is used here, other cutoff values delivered the same results.

$${}^S\mathbf{v}_i = {}^{SO}\mathbf{R}(\boldsymbol{\theta}) \cdot {}^O\mathbf{v}_i, \quad i=1 \dots N \quad (1)$$

Where:

${}^S\mathbf{v}_i$ = angular velocity measured with IMU

${}^{SO}\mathbf{R}(\boldsymbol{\theta})$ = Orientation of IMU casing related to Vicon markers on IMU

${}^O\mathbf{v}_i$ = angular velocity as derived from Vicon markers.

Equation (1) can be written as

$$[{}^S\mathbf{v}_1 \dots \dots \dots {}^S\mathbf{v}_N] = {}^{SO}\mathbf{R} \cdot [{}^O\mathbf{v}_1 \dots \dots \dots {}^O\mathbf{v}_N]$$

When having enough data around three axis of rotation, this equation can be solved using a least squares:

$${}^{SO}\mathbf{R}^{init} = [{}^S\mathbf{v}_1 \dots \dots \dots {}^S\mathbf{v}_N] \cdot [{}^O\mathbf{v}_1 \dots \dots \dots {}^O\mathbf{v}_N]^{-p}, \text{ where }^{-p} \text{ denotes the pseudoinverse.}$$

Due to small measurement errors, the above solution will give a rotation matrix that is

slightly nonorthogonal. This can be solved by an orthogonalization.

3

Functionally interpretable local coordinate systems for the upper extremity using inertial & magnetic measurement systems

W.H.K. de Vries^{1,2}, H.E.J. Veeger^{1,3}, A.G. Cutti⁴, C. Baten², F.C.T. van der Helm¹

Journal of Biomechanics 43 (2010) 1983–1988

1) Department of Biomechanical Engineering, Faculty of Mechanical, Maritime & Materials Engineering, Delft University of Technology, the Netherlands.

2) Roessingh Research & Development, Enschede, the Netherlands

3) Research Institute MOVE, Department of Human Movement Sciences, VU University Amsterdam, the Netherlands

4) INAIL Prosthesis Center, Vigorso di Budrio (BO), Italy

Abstract

Background: Inertial Measurement Units (IMU's) are becoming increasingly popular by allowing for measurements outside the motion laboratory. The latest models enable long term, accurate measurement of segment motion in terms of joint angles, if initial segment orientations can accurately be determined. The standard procedure for definition of segmental orientation is based on the measurement of positions of bony landmarks (BLM). However, IMU's do not deliver position information, so an alternative method to establish IMU's based, anatomically understandable segment orientations is proposed.

Methods: For five subjects, IMU's recordings were collected in a standard anatomical position for definition of static axes, and during a series of standardized motions for the estimation of kinematic axes of rotation. For all axes, the intra- and inter individual dispersion was estimated. Subsequently, local coordinate systems (LCS) were constructed on the basis of the combination of IMU's axes with the lowest dispersion and compared with BLM based LCS.

Findings: The repeatability of the method appeared to be high; for every segment at least two axes could be determined with a dispersion of at most 3.8°.

Comparison of IMU's based with BLM based LCS yielded compatible results for the thorax, but less compatible results for the humerus, forearm and hand, where differences in orientation rose to 17.2°.

Interpretation: Although different from the 'gold standard' BLM based LCS, IMU's based LCS can be constructed repeatable, enabling the estimation of segment orientations outside the laboratory.

Conclusions: A procedure for the definition of local reference frames using IMU's is proposed.

Keywords: Sensors, Upper Extremity, Coordinate system, Functional Axes

Introduction

Inertial & Magnetic Measurement Systems (IMU's) are small devices containing accelerometers, gyroscopes and magnetometers. IMU's modules deliver total acceleration including gravity, angular velocity and the earth magnetic vector, all in 3D, expressed in the sensors local coordinate system. With a proper algorithm, based on the three types of data, sensor orientation estimations with respect to a global coordinate system can be made with an accuracy of 1° in static, and 2° RMS during dynamic movements (MTx specifications, XSens, Netherlands;(Cutti et al., 2008)). IMU's are becoming increasingly popular for monitoring of functional activities, since they are relatively cheap and, in contrast with video based systems, easily allow for measurements outside the motion laboratory in a, in principle, unlimited measurement volume (Brodie et al., 2008). IMU's have been used for the classification and quantification of physical activity in terms of postures and tasks (Coley et al., 2008; Janssen et al., 2008), using statistical correlation methods. With the current generation of IMU's, with a proper calibration method, the ambulatory measurement of segment motion, in terms of joint angles is now also feasible (Cutti et al., 2008; Picerno et al., 2008). Furthermore, the recording of segment motion combined with the external load will allow for the estimation of biomechanical loading of joints. For the estimation of the load on the upper extremity under everyday conditions, outside the laboratory, we intend to record segment motions using IMU's and use these as input for an existing musculoskeletal model of the shoulder (van der Helm, 1994b).

For the calculation of joint- and segment motion, the relationship of the IMU's coordinate system and a segments local coordinate system (LCS) is needed. The standard procedure for the definition of a LCS is based on the measurement of the

position of bony landmarks (BLM) (Wu et al., 2005; Cappozzo et al., 1995). This is not a practical solution when IMU's are being used in the field since it would require the use of an additional measurement system to record segments BLM positions in 3D, relative to the orientation of these IMU's (Picerno et al., 2008). Avoiding the use of such additional equipment, required expertise and analysis would simplify the use of IMU's in obtaining segment kinematics in the field. It can be stated that there is a need for an "in the field" calibration procedure for inertial sensors, to determine the relation between IMU's and segment LCS, with comparable accurate results as in procedures developed for optical recording systems(Kontaxis et al., 2009).

Two options can be considered to construct a segments LCS based on IMU's data (Kontaxis et al., 2009):

First, the so-called reference method where IMU's recordings from the standard anatomical position (SAP, standing straight, arms hanging along the body, hand palms pointing to the front) are related to the standard anatomical axis definitions. Second, a functional method in which segments LCS are constructed from estimations of the functional axes of rotation of a segment. For a well defined, uni-axial movement the angular velocity as measured by the sensors represents the functional axis of rotation, by definition. These functional axes of rotation can be with respect to an adjacent segment, or to the global coordinate system. Of course, a combination of both methods (reference and functional) is also possible. Since for each segment multiple combinations of axes are realizable, it has to be determined what the best combination of axes is. In addition, these constructed LCS are likely to differ from the standard BLM coordinate systems and the magnitude of this difference has to be determined.

Therefore we will, for the thorax and the upper extremity, excluding the scapula and clavicle:

- 1) determine IMU's based "reference" and / or "functional" axes to be used for the construction of segment LCS;
- 2) determine the inter- and intra-subject repeatability of this procedure;
- 3) construct segment LCS using the axes with the highest repeatability;
- 4) compare these IMU's based LCS with BLM based LCS;
- 5) propose a procedure for the definition of LCS using IMU's.

Methods

Five healthy subjects (age 27 ± 1.9 year, stature 189 ± 6 cm, weight 83 ± 8.9 kg), without a history of shoulder complaints, participated in this study after giving their informed consent. The protocol of the study was approved by the VU University's local ethical committee. Four sensor units were attached to a bus master (MT-X sensors and a XM-B-3 bus master, Xsens Technologies, Netherlands), operating at 50 Hz. The XSens MT-manager software (v1.5.0, SDK v3.1) was used for logging; the implemented Kalman filtering (Roetenberg et al., 2005) was set at the "human scenario". As reference system a Vicon MX13 setup with 6 MX cameras (50Hz, electronically synchronized) was used. For the comparison between the inertial (IMU's) coordinate systems and the opto-electronic lab-based coordinate system, an alignment procedure was applied as described in (de Vries et al., 2009).

MTx sensors were placed (1) on thorax-sternum, (2) latero-distally on the right humerus, (3) dorso-distally on the right forearm, close to the wrist and (4) on the right hand, on Metacarpale II and III (MCII & MCIII). The sensors were attached using dedicated neoprene cuffs. Reflective markers were placed on Bony Landmarks conform the ISB standard for upper extremity measurements (Wu et al., 2005), see also Figure 1.

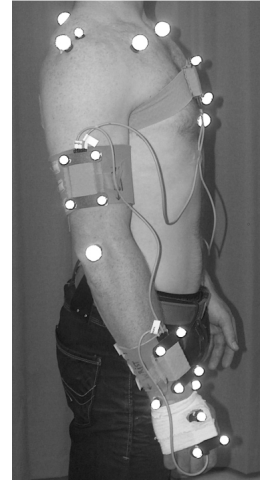


Figure 1,
A subject equipped with IMU's
and reflective markers on BLM.

Subjects started each trial in the SAP for five seconds and collected IMU's data were used for the determination of the following segment axes: the gravity vector (when standing still gravity is the only acceleration measured; averaged over time and normalized to unit length) was used as an estimator for the longitudinal axis of a segment; the magnetic vector (averaged over time, normalized to unit length) as an estimator of the frontal axis. The derived BLM-based segment orientations during the SAP were used as a reference in which all subsequent trials were expressed.

To determine functional axes of rotation, subjects performed the following series of well defined, uni-axial rotations, five times each, avoiding the extremes of the range of motion:

- Thorax:
 - flexion – extension;
 - lateral flexion;
 - axial rotation.
- Humerus:

-
- arm forward flexion, elbow extended, holding a light bar at shoulder breadth, thumbs pointing lateral;
 - ab – adduction;
 - endo- and exorotation, with the elbows supported at the olecranon;
 - elbow flexion (the movement of the forearm expressed in the humeral IMU's).
 - Forearm:
 - flexion – extension, while holding a light bar, thumbs pointing laterally to fix the forearm from pro- and supination, elbows supported at the olecranon;
 - pro- and supination, free in the air, hand kept straight in line with the forearm;
 - pro- and supination, elbow and ulna supported.
 - Hand:
 - hand flat on the table for 5 seconds;
 - dorsal flexion with the forearm supported, palm of the hand facing the table;
 - same position, performing radial ulnar deviation, by sliding the palm of the hand over the surface.

Angular velocity as measured with the IMU's was used as an estimate of the functional axis of rotation (averaged over time, and normalized to unit length) (Luinge et al., 2007). To enable a clear segmentation, each series of movements was followed by a stop of at least two seconds. To ensure a high signal-to-noise ratio, a cut-off of 30% of the maximal angular velocity amplitude was used.

To be able to assess within-subject variability, the complete protocol was repeated six times for each subject. The variation over trials was calculated as $\mathcal{E}_{dispersion}$,

the average of the six individual smallest angles ($\Delta\vec{v}_{i1}$) between 1) the axes determined in the six trials (\vec{v}_{i1}), and 2) the average orientation of these axes over the six trials (Equation 1):

$$\Delta\vec{v}_{i1} = \arccos \left(\vec{v}_{i1} \bullet \frac{\sum_{i2=1}^6 \vec{v}_{i2}}{6} \right), i1 = 1:6.$$

$$\mathcal{E}_{dispersion} = \frac{\sum_{i1=1}^6 \Delta\vec{v}_{i1}}{6} \quad \text{Equation 1}$$

Where:

- vectors \vec{v}_i is a functional or reference axis
- \vec{v}_i and \vec{v}_2 have unit length

The two non-aligned axes which had the lowest dispersion over trials and subjects were chosen for the construction of a local coordinate system, following the same rule as that for the calculation of local coordinate systems based on anatomical landmarks (Picerno et al., 2008; Wu et al., 2005; Cappozzo et al., 1995; Kontaxis et al., 2009). Taking two concurrent cross products of the chosen axes assures orthogonality of the LCS [see Appendix 1 for details].

To determine the difference between methods, for each segment the IMU's based local coordinate systems were compared with the bony landmark-based local reference frames expressed as Δ_{local} , the angle of rotation between the BLM and IMU's based reference frames :

$${}^{BLM \text{ frame}} R_{IMMS} = {}^{Global} R_{BLM \text{ frame}}^{Transpose} \bullet {}^{Global} R_{IMMS}$$

$$\Delta_{local} = \arccos \left[\frac{(\text{trace}({}^{BLM \text{ frame}} R_{IMMS}) - 1)}{2} \right]$$

Where:

${}^{Global} R_{IMMS}$ = Segment Orientation based on IMMS axes

${}^{Global} R_{BLM \text{ frame}}$ = Segment orientation based on BLM method

${}^{BLM \text{ frame}} R_{IMMS}$ = Relative orientation of IMMS based LCS to BLM based LCS

Δ_{local} = Angle of rotation between IMMS and BLM based LCS

Equation 2

In addition, the angles between the individual X,Y, and Z axes from both IMU's and BLM based LCS were expressed as the smallest angle between these two vectors. Since a LCS is an orthogonal matrix, the individual axes are vectors of unit length, and the smallest angle between two corresponding axes can be calculated according to Equation 3.

$$\Delta X = \arccos({}^{BLM, x} R^{Transpose} \bullet {}^{IMMS, x} R)$$

$$\Delta Y = \arccos({}^{BLM, y} R^{Transpose} \bullet {}^{IMMS, y} R)$$

$$\Delta Z = \arccos({}^{BLM, z} R^{Transpose} \bullet {}^{IMMS, z} R)$$

Where:

${}^{IMMS, x} R$ = x axis of the IMMS based LCS

ΔX = smallest angle between both X-axes of IMMS and BLM based LCS

\bullet denotes the dot product

Equation 3

Per segment, a repeated measures ANOVA was performed on dispersion (e.g. for the Thorax: gravity vector during anatomical stance, thorax flexion axis, lateral

flexion axis and torsion axis). When a significant difference in overall dispersion was found, paired-samples T-tests with Bonferroni correction were performed. The same procedure was followed to test for the compatibility of the functional and BLM method between segments. As a further detailed analysis, paired-samples T-tests were applied to the individual ΔX , ΔY and ΔZ from the reference frames, to determine which axes deviated significantly.

A significance level of $p = 0.05$ was used for all tests.

Results

Mean dispersions of axes were quite low (Table 1, Figure 2). Standard deviations of dispersions over trials were generally well below 1° . The highest mean dispersion of 8.9° appeared to be of the magnetic vector measured at the hand in the SAP. The forearm 'pro-supination', and 'pro-supination fixed', and humeral 'endo-exo rotation' axes showed the lowest mean dispersion of 1.2° , 1.3° and 1.6° , respectively.

In the SAP the gravity vectors showed a low dispersion of about 2° to 3° , except for the hand where dispersion was 6.6° . For all segments, the dispersion of the magnetic vector ended highest in the variation ranking, from 4.4° at the thorax up to 8.9° at the hand.

Thorax			N=5			Humerus		
Flexion	2.0	± 0.8	Endo rotation	1.6	± 0.8			
Gravity Vector	2.9	± 2.3	Gravity Vector	2.0	± 0.5			
Torsion	3.0	± 2.4	Elbow Flexion	2.8	± 0.9			
Lateral Flexion	3.9	± 1.3	Abduction	4.6*	± 1.5			
Magnetic Vector	4.4	± 2.4	Ante Flexion	5.0*	± 1.9			
			Magnetic Vector	5.2	± 4.3			

Forearm			Hand		
Pro-Supination	1.2	± 0.4	Gravity Hand Flat	2.4	± 0.8
Pro-Supination Fixed	1.3	± 0.6	Dorsal flexion	2.9	± 0.5
Gravity Vector	2.6*	± 0.9	Radiar Ulnar deviation	5.5*	± 1.4
Elbow Flexion	3.8*	± 1.2	Gravity Vector	6.6*	± 2.8
Magnetic Vector	6.3*	± 2.9	Magnetic Vector	8.9*	± 3.1

Table 1, Mean dispersion of reference (gravity and magnetic vectors) and functional axes (movements) over five subjects, in degrees. Dispersion of these axes is calculated per subject, as the variation in orientation over trials (see equation 1). Per segment, axes are ranked to Mean dispersion. * denotes a significant difference in paired T-tests over subjects (with Bonferroni correction, initial $p < 0.05$). For the relation of these differences see text.

The axes of the thorax showed no significant difference in dispersion indicating that any combination of axes can be used to construct a local reference frame. The thorax flexion and the gravity vector in the SAP were subsequently used for the construction of the thorax local coordinate system.

The dispersion of the axes of the humerus, forearm and hand were significantly different ($p = 0.025$, $p=0.000$ and $p=0.000$, respectively).

Humeral abduction and forward flexion axes had a higher dispersion than internal rotation and the gravity vector while the humeral forward flexion axis also showed significantly higher dispersion than the 'elbow flexion' axis (paired-samples T-test, all $p < 0.05$). These results led to the selection of internal rotation and elbow flexion for calculation of the humerus local coordinate system.

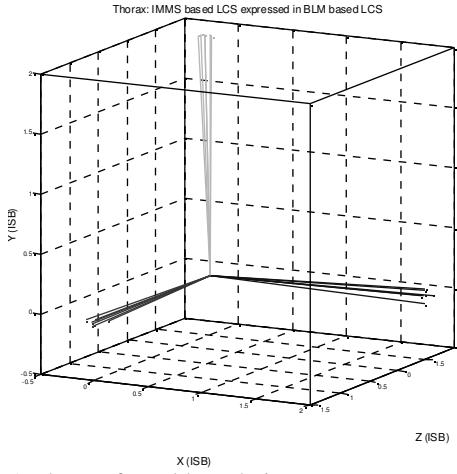
For the forearm, the dispersion of the gravity vector, elbow flexion and the magnetic vector were significantly higher than dispersion for the pro- and supination axes. Elbow flexion and the magnetic vector also differed from the gravity vector (paired-samples T-test, all $p < 0.05$). The pro-supination axis was chosen as the first axis for the construction of the forearm coordinate system. Elbow flexion is chosen as the second axis.

The gravity vector (measured with the hand flat on a table) and dorsal flexion both differed significantly from the other three functional axes and were selected for the construction of a local frame of reference for the hand.

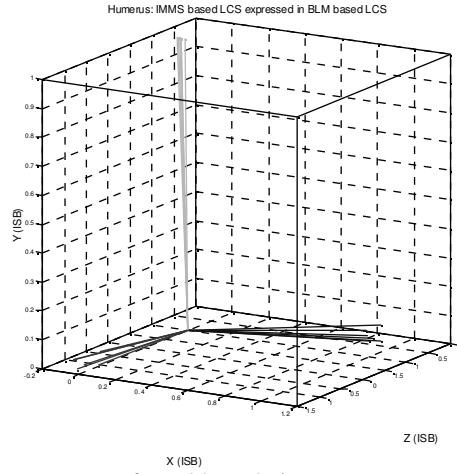
Resuming the above, the ‘reference’ and the ‘functional’ method showed dispersion in the determination of the various axes of 1° to 9° over subjects. However, for every segment two axes could be determined with a dispersion of at most 3.8° over six trials.

The constructed IMU’s coordinate systems were expressed in the corresponding segment BLM coordinate system (Figure 2, Table 2).

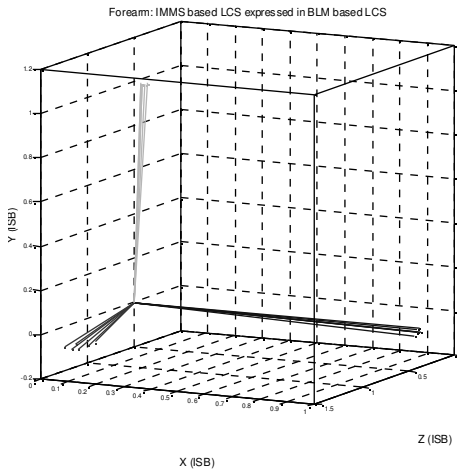
IMU’s-based and the BLM based local coordinate systems were overall different ($p=0.016$). This mean difference was smallest for the thorax with 6.4° , and rose up to 17.2° for the forearm (Table 2). When looking into more detail to these differences it appeared that the longitudinal axis of the forearm based on IMU’s data differed only 4° from its BLM based equivalent, but lateral and frontal axes differed about 17° between IMU’s and BLM based axes (Table 2).



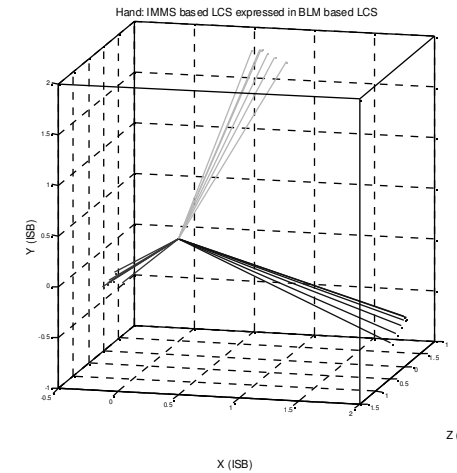
A Thorax, frontal-lateral view



B Humerus, frontal-lateral view



C Forearm, frontal-lateral view



D Hand, frontal-lateral view

Figure 2, A typical example (Subject03) of IMU's based LCS, a compilation of six trials expressed in the segment's BLM based LCS. Dispersion can be noticed by the bundles of lines, the difference with the BLM LCS by the relative orientation of the axes of the IMU's based LCS with respect to the axes of the figure.

Thorax					Humerus			
	Total	X	Y	Z	Total	X	Y	Z
Mean	6.4	5.9	5.4	3.8	8.7	7.6	6.8	6.0
SD	4.7	4.8	3.7	3.0	4.0	4.4	3.9	2.5
Forearm					Hand			
	Total	X	Y	Z	Total	X	Y	Z
Mean	17.2	16.9	4.0	17.0	15.6	12.5	14.8	9.9
SD	6.3	6.3	1.3	6.5	8.5	7.5	8.4	5.2

Table 2,

Difference between BLM LCS and IMU's LCS, averaged over five subjects, expressed as smallest rotational angle (in degrees), and as angle (degrees) between the individual X,Y and Z components of both LCS.

When IMU's recordings of humeral motion are applied to the IMU's based LCS and compared with humeral orientation obtained by an optoelectronic system which uses a BLM based LCS, a difference in orientation during movement can be observed. Figure 3 shows the effect on humero-thoracal orientations during forward flexion, lateral flexion and internal rotation, decomposed in Euler-angles. Differences between methods vary over movements and segment positions, up to 20°, but are lower for the elevation angle, up to 10°.

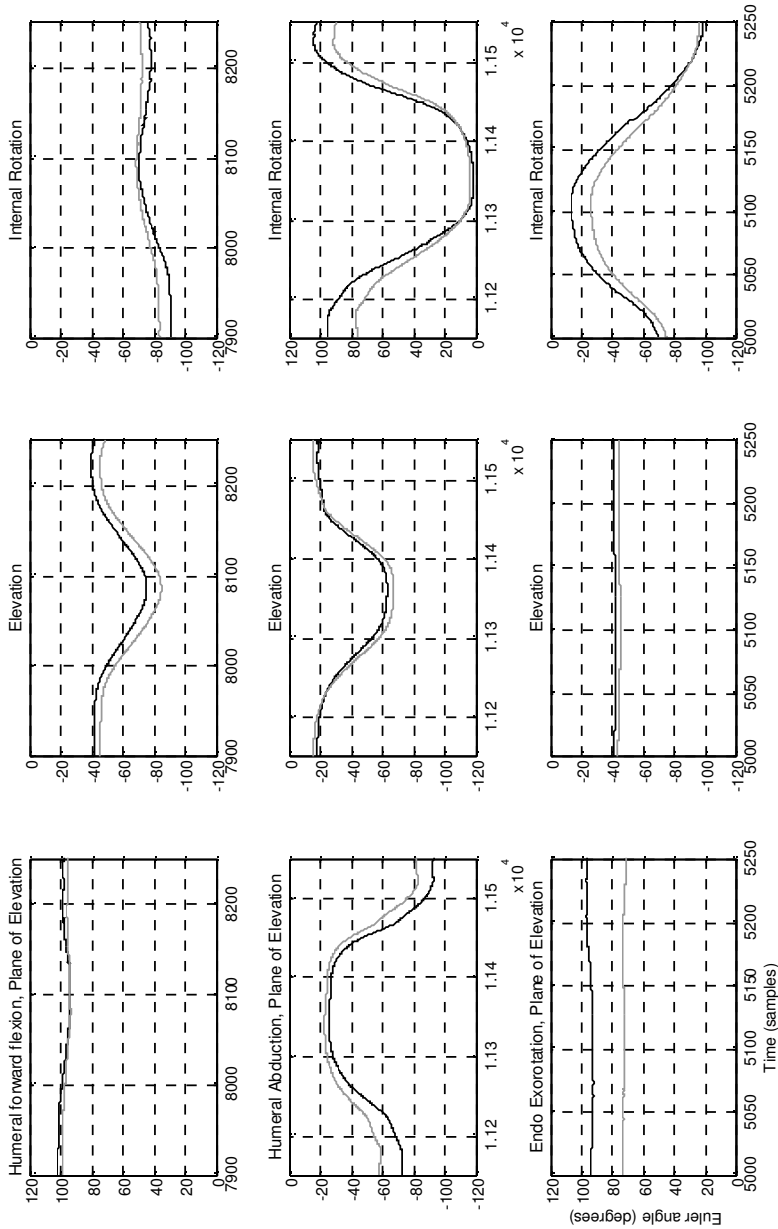


Figure 3, Orientations of the humerus (with respect to the thorax) over time [samples], from BLM (black line) and IMU's based LCS (grey line), during three types of motion; humeral forward flexion (top row), lateral flexion (middle row), and internal rotation (bottom row), one movement each. Humeral orientations are decomposed in Euler angles [in degrees], in the following order: plane of elevation (left column), elevation (middle column) and internal rotation (right column), conform the ISB proposal.

Discussion

The aim of this study was to determine and propose a simple and easy ‘IMU’s to segment’ calibration, or Local Coordinate Systems (LCS), for the thorax and upper extremity.

The results of this paper reveal that when an appropriate protocol is used, with a well-controlled reference position and in which movements to obtain functional axes are performed in a standardized manner, a low dispersion over trials can be obtained (Table 1). Low dispersion, by definition, means high repeatability. This was the first requirement for the development of an ‘IMU’s to segment’ calibration. Additionally, the method is independent of 3D position information, and therefore independent on equipment of a motion lab and/or expertise of a lab technician.

Direct comparison of dispersion results with previously published values was quite difficult, since most of those data concern the lower extremity and data that are based upon the BLM method. However, the reported variation obtained in this experiment was comparable to the dispersion of 2.2° to 15.7° as published by (Stokdijk et al., 2000) for the elbow flexion extension axis and the directional accuracy of $4.36 \pm 2.12^\circ$ for pro-supination as reported by (Tay et al., 2008).

The comparison of BLM and IMU’s-based LCS yielded both compatible (thorax) and quite different results (humerus, forearm and hand). For the humerus, the two methods showed a relatively large difference of around 9°, with two potential causes: first, soft tissue artifacts might have affected the orientation of the sensor on the humerus in two ways; the sensor does not follow the complete excursion of the humeral bone during internal rotation (Cutti et al., 2006), and the sensor might be tilted during elbow flexion. Second, the fixation of the forearm with a light wooden bar, which should prevent lateral sway, might have induced unwanted pro-and supination of the forearm during elbow flexion. This then results in a

composite axis, pointing more dorsally and caudally than the anatomical flexion extension axis known from the literature (Cutti et al., 2008; Stokdijk et al., 2000) (Cutti et al., 2006; Ericson et al., 2003). Since, however, the dispersion of this movement is rather low, it is still a suitable candidate. For the forearm the same effect might have occurred since the flexion axis was derived using the same procedure.

For the hand, the differences between the IMU's -based LCS and the BLM based LCS deserve special attention, since these differences were rather large, significant, and varied over subjects. An important cause to these differences might be based in the choice of bony landmarks PU, PR and MCIII to construct the LCS of the hand, where PU and PR are in fact landmarks on two different segments. Since the ISB proposal does not include a final definition of BLM to be used for the construction of a LCS for the hand, it is of course possible to further explore different BLM that would lead to a closer fit of the two coordinate system derivations.

It should be noted that the differences between BLM and IMU's based orientation in segment motion, as visualized for the humerus in figure 3, are a cumulated effect. First, the different definition of the LCS which can cause an offset between methods, and second, soft tissue artefacts (STA) having a dissimilar effect on both systems used (markers on BLM versus IMU's), of both segments involved (humerus and thorax), which can result in variation over time.

Limitations of the method

To enable a proper comparison of the IMU's-based method with data derived from BLM, or the transformation of the one into the other, norm data on both methods are needed as well as consensus on the most appropriate methods. A

transformation matrix from IMU's based to BLM based LCS would enable comparison of kinematics based on functional axes. It should, however, be kept in mind that inter-individual differences do exist and that no single, unique transformation will exist that can be used to map the one reference frame onto the other for all individuals. In that sense this process will always be an estimate. The dataset in this experiment was collected with the help of healthy subjects, with no history of upper extremity complaints, or any pathological restrictions in movement performance. The application of the functional method might be limited in individuals with musculoskeletal disorders because of limited ranges of motion, or compromised joint rotation (as in severe osteoarthritis). Depending on type and severity of the restriction, alternative motions might be necessary, or the BLM method might work out to be the only suitable procedure for the construction of LCS.

Since the scapula is not under voluntary control, and can only be measured for a restricted range of motion (van Andel et al., 2009; Karduna et al., 2001), this segment is not addressed in the method. To obtain the 3D orientation of the scapula for the full range of motion, to serve as input for a musculoskeletal model, a regression method is preferred (de Groot and Brand, 2001), in this stage of the project. However, these regression equations are only valid and applicable to healthy subjects. When aiming at musculoskeletal modeling on patient data, tracking scapular orientations conform (Cutti et al., 2008), although for a restricted range of motion, will be more appropriate.

Conclusions

The method to determine IMU's based axes is repeatable. Using the axis with the lowest dispersion as the main axis for constructing a LCS seems a logical choice; analog to the ISB proposal, where the longitudinal axis, based on markers on

BLM, is argued to be the most stable and repeatable axis. Appendix 1 comprises a proposal for the construction of LCS when using IMU's.

Acknowledgements

This research project is conducted within the Freemotion Consortium, which is granted by Senter (a delegate of the Dutch Ministry of Economic Affairs).

Appendix 1: Construction of local frames of reference with functional axes.

IMMS placement (based on ‘best practice’)

- Thorax: on sternum, double sided tape to avoid sliding down, elastic / neoprene bandage to avoid loosening from tape;
- Humerus: on latero-caudal side of the humerus, with a neoprene cuff;
- Forearm: on the dorso-caudal side of the forearm, close to the wrist, with a neoprene cuff, connectors and cables pointing to the elbow, to avoid contact friction with the hand IMMS during dorsal flexion of the hand;
- Hand: with a neoprene cuff or gloves, base on MCII and MCIII, on dorsal side of the hand, with connectors and cables pointing to the fingers, to avoid contact and friction with the forearm IMMS during dorsal flexion.

Movement protocol

All movements should be performed at a moderate speed.

Thorax

- Primary axis: Five times forward flexion of the trunk (0° to 40° flexion). Keep the arms aligned with the thorax, try to avoid neck flexion. Start and end with standing still and upright for a few seconds.
- Secondary axis: From standing still in anatomical reference position for 5 seconds.

Humerus

- Primary axis: while seated, the olecranon supported at a table, elbow flexed at about 90° , perform five times endo-exo rotation of the humerus. Try to avoid elbow flexion-extension, or forearm pro and supination during the movement.
- Secondary axis: while seated, both elbows (olecranon) supported at a table, elbows at shoulder breadth, holding a stick with both hands at shoulder breadth, thumbs pointing laterally, perform five times elbow flexion and extension, ranging from 20° to 50° flexion. Since movement of the forearm is used to define the lateral axis of the humerus which is not moving, data from the IMMS on the forearm is expressed in the coordinate system of the IMMS on the humerus.

Forearm

Primary axis: while seated, olecranon supported at a table, ulna supported and fixated to avoid endo exo rotation of the humerus during the movement, perform five times pro and supination of the forearm.

Secondary axis: Elbow flexion, same procedure as in obtaining the secondary axis of the humerus. IMMS data of the forearm is now used with respect to the forearm IMMS.

Hand

Primary axis: while seated, keep the hand flat on a table, for five seconds. Use the gravity vector obtained during this measurement.

Secondary axis: while seated, start with the forearm and hand flat on a table, perform five times dorsal flexion of the hand, from 0° to 30°.

Construction of the local coordinate system (LCS)

IMMS data are first processed into functional axes; subsequently these axes are used to construct a LCS with respect to the sensor and transformed into segment orientation, according to the general formula below:

$$a = v_{\text{functional axis 1}}$$

$$b = v_{\text{functional axis 2}} \times a$$

$$c = a \times b$$

$${}^{IMMS}R_{\text{segment}} = [a \quad b \quad c], \quad {}^{IMMS}R_{\text{segment}} = \frac{{}^{IMMS}R_{\text{segment}}}{\|{}^{IMMS}R_{\text{segment}}\|}$$

$${}^{global}R_{\text{segment}} = R_{IMMS \text{ on segment}} \bullet {}^{IMMS}R_{\text{segment}}$$

Where:

$v_{\text{functional axis 1}}$ = functional axis with lowest dispersion

$v_{\text{functional axis 2}}$ = functional axis with second lowest dispersion

${}^{IMMS}R_{\text{segment}}$ = segment LCS with respect to IMMS

${}^{global}R_{\text{segment}}$ = segment orientation in global based on IMMS data and LCS based on functional axes

\times denotes the cross product

\bullet denotes matrix multiplication

To obtain a right handed, orthogonal LCS which matches the naming conventions of the ISB proposal, the following order in the determination of segment orientation is proposed.

Thorax:

$$c = v_{flexion-extension}$$

$$a = v_{gravity\ in\ SAP} \times c$$

$$b = c \times a$$

Where

$v_{flexion-extension}$ = functional axis obtained from thorax flexion

$v_{gravity\ in\ SAP}$ = acceleration vector during standard anatomical position

Humerus:

$$b = v_{endo-exorotation}$$

$$a = b \times v_{flexion-extension}$$

$$c = a \times b$$

Where:

$v_{endo-exorotation}$ = functional axis obtained from humeral endo and exo rotation

$v_{flexion-extension}$ = functional axis obtained from elbow flexion-extension

Forearm:

$$b = v_{pronation-supination}$$

$$a = b \times v_{flexion-extension}$$

$$c = a \times b$$

Where:

$v_{pronation-supination}$ = functional axis obtained from forearm pronation-supination

$v_{flexion-extension}$ = functional axis obtained from elbow flexion-extension

Hand:

$$a = -v_{\text{gravity, hand flat}},$$

$$b = v_{\text{dorsalflexion}} \times a,$$

$$c = a \times b$$

Where:

$-v_{\text{gravity, hand flat}}$ = acceleration vector obtained with the hand flat on a table

$v_{\text{dorsalflexion}}$ = functional axis obtained from dorsal flexion of the hand

4

Determining a long term ambulatory load profile of the shoulder joint: Neural networks predicting input for a musculoskeletal model

de Vries, W.H.K.^{ab}, Veeger, H.E.J.^{ac}, Baten, C.T.M.^b, van der Helm, F.C.T.^a

Human Movement Science (31-2), 419-428

a Department of Biomechanical Engineering, Faculty of Mechanical, Maritime and Materials Engineering, Delft University of Technology, Mekelweg 2, 2628 CD, Delft, Netherlands

b Roessingh Research and Development, Roessinghsbleekweg 33B, 7522 AH, Enschede, Netherlands

c Research Institute MOVE, Department of Human Movement Sciences, VU University Amsterdam, van der Boechorststraat 9, 1081 BT, Amsterdam, Netherlands

Abstract

To gain more insight in the development of joint damage, a long term load profile of the shoulder joint under daily living conditions is desirable. Standard musculoskeletal models estimate joint load using kinematics and external force. However, the latter cannot be measured continuously in ambulatory settings, hampering the use of these models. This paper describes a method for obtaining such a load profile, by training a Neural Network (NN), using kinematics and EMG.

A small data set of specified movements with known external force is used in two ways. First, the model calculates several variables of joint load, and a set of Generalized Forces and Net Moments (GFNM) around the models degrees of freedom. Second, using kinematics and EMG, a NN is trained to predict these GFNM, which can concurrently be used as input for the model, resulting in full model output independent of external force. The method is validated with an independent trial. The NN could predict GFNM within 10% relative RMS, compared to output of the model. The NN–model combination estimated joint reaction forces with relative RMS values of 7 to 17 %, enabling the estimation of a detailed load profile of the shoulder in daily conditions.

Keywords: Ambulatory; Upper Extremity; Joint Reaction Forces; Musculoskeletal model; Neural Network.

Introduction

It is commonly accepted that the mechanical loading of the shoulder joint plays a role in the development of shoulder complaints when exceeding biological limits (in the case of a healthy shoulder), or when exceeding design limits in the case of a shoulder endo-prosthesis. However, neither biological limits in shoulder joint loading are known, nor are the load profiles on the joint in daily conditions. To gain more insight into the underlying mechanisms of the development of joint damage, and to enable the future development of enhanced endo-protheses, a long term load profile of the shoulder joint under daily living conditions is a necessity. Such a load profile, in terms of Net Moments (NM) around a joint, Joint Reaction Forces (JRF), and individual Muscle Forces (MF) can be estimated with a detailed musculoskeletal model (van der Helm, 1994b) (Dutch Shoulder and Elbow Model, DSeM), using upper extremity 3D kinematics and external force as input. To obtain the kinematics, Inertial Magnetic Measurement Systems (IMU's) have been shown to be an adequate candidate for the ambulatory measurement of upper extremity kinematics (Cutti et al., 2008; de Vries et al., 2010). Obtaining external force data in daily conditions is not yet feasible and therefore an inverse dynamic musculoskeletal model cannot be directly applied in daily living conditions outside the motion lab. However, the musculoskeletal response to external loads and tasks can be sampled and might be useful for the estimation of input data, in combination with 3D kinematic input. Neural networks have been used for muscle force prediction from EMG (Liu et al., 1999), the mapping of EMG to joint angles (Cheron et al., 2003; Shrirao et al., 2009), and the prediction of net moments around the elbow joint based on EMG (Song and Tong, 2005). Others compared NN prediction of isokinetic knee torque, based on EMG, joint kinematics and several other parameters, with a

forward stepwise regression model, showing NN results to be more accurate (Hahn, 2007).

In a previous study we (de Vries et al., 2014) explored the feasibility of using a Neural Network (NN) with upper extremity 3D kinematics and EMG as input for the prediction of one parameter (JRF) of the mechanical loading of the shoulder joint directly. No information on external force was needed, apart from some initial trials to generate training data for the NN, prior to the long term ambulatory measurements. However, to obtain a more detailed load profile, including Net Moments and Joint Reaction Forces around all joints involved, more extended model output is desirable.

The musculoskeletal model used in this experiment (van der Helm, 1994b) consists of thorax, clavicle, scapula, humerus, and forearm, including all muscles and their musculoskeletal parameters. The DSeM transforms external force and upper extremity 3D kinematics into “Generalized Forces and Net Moments” (GFNM) around its degrees of freedom. In a second step the required muscle force to accomplish this task is calculated using a cost function to minimize the load sharing problem. A basic cost function is used by the minimization of summed muscle stress, weighted by physiological cross-sectional area (van der Helm, 1994b). To minimize computational load, but maintain a mechanically consistent system, this optimization is performed around the eight most important degrees of freedom. These are “Generalized Forces” at the acromioclavicular joint in cranial and posterior direction, at the trigonum spinae in lateral direction, net moments around the humeral head in 3D, flexion moment at the elbow, and pro-supination moment of the forearm.

The DSeM can also accept these GFNM as input. To enable full model output independent of external force, a two stage approach in estimating a detailed shoulder joint load profile in daily conditions is presented here.

1. The first stage is the training of a NN, with upper extremity 3D kinematics and surface EMG of relevant muscles as input, to predict the Generalized Forces and Net Moments.
2. In the second stage, the Generalized Forces and Net Moments predicted by the trained NN are used as input for the model to calculate full model output.

In this experimental setting the external force were recorded or could be calculated from the weight and its measured acceleration. Every result from the two stage NN approach can be compared to output obtained with the standard approach, the inverse dynamic musculoskeletal model using kinematics and external force.

The goal of this study is the development of a method to assess a general load profile on the shoulder in daily conditions, based on variables that can be measured in an ambulatory setting, e.g. kinematics and EMG. Based on previous results, the NN approach is expected to achieve an accuracy of 10% (relative RMS value over a complete trial) in predicting the Generalized Forces and Net Moments. Output of the DSeM based on input as predicted by the NN will therefore differ from output estimated with the standard method, which uses kinematics and measured external force. For variables like JRF a difference of 10% to 15% relative RMS over a complete trial is considered acceptable, and useable for the ambulatory assessment of a joint load profile.

Methods

A healthy subject (age 30 years, stature 180 cm, weight 80 kg), with no history of shoulder dysfunction, was invited to participate in this pilot study. The study was approved by an IRB, and standard guidelines considering experiments with human subjects and the measurement of human motion were followed. After explanation of the aims and procedures of the study, informed consent was signed. An IMU's consisting of four sensors and a busmaster (MTx sensors, XM-B-3 busmaster, Xsens Technologies, Netherlands) was used for recording kinematics of thorax, humerus, forearm and hand (figure 1). MT-manager logging software was used, the implemented kalmanfilter was set at the "human scenario" with a sample frequency of 50 Hz. (Based on the chosen scenario the implemented

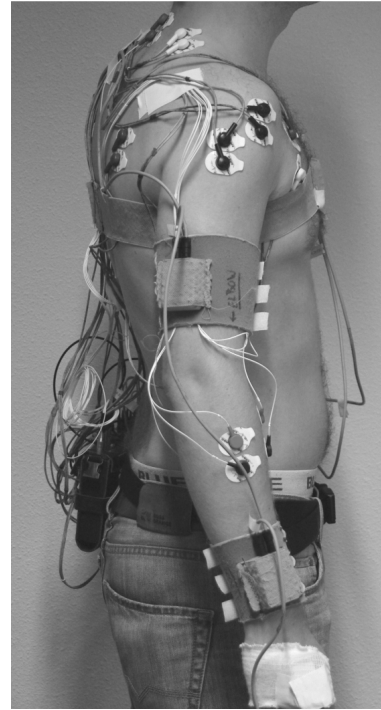


Figure 1, a fully equipped subject, with four IMU's units on thorax-sternum, right upper arm, right forearm and hand, and 13 channels of surface EMG.

kalmanfilter will apply appropriate filter settings recommended for the application, being human motion, not fast movements, nor robotic or industrial movements). Sensor to segment calibration was performed following (de Vries et al., 2010). To enable the orientation estimation of clavicle and scapula over the full range of motion a regression equation was used (de Groot and Brand, 2001), the required initial orientations of clavicle and scapula were measured using an additional sensor unit on a scapula locator (van Andel et al., 2009).

The IMU's were electrically synchronized with a 16 channel wireless EMG measurement system (Biotell 99, Glonner, Planegg, Germany), which was used to record the EMG of thirteen muscles around the shoulder girdle (table 1). Bi-polar Ag/AgCl electrodes were placed following the guidelines proposed by (Hermens and Freriks, 1997). EMG data were sampled at 1000 Hz (bandpass filter 16 – 400 Hz). Subsequently off line processing into srEMG was performed by applying a 2nd order Butterworth low pass filter with cutoff frequency of 2.18 Hz to create a linear envelope after offset removal and rectification of the signal.

Table 1, Muscles selected for the recording of surface EMG

1	M. Trapezius ascendens
2	M. Trapezius transversa
3	M. Trapezius descendens
4	M. Deltoideus anterior
5	M. Deltoideus medial
6	M. Deltoideus posterior
7	M. Latissimus dorsi
8	M. Infraspinatus
9	M. Serratus anterior
10	M. Pectoralis major, pars Sternalis
11	M. Pectoralis major, pars clavicularis
12	M. Triceps, caput longum
13	M. Biceps, caput longum

MVC values were obtained for all muscles or muscle groups following guidelines by (Hermens and Freriks, 1997). For normalization of the EMG the maximum 1-second average srEMG value was used.

To generate training data for the Neural Network the following trials were performed by the subject:

1. Random movements for one minute, through the complete range of motion of the upper extremity, at varying velocity, while holding a known mass in the right hand. Masses ranged from 0 to 2.5 kg in steps of 0.5 kg, resulting in six trials total.
2. Five activities of daily living (ADL): Brushing teeth, combing hair, perineal care, washing armpits, eating, 10 seconds each, while holding a

known mass in the right hand. Masses ranged from 0 to 1.5 kg, in steps of 0.5 kg, resulting in 4 separate trials.

One separate trial with ADL movements with a mass of 0.2 kg in the right hand was kept apart, e.g. not used in the training of the NN, and used for validation purposes. As a final step, all motion data were filtered with a 2nd order zero lag low pass Butterworth filter with cutoff frequency of 3 Hz.

A standard Neural Network was constructed, similar to (de Vries et al., 2014), with the following structure: an input layer of 40 cells (3D Kinematics of segments, orientations, accelerations, angular velocity, and 13 channels of normalized srEMG), one hidden layer of 30 cells, and one output layer of eight cells representing the Generalized Forces and Net Moments. The transfer function from input to the hidden layer was a tangent sigmoid function, from hidden to output layer a linear function was used. The network was trained with back propagation, using the Levenberg-Marquardt algorithm at a learning rate of 0.05, and with momentum of 0.7. Training of the NN was stopped when the mean sum of squares of the network errors dropped below a goal set at $MSSE=0.01$ (determined by experiment), or when network error on a subset of data used for validation began to rise for a certain number of iterations to prevent over fitting.

Validation of the trained neural network (figure 2A) was performed by simulating a complete motion trial. This independent trial of ADL movements with 0.2kg in the right hand was not used for training. Neural Network predictions of Generalized Forces and Net Moments were compared to those calculated by the musculoskeletal model by expressing the differences between both methods as absolute and relative RMS values over the complete trial. Relative RMS is expressed here as the absolute RMS value related to the range of values of that variable as calculated by the musculoskeletal model.

NN Training & Validation

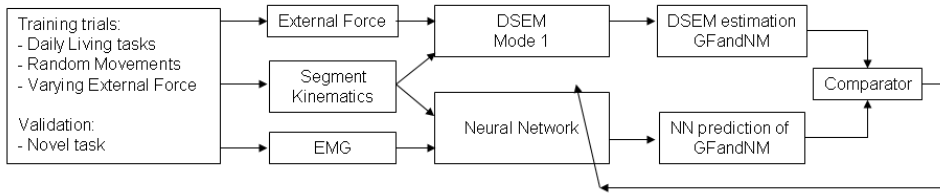


Figure 2A, Schematic of the procedure used to train a Neural Network with back propagation in predicting generalized forces and net moments in the shoulder girdle. Only during this training phase, known external force are required as one of the inputs for the musculoskeletal model. This can be a known mass in the hand, and its kinematics, or data from a force transducer measuring actual external force. The comparison of NN output, and its target (calculated by the musculoskeletal model), and the update of internal parameters of the neural network is implemented in the NN toolbox which was used for the construction, training and validation of this procedure.

Validation of the complete procedure was obtained by using the generalized forces and net moments predicted by the Neural Network from the independent trial as input for the musculoskeletal model. From full model output, as an example, JRF of Sternoclavicular, Acromioclavicular, Glenohumeral and Humero-ulnar joint were compared. Differences in JRF between both methods were described as relative RMS values over the complete trial. Figure 2A and 2B depict the schematics of the described validation procedures.

Validation of complete procedure

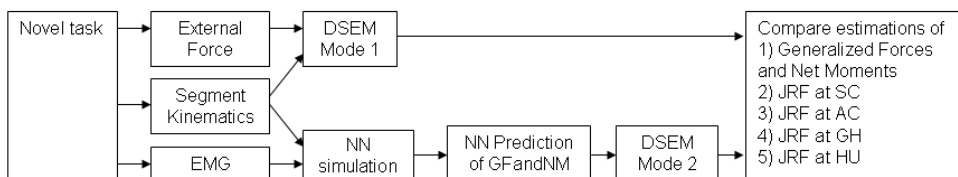
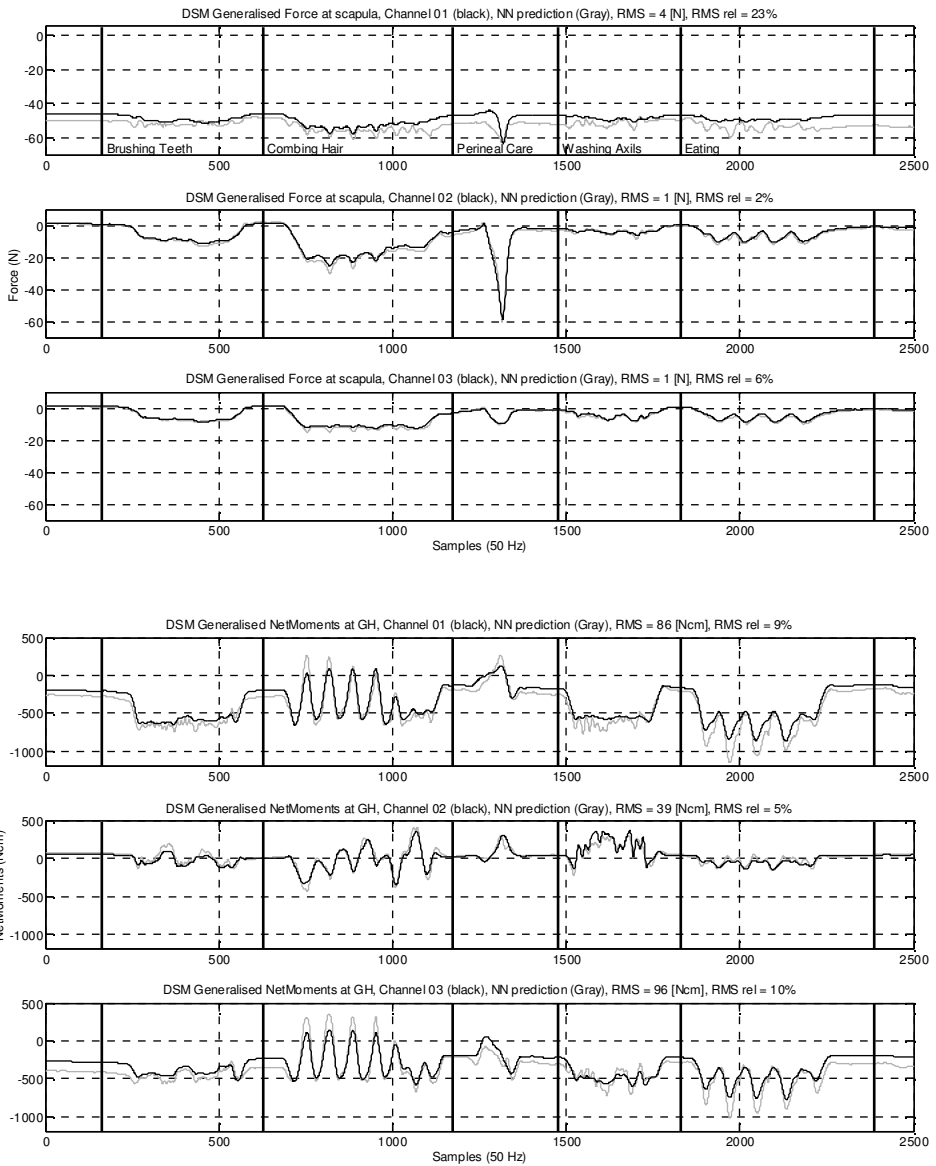


Figure 2B, Schematic of the validation of the complete procedure, in which a novel, independent task, not used in the training, is simulated with the trained NN, and its prediction of Generalized Forces and Net Moments, is used as input for the musculoskeletal model (Mode 2). Output of the combination NN-musculoskeletal model is compared to corresponding output of the musculoskeletal model using external force (known mass in the hand) and upper extremity kinematics (Mode 1). This paper addresses the validation of GFNM and JRF at the various joints of the shoulder complex.

Results

The first step in validating the trained neural network is the simulation of an independent trial, not used in training, and the comparison of the output of the NN with its equivalent, the generalized forces and net moments as calculated by the musculoskeletal model. The independent trial consisted of ADL movements while holding a mass of 0.2 kg in the right hand. This resulted in a moderate loading of the shoulder girdle, with Net Moments around the GH joint varying from 2 to 10 Nm, and maximum JRF of about 70 N, 140 N, 350 N and 250 N for the SC, AC, GH and HU joint respectively. Although a certain overshoot can be observed for peak values from the NN prediction, the relative RMS values calculated over the complete trial were below 10% for seven of the eight components of the Generalized Forces and Net Moments (figure 3). The prediction of the generalized force at the Acromioclavicular joint in cranial direction (Netforce channel 01) shows an acceptable low absolute RMS value of 4 Newton, which is comparable to the absolute RMS values of the other two Generalized Forces; however, due to the low variation of the signal over the trial a high relative RMS value of 23% is obtained.



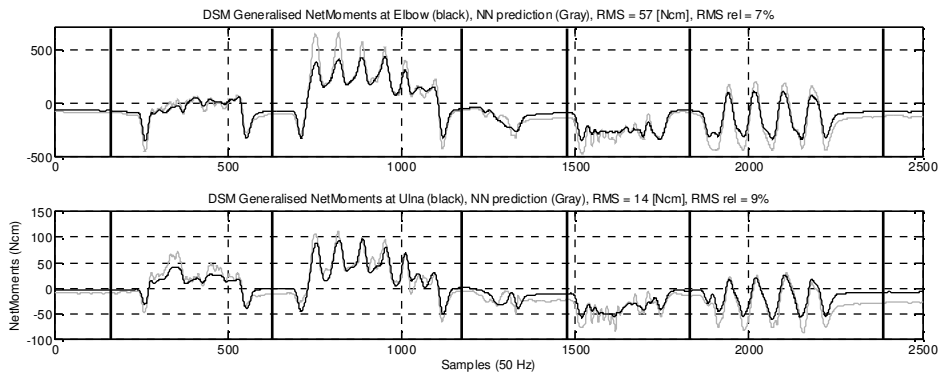


Figure 3, the eight components of the generalized forces and net moments, as calculated by the DSeM (Black), and predicted by the Neural Network (Gray).

These Generalized forces and Net Moments, predicted by the NN based on data of the independent trial, were subsequently used as input for the DSeM to calculate full model output. From the resulting output the estimations of the JRF at the Sternoclavicular (SC), Acromioclavicular (AC), Glenohumeral (GH) and the Humero-ulnar (HU) joint were compared to their equivalents as obtained by the DSeM using external force and upper extremity 3D kinematics as inputs. For the sake of clarity, the relative RMS value of a variable is the RMS value between time series of that variable from output of NN-DSeM predictions and DSM calculations, related to the range of that variable (maximum – minimum) as calculated by DSeM.

As an example, Glenohumeral Joint Reaction Forces in 3D are depicted in figure 4. With full model output available, not only the order of magnitude, but also the direction of the JRF can be examined. Deviation of the NN-DSeM estimation of Total Glenohumeral JRF is 12% relative RMS. However, several spikes can be observed during the task “Washing Armpits” and an overestimation of the NN-DSeM prediction during the task “Eating”. The JRF in Y-direction (longitudinal axis of the humerus) as estimated by NN-DSeM shows the highest relative RMS

value of 18%, for respectively X and Z direction the relative RMS value is 13% and 11%. During the task “Perineal Care” the output of the NN yielded an incompatible set of Generalized Forces and Net Moments, which could not be “solved” by the DSeM. Therefore results of this task could not be compared, and are not shown in the graph.

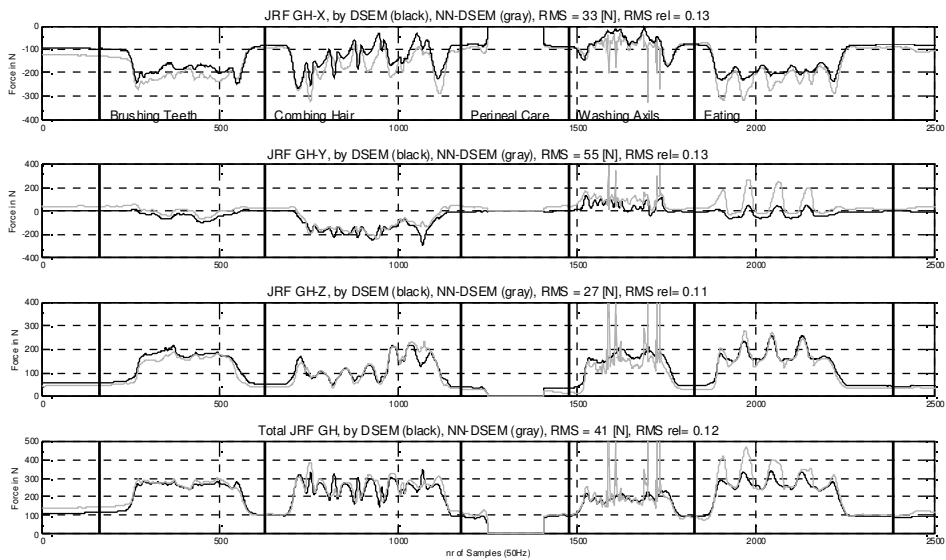


Figure 4, JRF of the glenohumeral joint, for its three axes and Total JRF (in N). Relative RMS values range from 11% to 13% over the complete trial. However, in the NN-DSeM prediction several spikes can be noticed during the task “washing armpits” and a clear overestimation in X and Y direction during the task eating.

Table 2 depicts the relative RMS values for the JRF of the SC, AC, GH and HU joint, in three dimensions. Although the relative RMS values of SC-X and AC-Y are noticeably higher, the absolute RMS values are at the same order of magnitude as at the other axes of that particular joint.

Table 2, relative RMS values of JRF between methods for four joints, in their local coordinates in 3D (X+ to the right, Y+ vertical up, Z+ pointing backwards) and Total JRF.				
	X	Y	Z	Total
Sterno-Clavicular	18%	14%	13%	14%
Acromio-Clavicular	12%	26%	14%	17%
Gleno-Humeral	13%	13%	11%	12%
Humero-Ulnar	4%	5%	8%	7%

The graphs in figure 5 show the Total JRF over time, for the independent trial not used in training of the neural network, for the four joints described. Relative RMS values between both methods (DSeM versus NN-DSeM) vary from 7% to 17% for the several joints. As can be noticed the spikes during the task “Washing Armpits” appear at the SC, AC and GH, but not at the HU joint, which will be addressed in the discussion.

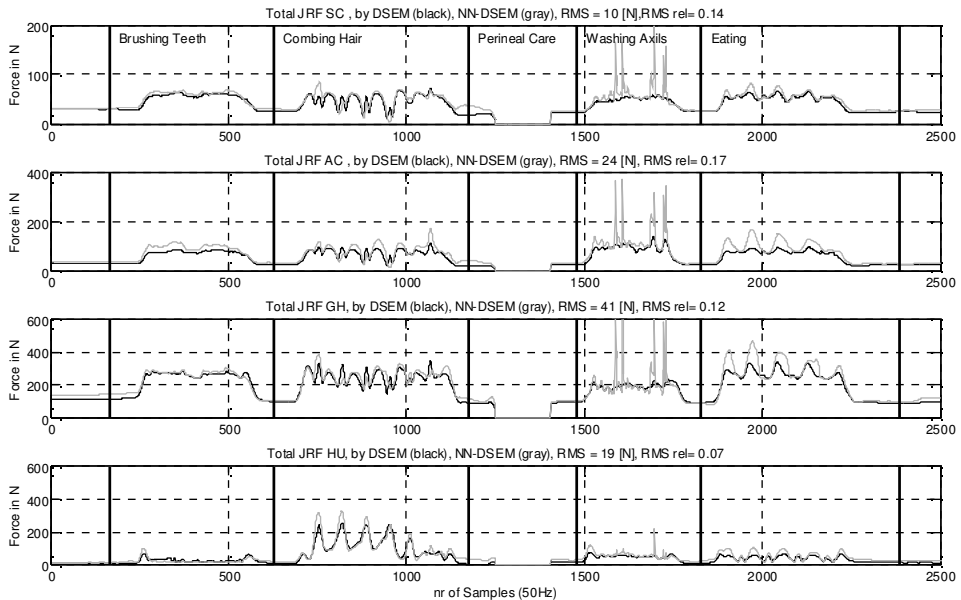


Figure 5, Total JRF of Sterno-Clavicular, Acromio-Clavicular, Gleno-Humeral, and Humero-ulnar joint, calculated by NN based DSM (gray lines) and the standard approach, DSM (black lines), for an independent trial, not used in the training of the neural network. Relative RMS values between methods vary from 7% to 17% for the various joints.

Discussion

The overall performance of the NN in predicting Generalized Forces and Net Moments for an independent trial, not used in the training of the NN is good. Predictions showed a relative RMS of less than 10% for seven of the eight components. The first component, Generalized Force at the acromioclavicular joint, showed an acceptably low absolute RMS value of 4 Newton, comparable to the RMS of the other components of Generalized Force, despite the calculation of the relative RMS amounted to a value of 23% (due to low variation in the signal over time). The same phenomenon can be observed for the calculation of relative RMS values of components of the JRF of the SC and the AC joint. Although the absolute RMS value of the Y component of the JRF of AC is higher than expected (a possible explanation is given below), the relative RMS value was doubled to 26% due to low variation in the JRF signal over time. Also here the absolute and relative error should not be used apart from each other.

A sensitivity analysis of the trained NN was performed. The network simulated a dataset with one of the inputs at 90% and 110%, for each input channel separately, and the output channel its gradients were calculated. The network generally showed a larger dependency on kinematic variables, but also fluctuation of this dependency over time. Peaks in sensitivity occurred at the extremes of the range of motion of the upper extremity kinematics. This phenomenon can be explained by the fact that NN are good in interpolation, but analog to regression equations, are not very suitable for extrapolation.

In this experiment, besides normalization, no further pre-processing of input data was performed. Since the extremes of range of motion are less represented in the data, the risk of extrapolation increases, and an increase in sensitivity for

fluctuations can be seen in these areas. As a result from this overestimation of Net Moments around GH-X and GH-Z during the task “Eating”, the NN-DSeM shows an overestimation of muscle forces (mainly M. Deltoid pars clavicularis, and M. Pectoralis, sternal and clavicular part) in these areas, which is reflected in a clear overestimation of the JRF in Y direction at the GH joint, but also the SC and the AC joint. This effect can possibly be reduced by a more dedicated selection of data on which the NN is trained. The NN can, for instance, be trained on data consisting of local peaks in the Generalized Forces and Net Moments instead of data from complete trials. In this way, the NN can probably be tuned to have a better prediction for these peak values, at the cost of a less accurate prediction of the lower range of these values. However, this will hamper the collection of a balanced Load Profile in daily conditions. Another possible method to improve the quality of NN-prediction is preprocessing of the dataset in such a way that all unique combinations of input samples have equal distribution. Numerous other options exist considering extended input, preprocessing of data, type and architecture of NN used, types of motion, etc. and will certainly be addressed in future research in estimating a load profile for unconstrained upper extremity motion.

Another phenomenon to be discussed is the occurrences of spikes in the NN-DSeM estimation of JRF during the task “washing armpits”. During this task faster humeral rotations were measured (endo- and exorotation, possibly including Soft Tissue Artifacts of sensors). Since the kinematics as measured with the sensors are used for both direct calculation of JRF with the DSeM and for the “NN-DSeM” combination (see Figure 2B), the cause of this phenomenon should be sought in another part of the scheme. A likely explanation is the sensitivity of the NN prediction of Net Moments around the GH joint for humeral kinematic input, since this sensitivity could easily lead to larger fluctuations. As a result, the

needed muscle forces as calculated by the DSeM can than easily be exceeded for the most effective but smaller muscles, which are, due to the load sharing optimization, accounted for by larger but less effective muscles, leading to unrealistic high JRF. Again, a more dedicated selection of input data for the training of the NN might possibly reduce the sensitivity for just one or a few of the input variables.

Overall performance of the NN-DSeM method is acceptable in obtaining a general load profile of the shoulder girdle over time, based on ambulatory obtainable variables. With the prediction of Generalized Forces and Net Moments by the NN, more extended output of the DSeM becomes available. JRF for four joints of the shoulder girdle were examined in 3D. Except for two components, most JRF components in three dimensions were estimated with an accuracy of about 5 to 15% relative RMS value. This opens the way to a more detailed load profile of the upper extremity in ambulatory settings, including Net Moments and Joint Reaction Forces in 3D around the joints involved. It is expected that with such a long term load profile insight can be gained into the mechanisms of the development of joint damage, or to enable the future development of enhanced endo-prostheses.

Role of the funding source

This research project is conducted within the “Freemotion Consortium”, and “Fusion Consortium”, which were both granted by Senter (a delegate of the Dutch Ministry of Economic Affairs). Senter had no involvement in study design, collection, analysis, interpretation of data nor the writing or submission of this paper.

5

Can shoulder joint reaction forces be estimated by neural networks?

W.H.K. de Vries^{1,2}, H.E.J. Veeger^{1,3}, C. Baten², F.C.T. van der Helm¹

Submitted.

- 1) Department of Biomechanical Engineering, Faculty of Mechanical, Maritime & Materials Engineering, Delft University of Technology, the Netherlands.
- 2) Roessingh Research & Development, Enschede, the Netherlands
- 3) Research Institute MOVE, Department of Human Movement Sciences, VU University Amsterdam, the Netherlands

Abstract

To facilitate the development of future shoulder endoprostheses, a long term load profile of the shoulder joint is desired. A musculoskeletal model using 3D kinematics and external force as input can estimate the mechanical load on the glenohumeral joint, in terms of joint reaction forces. For long term ambulatory measurements, these 3D kinematics can be measured by means of Inertial Magnetic Measurement Systems. Recording of external force in daily conditions is not feasible; estimations of joint loading should preferably be independent of this input. EMG signals reflect the musculoskeletal response and can easily be measured in daily conditions. This study presents the use of a neural network for the prediction of glenohumeral joint reaction forces based upon arm kinematics and shoulder muscle EMG. Several setups were examined for NN training, with varying combinations of type of input, type of motion, and handled weights. When joint reaction forces are predicted by a trained NN, for motion data independent of the training data, results show a high intraclass correlation (ICC up to 0.98) and relative SEM as low as 3%, compared to similar output of a musculoskeletal model. A convenient setup in which kinematics and only one channel of EMG were used as input for the NN's showed comparable predictive power as more complex setups. These results are promising and enable long term estimation of shoulder joint reaction forces outside the motion lab, independent of external force.

Keywords: Ambulatory, IMU's, Joint Reaction Forces, Upper extremity, Neural networks.

Introduction

In the process of developing future endoprostheses for the shoulder, information on the mechanical loading of the shoulder is essential. Ideally, this information embraces a long term load profile of the shoulder joint under daily living conditions. The glenohumeral joint reaction force represents the resultant of muscle forces and passive forces like ligament strain working on the shoulder joint, rendering it into a natural candidate for the indication of mechanical loading.

Under laboratory conditions shoulder joint moments and reaction forces have been estimated with a large scale musculoskeletal model for a variety of tasks [Delft Shoulder and Elbow Model, DSEM, (van der Helm, 1994b), (van der Helm, 1994a)], using upper extremity 3D kinematics and external force as input. If load profiles are to be recorded in daily conditions, these input variables have to be measured ambulatory.

It has been shown that Inertial Magnetic Measurement Systems (IMU's) are an adequate candidate for the ambulatory measurement of upper extremity kinematics [(Cutti et al., 2008), (de Vries et al., 2010)]. Although external force can be measured under laboratory conditions, long term ambulatory recordings should preferably be independent of the complex measurements of external force. Several alternative methods in the determination of the mechanical loading of the shoulder joint in daily conditions exist. Westerhoff et al (Westerhoff et al., 2009a) used instrumented endoprostheses, enabling the direct measurement of JRF-GH in daily conditions. Despite interesting results, this method is rather invasive, limited to a small group of patients who opt for a shoulder joint replacement, and therefore will render only a small sample size for research. Besides that, for a more detailed load profile, additional measurement of movements or actions resulting in higher loads at the endoprosthesis is required.

As in EMG driven models, EMG signals reflect the musculoskeletal response and can easily be measured in daily conditions. Several studies have used EMG combined with other variables as input for Neural Networks in the prediction of kinematics or kinetics, like muscle force prediction from EMG [(Liu et al., 1999)], the mapping of EMG to joint angles [(Cheron et al., 2003; Shirao et al., 2009)], and the prediction of net moments around the elbow joint based on EMG [(Song and Tong, 2005)]. Kingma et al [(Kingma et al., 2001)] compared a linked segment model, an EMG driven model, and a neural network approach in the prediction of spinal loading. Isokinetic knee torque as predicted by a Neural Network using EMG, joint kinematics and several other variables showed higher accuracy than a forward stepwise regression model [(Hahn, 2007)]. Luh et al [(Luh et al., 1999)] showed that moments around a single joint axis can be estimated by a Neural Network (NN), using segment kinematics and surface EMG as inputs.

These results inspired us to investigate a NN approach in the direct prediction of the glenohumeral joint reaction force under unconstrained daily conditions, based on ambulatory obtainable variables like body segment kinematics and EMG. Inertial Magnetic Measurement Systems (IMU's) enable the long term ambulatory measurement of 3D upper extremity kinematics in an almost unlimited measurement volume. Developments in the past decade resulted in truly wearable EMG measurement equipment. With these two systems available all the necessary information can be collected ambulatory, as needed for the chosen approach, with a relative simplicity.

One major question remains open: Are Neural Networks indeed able to learn the complex relationship between upper extremity kinematics and muscle activity patterns to predict glenohumeral joint reaction force, for the irregular, unconstrained humeral motion in daily conditions?

Methods

One healthy subject (age 29 years, stature 180 cm, weight 78 kg), with no history of shoulder dysfunction, was invited to participate in this pilot study, after consulting a local ethical committee. After explanation of the goal and procedures of the study, informed consent was signed.

Training data for the NN method were generated by performing several series of pre-described upper extremity movements while holding a variety of known masses in the hand. Upper extremity 3D kinematics and EMG were measured, external force on the hand were calculated by multiplying the known mass by measured acceleration. The glenohumeral joint reaction force was calculated using a musculoskeletal model (DSEM), and used as target for the training of the NN. This approach produced input for the musculoskeletal model (3D upper extremity kinematics and external force), as well as data to train the NN method (3D upper extremity kinematics and EMG), all measured simultaneously, not limited to laboratory conditions. After sufficient training, the NN should be able to predict glenohumeral joint reaction forces using only 3D kinematics and EMG.

To examine a NN method being successful in the prediction of the joint reaction forces in daily conditions, the influence of the following factors has been studied:

1. The type of movements that should be performed; Activities of Daily Living (ADL) or Random Movements;
2. The type of input needed for the NN;
 - a. 3D kinematics and surface EMG of 13 muscles of the upper extremity;
 - b. Upper extremity 3D kinematics and the EMG of the medial Deltoid, which was considered to be most active during mentioned tasks;

3. Variation of external weights, should the range of weights used for training cover the external force exerted during ADL movements; or stated differently, how good is a trained NN in intra- and extrapolating?

Kinematics

Four IMU's were attached to a bus master (MT-X sensors and a XM-B-3 bus master, Xsens Technologies, Netherlands), operating at 50 Hz. The XSens MT-manager software (v1.5.0, SDK v3.1) was used for logging; the implemented Kalman filtering [(Roetenberg et al., 2005)] was set at the "human scenario". As depicted in figure 1, IMU's were attached by means of dedicated neoprene cuffs to guarantee a comfortable, long term fixation on sternum, humerus, forearm and hand.

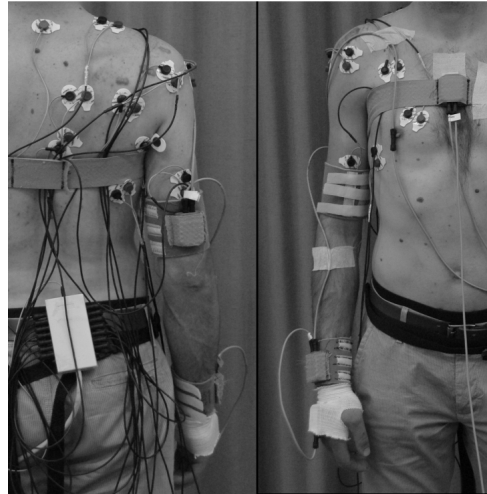


Figure 1, a fully equipped subject, with four sensor modules on sternum, humerus, forearm and hand, and 13 channels of surface EMG.

Sensor to segment calibration was performed following [(de Vries et al., 2010)]. Orientation estimations of clavicle and scapula were based on the regression equations by De Groot & Brand [(de Groot and Brand, 2001)]. The required initial orientation of clavicle and scapula were measured using an additional sensor unit on a scapula locator [(van Andel et al., 2009)]. Kinematic data were expressed in the reference frame of the DSEM model, with the positive X-axis from left to right, positive Y-axis vertical upwards, and positive Z-axis pointing backwards.

EMG

Thirteen muscles around the shoulder joint were selected for the recording of surface EMG, see table 1. Bi-polar Ag/AgCl electrodes were placed following the guidelines proposed by [(Hermens and Freriks, 1997)]. EMG data were sampled at 1000 Hz, digitally filtered with a first order high pass filter at 16 Hz and recorded (Biotel 99, Glonner, Planegg, Germany). Offline, EMG signals were rectified and smoothed (unidirectional low pass 2nd order Butterworth filter at 3 Hz) to obtain smooth rectified EMG envelopes (srEMG) in an attempt to have a resemblance in envelope shape close to muscle force output [(Olney and Winter, 1985)].

1	M. Trapezius ascendens
2	M. Trapezius transversa
3	M. Trapezius descendens
4	M. Deltoideus anterior
5	M. Deltoideus medial
6	M. Deltoideus posterior
7	M. Latissimus dorsi
8	M. Infraspinatus
9	M. Serratus anterior
10	M. Pectoralis major, pars Sternalis
11	M. Pectoralis major, pars clavicularis
12	M. Triceps, caput longum
13	M. Biceps, caput longum
Table 1, Muscles selected for the recording of surface EMG.	

External force

To obtain different levels of external force during motion, subjects were holding different (known) masses ranging from 0.5 to 2.5 kg in the right hand. External force was calculated by multiplying the mass with measured acceleration of the hand.

Experimental protocol

Two types of datasets were generated. During the first series of measurements, labeled as RND (random), the subject performed random upper extremity

movements for one minute each, holding a known mass (0, 0.5, 1.0, 1.5, 2.0, or 2.5 kg). The subject was instructed to cover the complete range of motion over all degrees of freedom, and to vary movement speed from slow to moderately fast. In the second series of measurements the subject was asked to mimic Active Daily Living (ADL) tasks with a mass (0, 0.2, 0.5, 1.0) in the right hand for ten seconds each. These tasks consisted of brushing teeth, combing hair, perineal care, washing the axils and eating.

Data analysis

The joint reaction force as calculated with the DSEM was used as target for training of the NN and as the standard in validating NN predictions for independent trials not used in training.

Inspired by the overview of [(Schollhorn, 2004)], for the type of data in this experiment a three layer feedforward network was constructed. From input to hidden layer a tangent sigmoid transfer function was used, from hidden to output layer a linear transfer function [(Schollhorn, 2004)]. The number of inputs depended on the stage of analysis:

- Stage 1: 36 input cells were used using segment 3D kinematics (orientation for all segments; forearm acceleration and angular velocity as measured with the IMU's) and 13 channels of upper extremity muscle srEMG;.
- Stage 2: 24 input cells were used based on kinematics and EMG of the medial Deltoid.

Based on results indicated by [(Schollhorn, 2004)] a number of 20 cells was chosen for the hidden layer. The output layer consisted of three cells to predict the joint reaction force at the glenohumeral joint in 3D. Neural networks were trained using Matlab's Neural Network Toolbox (Matlab R2012a, NN toolbox V7.0.3). Network training was epoch based for a maximum of 500. A Levenberg-Marquard backpropagation algorithm with a momentum of 0.8 at a learning rate

of 0.05 was applied. To prevent overfitting, training was stopped when internal validation failed to decrease for ten successive iterations. The training procedure is schematized in figure 2.

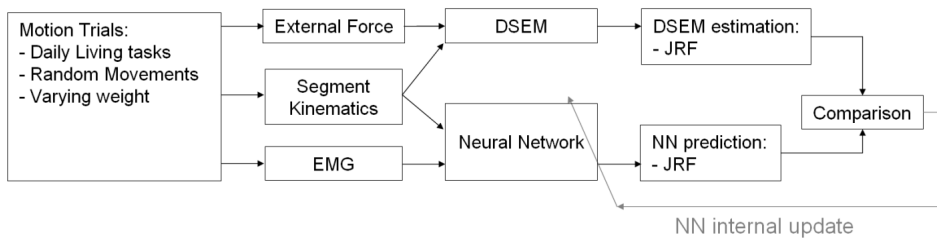


Figure 2, Schematic of the procedure used to train a Neural Network with back propagation in predicting joint reaction forces at the glenohumeral joint. During the training phase, known external force are required as one of the inputs for the musculoskeletal model (Exerted Force = [known mass in the hand] times [measured acceleration of the hand]). The comparison of neural network output and its target (calculated by the musculoskeletal model), and the update of internal parameters of the neural network is implemented in the Matlab Neural Network toolbox which was used for the construction and training of this procedure. Validation was performed by simulating an independent dataset with the network, and compare its prediction with results as calculated with the musculoskeletal model.

Since the initialization of a NN comprises random weight assignment to all internal connections, followed by training; when repeated this might lead to different behavior and performance of the individually trained NN. Therefore, for each test condition 10 individual networks were initialized, trained and externally validated by simulating the trained NN with an independent dataset, not used for training. Intra Class Correlation (ICC) between prediction and corresponding output by the DSEM (joint reaction force) were calculated using custom written Matlab-routines. From these ICC's, the Standard Error of Measurement (SEM) was derived following (Weir, 2005). To compare test conditions with different external loads, SEM values were expressed as a percentage of the range of the signal (SEM_rel). Finally, from the 10 neural networks individually trained for each test condition, the neural network producing the lowest SEM_rel was considered the best performing network.

Several combinations of input type, movement type, and weight ranges were examined during this validation, as depicted in table 2. The trials with the label “lower weight” were excluded from training and subsequently used for simulation with the trained NN for the external validation procedure as described above. These “lower weight” trials were within the range of weights used for training, serving as a test case for the performance of the NN while interpolating. The trials with the label “heavy weight” served in a similar way as a test case for extrapolation of neural network predictions.

Results

The neural networks showed good convergence during training, meaning that the neural networks were able to learn the relationship between input and target (preferred output for the training dataset). Over all conditions, for the best performing network the ICC values ranged from 0.98 to 0.83, whereas the SEM_rel varied from 3% to 21%, between NN-predictions and corresponding output from the musculoskeletal model. For the best performing NN of each conditions these ICC and the SEM_rel, are depicted in table 2.

Results from stage 1, (3D kinematics and 13 channels of EMG) for ADL type movements indicate that performance was best when NN were trained with ADL type movement trials and external load within the training range, resulting in a SEM_rel of 11, 5 and 6%, for the x, y and z dimensions respectively. Initially it was assumed that RND type movements would cover the complete range of motion of the upper extremity, and thus would deliver a generally trained NN, for ‘any’ type of motion. However, the combination of ADL and RND type movements as training dataset for the network did not improve performance in predicting joint reaction forces for ADL type movements, raising the SEM_rel to

10, 7 and 7%. When using only RND type movements as training data, the performance of NN in predicting joint reaction forces for ADL type movements decreased further to SEM_rel values of respectively 19, 14 and 12%. On the contrary, when predicting joint reaction forces for RND type movements using RND, or a combination of RND and ADL type movements as training data sets for the NN, SEM_rel values ranged between 6% to 11%, strengthening the notion that NN should be trained with task specific data.

NN predictions for ADL type movements performed with higher weights than those used for the training of the NN resulted in SEM_rel values ranging from 4 to 9% for ADL type motion, and 4% to 11% for RND type motion. These results indicate that even in extrapolation, the Neural Network approach remains consistent in its predictive power.

Results from the second stage, in which segment kinematics and just one single channel of EMG served as input for the NN, show similar results as stage one, where 13 channels of EMG were used. These results show the potential of the NN approach with an appealing simplicity in equipment needed: The ambulatory measurement of shoulder joint reaction forces, with one sensor per segment, and only one channel of EMG.

Kinematics, 13 channels EMG												
Training	Simulation ADL			Simulation ADL			Simulation RND			Simulation RND		
	Light Weights			Heavy Weights			Light Weights			Heavy Weights		
ADL	X	Y	Z	X	Y	Z	X	Y	Z	X	Y	Z
ICC	0,91	0,97	0,97	0,86	0,96	0,93						
SEM_rel	11	5	6	8	4	6						
ADL&RND												
ICC	0,93	0,95	0,95	0,85	0,94	0,94	0,93	0,94	0,96	0,89	0,91	0,88
SEM_rel	10	7	7	9	5	7	8	6	6	7	5	9
RND												
ICC	0,83	0,86	0,91				0,91	0,93	0,94	0,90	0,92	0,86
SEM_rel	19	14	12				11	7	7	7	4	9
Kinematics, 1 channel EMG												
Training	Simulation ADL			Simulation ADL			Simulation RND			Simulation RND		
	Light Weights			Heavy Weights			Light Weights			Heavy Weights		
ADL	X	Y	Z	X	Y	Z	X	Y	Z	X	Y	Z
ICC	0,88	0,98	0,95	0,88	0,95	0,93						
SEM_rel	13	4	7	7	5	6						
ADL&RND												
ICC	0,94	0,98	0,96	0,88	0,95	0,95	0,92	0,94	0,93	0,86	0,94	0,84
SEM_rel	9	3	6	7	5	6	10	6	7	8	4	10
RND												
ICC	0,84	0,88	0,90				0,90	0,96	0,95	0,89	0,93	0,88
SEM_rel	21	13	13				11	5	7	7	4	9

Table 2, Results of simulation with a trained NN in predicting JRF-GH, Relative SEM (3D average) for the several conditions tested. Each cell contains Relative SEM values of the best performing NN of 10 individually trained. Left column depicts which set of EMG (13 channels, or just one), and what type of motion trials were used for NN training; ADL type, ADL and RND, or only RND. Each row depicts what type of motion trial was simulated (ADL type, or RND), with a low (interpolation) or heavy weight (extrapolation). Simulation took place with measurement trials not used in the training of the NN.

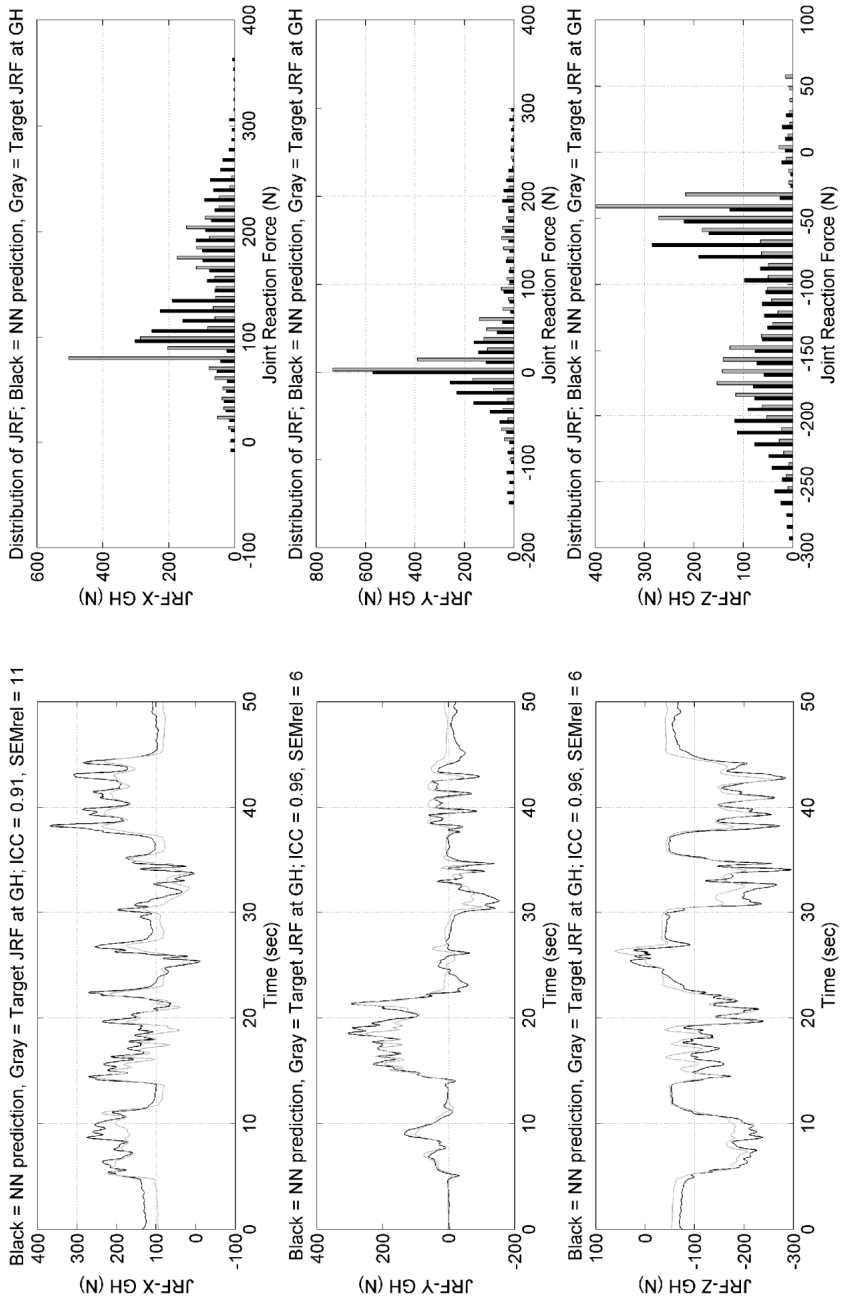


Figure 3A

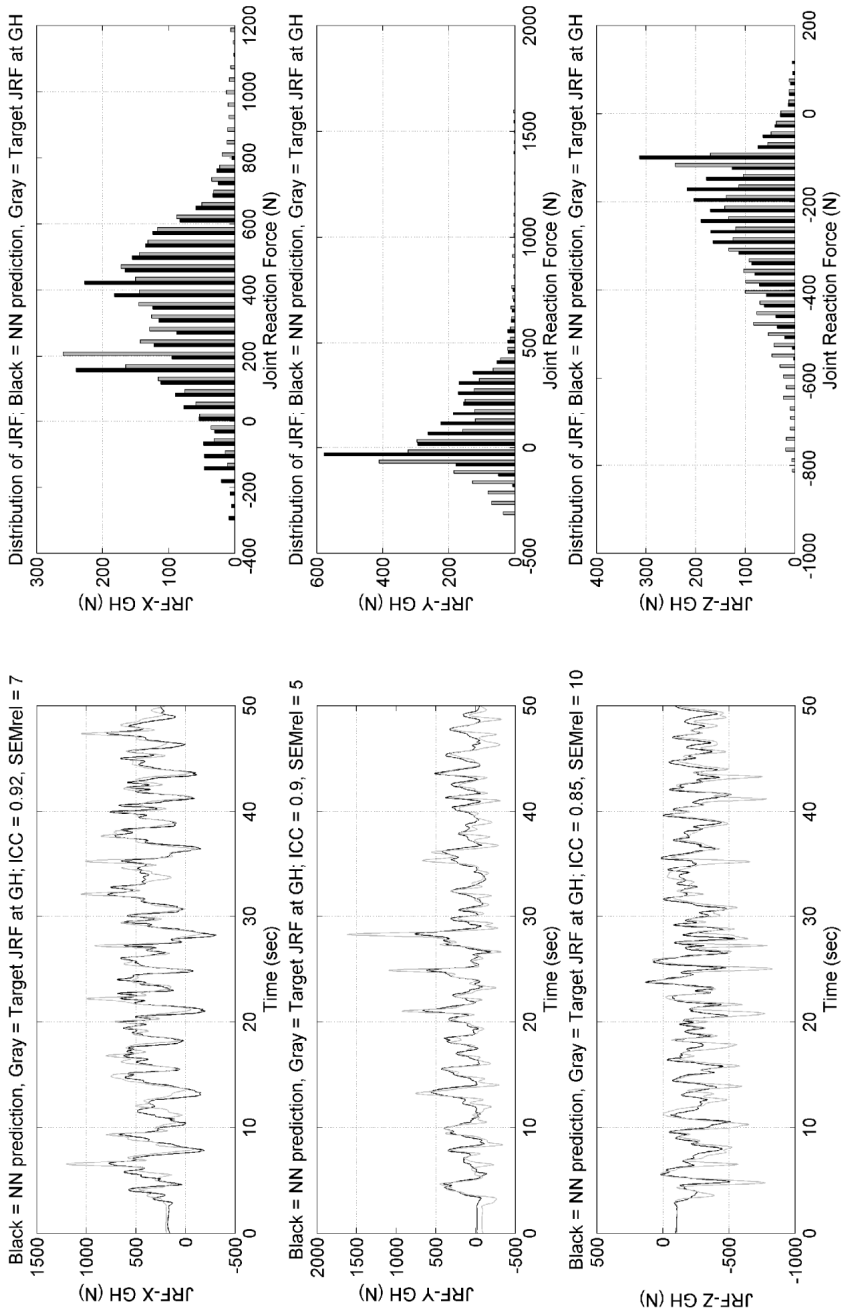


Figure 3B

Figures 3 depict time series, and distributions of glenohumeral joint reaction forces, from both NN predictions (black lines) and the musculoskeletal model (gray lines), the latter being the reference signal. Figure 3A shows results from a NN with kinematics, sensor data and 13 channels of EMG as input, trained on ADL type movement, predicting Low Weight ADL type movement. Figure 3B shows results from a NN with kinematics, sensor data and only one channel of EMG as input, trained on RND type movement, predicting a Heavy Weight RND type movement.

Figure 3A shows data of a NN, trained with ADL type movements, and simulating an independent ADL type movement while holding a light weight (0.2 kg) in the hand. Movements performed were brushing teeth, combing hair, perineal care, washing axils and eating (bringing hand to mouth). NN prediction overshoot can be observed at the peaks in the references signal, and a certain offset for some parts of the trial. In figure 3B, showing results for NN trained with kinematics and one channel of EMG, predicting joint reaction forces for Heavy Weight trials of RND movement, deviations can be observed at the peaks in the signal, where NN do predict lower values than the joint reaction force as calculated by the musculoskeletal model. However, the distribution of the joint reaction force over time, as predicted with the neural network method, shows good correspondence with the reference signal, and allows for an initial estimation of shoulder joint loading over time.

Discussion

The intention of the current experiment was to evaluate the neural network approach as a reliable and practical method, to enable a reasonable long-term estimation of joint reaction forces in daily conditions using ambulatory obtained data. A practical method should have an appealing simplicity concerning the amount of equipment used and preparation time needed. Aiming at such simplicity, neural networks were trained for several conditions. Two types of movements were used, mimicking Activities of Daily Living, and Random Movements. Furthermore two groups of input parameters were examined;

kinematics and 13 channels of EMG; kinematics and one channel of relevant EMG. NN predictions of glenohumeral joint reaction forces were referenced against a musculoskeletal model. Although there is room for improvement, results were promising and relevant influences to the predictive power of the method have been identified. Current results do at least allow for a modest application of the described neural network method in this estimation.

Figure 3A indicates the performance for conditions where neural networks were trained using ADL type kinematics and full EMG as input, predicting ADL type movements with a light load. Almost same results were obtained for the Heavy Weight condition. When trials with RND type movement were added to the training data set, predictive power decreased a little. When using only RND type movement in training, and predicting ADL type movement, predictive power decreased further, as can be noticed from table 2. This was unexpected, since it was initially assumed that the addition of more variation to the training data set of the NN should result in a 'better' prediction of the NN. This suggests that training data for the NN should be focused to the type of movement of interest. This can be seen as a drawback for the general applicability of the method. On the other hand, taking this phenomenon into account might improve the predictive power of the method when examining more specific movements.

The use of 13 channels of upper extremity EMG is not a convenient setup for ambulatory measurements. For the sake of a practical setup stage 2, with only one channel of EMG, was introduced and examined. The fact that results from stage 2 simulations corresponded well with results from Stage 1, this suggests that this setup is favorable for ambulatory measurements.

No preprocessing of data took place to enhance uniformity. Movements at the extremes of the range of segment motion (ROM) were potentially less represented in the data sets used, thereby of less influence in the training process of the NN. This might account for the effect of the under- and overestimation of the neural networks prediction seen at the peaks of joint reaction forces. More sophisticated modeling of EMG signals into a measure of external force might also contribute to a better prediction at peak forces. Both topics, data preprocessing and EMG force modeling, deserve to be examined in future research.

Glenohumeral joint reaction force as estimated by the musculoskeletal model was used as target signal in the training of NN, and as reference for comparison. Model estimations of muscle activity have been qualitatively validated against EMG patterns [(van der Helm, 1994b);(van der Helm, 1994a)]; estimations of glenohumeral joint reaction force have been quantitatively validated recently against in vivo measured joint reaction forces [(Nikooyan et al., 2010)]. For dynamic tasks up to 90° of humeral elevation values were comparable, although peak forces were underestimated by the model; for higher angles a deviation in force direction was observed, and for force exerting tasks an underestimation of the models JRF was found. Possibly this behavior of the musculoskeletal model results in an inconsistent training set, thereby disturbing the learning process of the NN method, resulting in the observed differences. Potentially the application of a NN method to in vivo measured JRF might show better correspondence, thereby expanding opportunities in obtaining a general load profile of the shoulder.

When applying the neural network method to obtain shoulder joint loading in patients, several topics deserve special attention. First of all, the used musculoskeletal model should be adapted to mimic the subjects abilities, for

instance, if present, rotator cuff tears should be simulated in the model as well. Secondly, if any pathological adaptation is present in upper extremity muscle activity, a redundant number of channels of EMG as input for the neural network should be considered. And thirdly, the type of motion used for training neural networks should be within the subjects ability.

From a mechanical point of view, joint reaction force is suspected to be related with joint damage. Although the glenohumeral joint reaction force, as a single resultant of all forces acting upon the joint, is a natural candidate for the indication of joint loading over time, the prediction of other variables like net moments can have meaning in the assembly of a load profile of the shoulder. However, theoretically, a zero net moment can occur while compressive forces are high, adding uncertainty to the predictive value of net moments as indicator for joint load. To obtain a complete load profile, at least joint reaction forces should be measured, and additionally other measures of joint load like net moments.

To enable the discrimination between the damaging effects of peak forces versus sustained duration of raised levels of JRF, for a broad range of movements as encountered in daily conditions, both levels should be estimated for a longer period of time. Current results do at least allow for a initial application of the described NN method in this estimation.

Conclusions

Shoulder joint loading in terms of JRF-GH can be estimated by a NN trained on ambulatory obtainable variables like srEMG and IMU's data of the upper extremity. The dataset should comprise sufficient "task specific" training trials. A convenient setup with IMU's on upper extremity segments and only one channel

of relevant EMG showed comparable results to a setup with IMU's and 13 channels of EMG.

Acknowledgements

This research project is conducted within the “Freemotion Consortium”, and “Fusion Consortium”, which are both granted by Senter (a delegate of the Dutch Ministry of Economic Affairs). Senter had no involvement in the study design, collection or the decision to submit this manuscript for publication.

6

General Discussion

General Discussion

This thesis describes a method with which a mechanical load profile of the human shoulder can be obtained in daily conditions, using ambulatory measurable variables like 3D kinematics, and surface EMG of relevant muscles of the upper extremity. With these variables a neural network can be trained to estimate net moments which can serve as input for a detailed musculoskeletal model. Another option is to train neural networks to predict joint reaction forces directly.

Results described in Chapter 4 show that neural networks could be trained to predict net moments around the glenohumeral joint. These net moments were subsequently used as input for a detailed musculoskeletal model, to compute full model output including individual muscle length and force, joint reaction force, and many other variables. When joint reaction force at the Sterno-Clavicular, Acromio-Clavicular, Gleno-Humeral and Humero-Ulnar joints, as estimated with the combination of neural network and musculoskeletal model were compared to corresponding output from the reference method (the laboratory based musculoskeletal model, using kinematics and external force) differences of 7% to 17% relative RMS were observed. When comparing the direct prediction of joint reaction force by neural networks to corresponding output from the reference (a laboratory based musculoskeletal model), differences of less than 10% relative Standard Error of Measurement were observed (Chapter 5).

Intra Class Correlation (ICC) between prediction and corresponding output by the DSEM (joint reaction force) were calculated. From these ICC's, the Standard Error of Measurement (SEM) was derived following (Weir, 2005; Weir, 2005). To compare test conditions with different external loads, SEM values were expressed as a percentage of the range of the signal (relative SEM).

Although the two distinct approaches (1: neural network prediction of net moments subsequently used as input for a musculoskeletal model and 2: direct prediction of joint reaction forces by neural networks) were not directly compared to each other, both approaches show promising results and enable the estimation of a load profile of the human shoulder in daily conditions. Further research with a larger group of subjects is advised to clarify which approach is more accurate and reliable. For now it can be stated that the first approach (using the neural network prediction of net moments as input for a musculoskeletal model) is more prone to error. When neural network predictions deviate from “true net moments” these deviations can have an enlarged effect by the calculations and optimization of the musculoskeletal model. In some occasions the neural network produced input which was incompatible with the musculoskeletal model, which couldn’t find a solution in it’s optimization. Besides that, using a musculoskeletal model can be very time consuming when processing large datasets. When for a given research questions the estimation of a single variable like joint reaction force is sufficient, the direct prediction of such a variable with a neural network has its advantages in terms of processing capacity and time needed.

In short the method works as follows:

Equipment used:

1. A subject is equipped with inertial sensors (Inertial Magnetic Measurement Systems, IMU’s) and EMG of shoulder and upper extremity muscles.

Sensor to segment calibration:

2. Sensor to segment calibration is performed by the execution of a set of well defined single axis movements by the subject, to measure the functional axes of movement of the upper extremity segments.

3. These functional axes of movement are used to define frames of reference for the segments of the upper extremity, and when related to sensor orientation, deliver segmental 3D kinematics over time.

Generating training data for the Neural Network

4. The subject is asked to perform another series of well defined movements, while holding a variety of known masses in the hand.
5. Upper extremity EMG is measured simultaneously.
6. For this relatively small set of movements, measured acceleration of the hand multiplied by the known masses in the hand deliver external force.
7. Upper extremity kinematics and calculated external force are used as input for a detailed musculoskeletal model, which
 - a. calculates net moments around the various joints of the shoulder
 - b. estimates joint reaction forces at the glenohumeral joint.
8. Using upper extremity kinematics and EMG as input and one of the described outputs from the musculoskeletal model as target, a neural network can be trained to predict:
 - a. net moments which can be used as input for the musculoskeletal model;
 - b. joint reaction forces directly.

When the neural network is trained adequately,

9. Only ambulatory measurements of kinematics and EMG are needed to:
 - a. predict net moments that can be used as input for the musculoskeletal model, to calculate full model output;
 - b. estimate joint reaction forces directly with the neural network.
10. Long term measurement of 3D kinematics and EMG in daily conditions can then be converted into a mechanical load profile of the shoulder.

Described as such, the method appears to be straightforward and easy to apply. However, several assumptions were made which require further articulation, to explicate the scope of the method.

As one of the required inputs for the described method, upper extremity kinematics can be measured ambulatory for longer duration by means of Inertial Magnetic Measurement Systems (IMU's). IMU's use three types of sensors and a dedicated algorithm to estimate sensor orientation in 3 dimensions.

Accelerometers measure sensor acceleration including gravity, gyroscopes measure the sensor's angular velocity, and magnetometers the earth magnetic field vector, all in three dimensions. A Kalman filter (Roetenberg et al., 2005) fuses the IMU's signals into a sensor orientation, correcting for specific characteristics like signal noise or sensor drift, under the assumptions of zero acceleration when averaged over 10 seconds (apart from gravity) and a homogenous earth magnetic field.

However, the orientation of the earth magnetic field vector can be altered by the presence of ferro-containing materials. Due to the widespread use of such material (constructive steel in buildings, furniture etc.), the "in-door" earth magnetic field is usually far from homogenous, which can be observed in measurement data by a changed norm of the vector. Despite considerable effort in the development of algorithms that estimate sensor orientation while correcting for any distortion in the earth magnetic field (Roetenberg et al., 2005), in long term measurements distortion of the earth magnetic field can and will have its disorienting effects. It is advised that for every experiment the measurement volume is verified to be within operation limits; a detailed method to define these operations limits in terms of measurement volume and time is described in chapter 2. If such is not possible, operation limits in terms of exposure time to distorted magnetic field should be obtained for the setup used, and long term measurements should be screened for exceeding values of the magnetic norm. Portions of the

measurements with exceeding values of the magnetic norm, for longer duration than these temporal limits should be labeled as suspect, and not be used for analysis. It is upon the decision of the experimenters to decide if the resulting loss of measurement data is acceptable. In extreme conditions, when upon experimenters decision, a too large part of the complete measurement is beyond described limits, it is advised to find another measurement volume to perform the measurements, or use an alternative measurement method like video based motion capture.

When measurement assumptions for IMU's measurements are met, they deliver sensor orientation in three dimensions. However, the required input for biomechanical analysis is the orientation of body segments, or joint kinematics. As part of a practically applicable method, the calibration procedure from sensor to body segment should be repeatable, deliver functionally interpretable local reference frames for the segments, and preferably correspond to the reference frames as used in standard methods. Besides that, the sensor to segment calibration should preferably be conducted ambulatory, independent of laboratory based equipment. Chapter 3 described a detailed method in obtaining these functional interpretable local frames of reference for the upper extremity and thorax. The method appeared to be highly repeatable, enabling ambulatory calibration. A dissimilar orientation of reference frames was obtained for humerus, forearm and hand, when compared to standard methods following ISB recommendations (Wu et al., 2005). This is due to the fact that following the ISB framework Bony Landmarks (BLM) are used to define anatomical frames of reference, which concurrently are used to describe segment kinematics. The axes of such BLM based anatomical frames of reference are often not fully aligned with the actual joint axes. When using these segment frames of reference for the description of joint kinematics, so-called kinematic crosstalk can be observed.

This is a matter of interpretation. Describing segment kinematics is a distinct goal from describing joint kinematics and the use of functional axes of movement is more appropriate in the latter. When using functional axes to build up a local reference frame, one of the joint axis is used in the definition of the local reference frame, which will minimize the so-called kinematics crosstalk. For the local reference frame of the hand this distinction and its effects on obtained kinematics are described in full detail in (de Monsabert et al., 2014). For a more general approach Kontaxis et al (Kontaxis et al., 2009) proposed a framework for the definition of standardized protocols for measuring upper extremity kinematics, in which a clear distinction is made between anatomical frames of reference and segment kinematics versus functional frames of reference and joint kinematics. It is expected that, by following the proposal of Kontaxis et al. in future research, a reduction in kinematic crosstalk can be achieved. Less kinematic crosstalk will lead to more congruency in measurement data, as muscle activity measured as EMG and the resulting joint kinematics will show more coherence. More congruency in the input data for the neural networks method is likely to improve its performance.

For the experiments conducted to build up this thesis the Delft Shoulder and Elbow Model (DSEM) was used as reference (van der Helm, 1994b; Nikooyan et al., 2010). This model is based on extensive and detailed measurements of one cadaver and, using kinematics and external force as input, describes the musculoskeletal response of the shoulder and upper extremity mathematically. It is a geometrical rigid body model, representing all relevant bones and joints. The 31 muscles crossing the various joints are divided in 139 muscle elements, from which fiber attachment sides, fiber course, wrapping surfaces and via points were measured; estimates of physiological parameters like force-length relation and optimal fiber length were also included in the model. The model balances the

measured joint moments by optimizing the load sharing of muscles using an energy based cost-function, while preserving a stability constraint; the joint reaction force should point into the scapular glenoid surface, to avoid shoulder luxation. With a model like this, individual muscle force contributions, and the resulting joint reaction forces can be estimated. Originally it was intended as a general model, and in the experiments of this thesis used as such. When using a general model, it should be kept in mind that a possible mismatch exists in morphology between model and the subject that is analyzed, which can lead to under- or overestimations of parameters of interest. Although several other musculoskeletal models have been developed, focusing on minimizing this potential mismatch, little evidence was found of their superiority over current models (Bolsterlee et al., 2013). This justifies the use of a general model for now, in this phase of exploring the potential use of a neural network method in the ambulatory assessment of shoulder joint load.

When the more complex, individualized models prove to deliver more accurate estimations of joint load, it is expected that more consistent input data is likely to improve neural network performance in predicting joint load.

Neural networks as a computational technique is one of the instruments used in this work, but it's fundamental working mechanisms have not been explained in detail. For a general introduction, and an overview of current applications of neural networks in the area of clinical biomechanics see (Schollhorn, 2004). To obtain sufficient information for the neural network to learn the desired relation, the type of inputs used for a neural network should cover the variables of influence on the target variable. For instance, when predicting joint reaction forces at the gleno-humeral joint, inputs used should comprise kinematics like posture, but also segment dynamics like angular velocity, or acceleration, and muscle activity. Expansion of the types of input used, increases the number of

inputs for the neural network, which amplify the number of connections between layers of the network, which in turn will slow down the training rate of the neural networks rapidly. The expansion to more variables to be measured and used as inputs for the training of the networks will also increase measurement complexity. For a practical applicable method this is not desirable. As shown in chapter 5, neural networks using only one channel of relevant EMG were performing as good as networks using 13 channels of EMG, but both conditions performed better than conditions without EMG used as input. This might illustrate the added value of EMG and simultaneously the unneeded redundancy of multiple channels of EMG. This phenomenon also raises further questions to be answered. Perhaps the multiple channels of EMG delivered too complex information to be handled by the relative simple neural network architecture used? Or are the features extracted from the EMG (smooth rectified EMG resembling an envelope shape close to muscle force output according to (Olney and Winter, 1985)) not accurate enough in terms of electromechanical delay? A further structured analysis of neural network architectures, types of input used, and effects of pre-processing and feature extracting might result in a more optimal configuration for the neural networks used in this approach, resulting in even better predictions of mechanical loading than obtained with the relative simple setup as described in this thesis. On the other hand, when starting with a simple setup, and neural network performance does not satisfy, the addition of an extra type of input might increase network performance.

As stated in the description of the method, upper extremity kinematics and EMG serve as inputs for a neural network, which is trained to predict net moments or joint reaction forces, using the corresponding output from the musculoskeletal model as target. When trained adequately, these net moments or joint reaction forces can be estimated by the neural network using only the ambulatory

measurements of kinematics and EMG. The following aspect of working with neural networks deserves special attention: A neural network is initialized by assigning random weights to the connections between input and output layers. By means of a back propagation algorithm, the relation between input and target is learned from examples, the training data set, and stored across the networks weights. Since the initialization of networks contains a random factor, multiple networks individual trained on the same dataset, can show different performance in prediction of the desired output. The neural network training can be trapped in a so called local minimum, and no further improvement will be achieved.

Although several training methods exist in the avoidance of local minima, and were applied in the analysis, when training only one network for a specific condition, the mentioned uncertainty remains. To overcome this uncertainty, it is advised to train several networks for a certain condition, validate with an independent data set, and choose the best performing neural network. This advice prompts three important questions; 1) how many individual networks should be trained, 2) how to validate a trained neural network, and 3) how to choose the best performing network.

To answer these questions a pilot experiment (not published) was conducted for the neural network configuration and dataset of the experiments described in chapter 5. For a given condition, 100 neural networks were individually initialized and trained. Every trained neural network was simulated with the same, independent dataset, not used in training. Predictions of these 100 simulations were compared to corresponding output of the musculoskeletal model, in terms of relative standard error of measurement (SEM related to the amplitude of the signal, relative SEM).

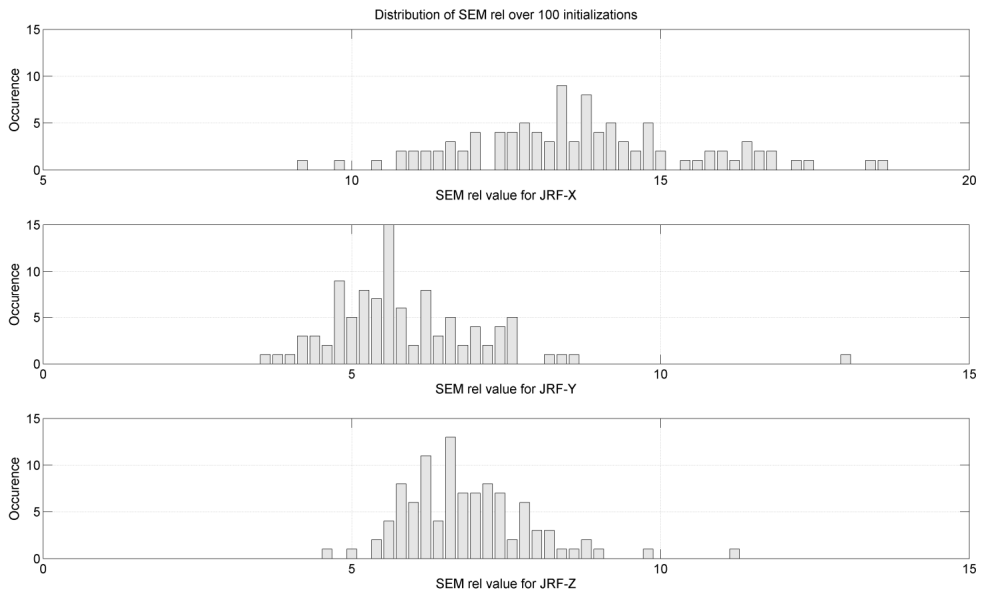


Figure 1, Distribution of SEM rel for 100 individually initialized and trained neural networks; all networks trained on the same training data set; all networks simulated the same independent validation data set, not used in the training of the networks. This figure shows the variable effect of random weight assignment in the initialization of neural networks, on the performance of networks when compared with the reference method.

From these 100 individual trained networks, the 10 best performing neural networks (the first ten neural networks with the lowest relative SEM) showed relative SEM values of less than 12% for the joint reaction force in X-direction, less than 5% in Y-direction, and less than 6% in Z-direction.

From these results it was deduced that when 100 individually trained networks result in 10 networks performing adequately (relative SEM less than 12%), a minimum of 10 individually trained neural networks will result in at least one network performing adequately, for the given configuration. For different architectures, configurations or inputs used, the described procedure should be repeated to reveal the minimum number of networks to be initialized and trained.

Doing so will give more guarantee to find the ‘best performing network’ with a minimum relative SEM when validated against the reference.

Based on the results described in chapter 5, the type of motions used for training the neural networks should encompass the type of motion for which joint reaction forces are to be predicted. When considering the performance of neural networks trained on “Random type Movement” while simulating Activities of Daily Life, this performance was less accurate than neural networks which were trained on a combination of “Random Type Movements” and “ADL type movements”. Best performance for the simulation of ADL type movements was found when neural networks were trained on ADL type movements only. This last condition recognizes a drawback when applied to long term measurements in daily conditions. When in long term measurements the variety in types of motion is larger than in the subset used as training data for the neural networks, prediction might become less accurate.

However, a training set for the neural networks consisting of a general set of movements from which ‘any’ type of motion can be predicted has not been found. It can be stated that the generalization of the neural network predictions is limited to the scope of the tasks trained. This means that the data set used for the training of the neural network should be customized to the specific situation of interest, which is in fact a limitation of the method. Some a-priori knowledge is needed of the daily conditions in which measurements will take place. This enables the proper customization and formation of the training data sets. This hampers a general application of the neural network method. A theoretical option is to execute the measurements in daily conditions first. Concurrently the most common movements performed can be extracted from the measured dataset. When the subject performs these extracted stereotype movements in a ‘last

measurement trial', this data can be used as training set for the neural network. Future research should point out if this approach is feasible.

In contrast to the use of a detailed musculoskeletal model, when using a neural network to predict a single variable like joint reaction forces at the gleno-humeral joint, neither other details of joint load can be examined, nor can the working mechanism of joint loading like muscle activation easily be recovered from neural network connection weights.

To enable the application of a detailed musculoskeletal model to ambulatory measurements in daily conditions the experiment described in Chapter 4 was conducted. A neural network was trained to predict net moments around the glenohumeral joint, which was then used as input for the aforementioned musculoskeletal model, to estimate full model output, like individual muscle force contributions and joint reaction forces. Although results were quite satisfactory, the 'processing chain' is growing longer and longer, including more assumptions along its way, and differences between standard method and the newly developed method are even more difficult to deduce.

Besides that, the initial advantage of a computational fast method like neural networks is counteracted by the computational heavy optimization of the musculoskeletal model, when larger datasets are to be processed. It might be an interesting option to train neural networks to predict multiple relevant variables of joint load directly, or train several distinct neural networks for those distinct variables, instead of forcing such a relatively unknown method to estimate all potentially relevant variables in one processing chain.

The variable used as indicator for the mechanical loading of the gleno-humeral joint is joint reaction force at the humeral head, which is the mathematical resultant of all forces acting on that joint. It comprises external force, active and

passive muscle forces, ligament forces constraining the joint excursions and stabilizing forces from rotator cuff muscles. Therefore it is a natural single variable to describe the mechanical loading of the joint over time. Other mechanical variables like net moments around a joint are easier to obtain and, as (Praagman et al., 2000) showed, do correlate quite well with joint reaction forces, for healthy subjects and static postures. However, (Nikooyan et al., 2010) showed that joint reaction forces at the glenohumeral joint, as measured with an instrumented shoulder endoprostheses, varied significantly between patients for a standard movement like humeral abduction. Such a difference couldn't be seen in net moments around the glenohumeral joint. When considering the option of co-contraction, or the activation of the rotator cuff muscles during weight relief lifting, the different effect on net moments and joint reaction force becomes even more clear; while for net moments that are about the same, joint reaction forces (including the sum of all muscle force delivered) can vary with the level of co-contraction. Another phenomena can be seen in spinal cord injury patients. Depending on lesion level different muscle groups are available for the execution of weight relief lifting. A simulation study from (van Drongelen et al., 2011) showed a difference in joint reaction force of 7% depending on lesion level, although statistically not significant in the cited experiment. But a different effect exists on net moments and joint reaction forces; when mechanical loading of joints is the topic of interest, joint reaction forces are the key variables to be obtained.

The subjects invited for the experiments building up this thesis were healthy subjects. When the method is to be applied to estimate the joint loading of patients, several adaptations are needed. The musculoskeletal model used for calculation of net moments or joint reaction force (which serve as target for the training of the neural networks) should be adapted to mimic the patient

characteristics in terms of available muscle groups (for SCI patients, depending on lesion level), or amount of available muscle force in the case of rotator cuff tears (Steenbrink et al., 2009; van Drongelen et al., 2013; Parsons et al., 2002). Since the effect of such adaptations to a musculoskeletal model have not been examined in current research, it is advised to repeat the protocols described in chapter 4 and 5 on such adapted models to verify if the neural network approach is still accurate and valid for those altered conditions.

Integrating the findings of the preceding chapters the method has proven to be a useful tool in the estimation of long term joint loading of the shoulder, in daily conditions. The observed differences of 10 % relative SEM or less, when compared to a laboratory based reference method, allow for further implementation of the method. When applied to larger groups of subjects, the collected joint load profiles can be used to gain more insight into the mechanical loading of the shoulder joints in daily conditions, and potentially be connected to the development of joint wear, or the gradual degradation of the shoulder and shoulder endoprostheses over time. The method is applicable to ambulatory settings, outside the laboratory, considering the required variables to be measured, the equipment to be used, as well as the required initial measurements to be performed to collect training data for the neural networks. For the current setup, the needed equipment is minimal, four IMU's and one channel of EMG, and a suitable data logger for these signals, although further research is advised to find an optimal configuration for the neural networks approach in terms of neural network architecture, and type and number of inputs needed for optimal predictive power. Initial measurements consist of sensor to segment calibration movements which can be performed in several minutes. The training data set for the neural networks can be collected within 10 minutes, the only extra's needed are a variety of known weights that can be held in the hand. The calculation of joint reaction

forces by the musculoskeletal model, which serve as target for the training of the neural networks, is the slowest part of the procedure, and can take several hours. However, smart distribution of this task over several computers seriously speeds up calculation. The training of neural networks can be accomplished in a couple of hours on a standard PC.

Finally, using ambulatory measurements of kinematics and EMG as input, the simulations and predictions of joint reaction forces by the neural networks, as described in chapter 5, were completed at 15000 samples per second. This means that for instance measurements at 50Hz with a duration of 5 hours (about the battery life of the used IMU's system) can be simulated by the neural network in one minute, demonstrating the high computational performance of trained neural networks. For long term measurements the approach in which joint reaction force are predicted directly by neural networks could serve as a first stage in selecting relevant time frames with high joint load. These selected timeframes can subsequently be analysed in much more detail by applying the approach in which neural networks predict net moments as input for the musculoskeletal model, to calculate full model output.

When comparing the described neural network approach to other means of estimating shoulder joint load in daily conditions, two distinct candidate methods show up; EMG driven models (Langenderfer et al., 2005; Laursen et al., 1998; Nikooyan et al., 2012), and the direct measurement of shoulder joint reaction forces by means of instrumented shoulder joint prostheses (Bergmann et al., 2007; Westerhoff et al., 2009a; Westerhoff et al., 2009b).

Since EMG driven models make use of the same sources of input as the neural network method, namely kinematics and EMG, at first sight they seem capable of estimating joint load in daily conditions. EMG driven models have the advantage of incorporating muscle co-contraction, a feature that most optimization-based

inverse-dynamics musculoskeletal models neglect, or which requires more advanced load sharing cost functions (Nikooyan et al., 2012). Keeping the concept of muscle co-contraction in mind, EMG driven models are developed with the aim of a better prediction of actual joint reaction forces, using the actual muscle activations as guidance for the optimization of the cost function. Also EMG driven models still require external force as input, which cannot be measured in daily conditions, or only with great difficulty, rendering the EMG driven models to a less suitable candidate for the long term estimation of joint loading in daily conditions.

Instrumented shoulder endo-prosthesis are a relatively new kind of measurement devices in the field of shoulder joint load. The actual joint forces and moments are measured within the body, which can aid to serious progress in gaining more insight in “true joint load” during motion. However, this is the case in subjects wearing such a device, people who’s shoulder joint is damaged due to severe wear or degeneration, and where joint replacement using an endo-prosthesis is indicated. It is unknown whether these subjects had different joint loading patterns leading to such a degeneration that joint replacement was advised, nor if the joint loading patterns after surgery are comparable to healthy subjects. Besides that, for larger studies, up till now the population of subjects with an instrumented endo-prosthesis is quite limited (6 former osteoarthritis patients).

Resume

When resuming the above, the answer is yes; the attractive idea of measuring the musculoskeletal response with wearable equipment like IMU’s and EMG for longer duration, in daily conditions and predicting a complex variable like joint reaction force, is possible with the developed method, within certain constraints. With such a method, the collection of a long-term joint load profile comes closer

at hand. By determining a load-profile over time, over subjects, more insight can be gained in the nature, magnitude and variation of the forces acting on the joints of the shoulder girdle, and possibly shed more light on the damaging effects of these forces. Increased insight in the ‘play of forces’ around the shoulder can also aid in the development of future endo-prostheses; such prostheses can than be designed to better withstand the forces they will be exposed to in the body, in daily conditions.

Future directions

Although successful, several future directions can be given which are expected to improve the predictive power of the neural network method. As a first step the procedure should incorporate an individualized musculoskeletal model, to ensure, from a biomechanical perspective, that the model output will be more coherent with signals measured from the subject. For instance, net moments around the shoulder as calculated by the model are directly influenced by segments length used. Also muscle properties like attachment sites (Bolsterlee and Zadpoor, 2013), and moment arms might result in deviating results for muscle activation in the optimization procedures used in the model, when subject characteristics are different from the geometry as used by the model. The measured musculoskeletal response is prone to be less coherent with the resulting estimated joint reaction force of the model if there is a mismatch between model and subject geometry. From that point of view an evident improvement can be expected with the use of individualized musculoskeletal models. However, individualization of musculoskeletal models isn’t as straightforward as it might seem, since “*only subsets of the parameters that describe model geometry and musculotendon properties can be obtained in vivo. Because most parameters are somehow interrelated the others should be scaled to prevent inconsistencies in the model’s*

structure, but it is not known exactly how.” (Literally cited from (Bolsterlee et al., 2013)).

Besides that, it is expected that the parameters needed for individualization of such a model cannot be collected ambulatory, rendering the procedure more complex and time consuming. Future research will prove if individualization of the model has added value in the estimation of joint load profile in daily conditions.

As described above, in the version of the DSEM used in the experiments co-contraction was not incorporated. Joint reaction forces from this model are used as target for neural network training, and in fact the neural network is at best mimicking the musculoskeletal model used, and will therefore lack the effect of muscle co-contraction on joint reaction forces. This is illustrated by the fact that a neural network with only one channel of EMG as input performed as good as a network with 13 channels of EMG. When EMG driven models are used as target for neural network training, it is expected that the concept of co-contraction can be learned by the neural networks, and incorporated in the prediction of joint loading. Probably the number of EMG channels needed as input for the neural networks has to increase above one, to represent the different combinations of co-contraction that can occur in human upper extremity motion.

Can the method be applied to patients? As stated above, the neural network is at best mimicking the musculoskeletal model that is used as target for training. So if the musculoskeletal model is adequately adapted to represent the musculoskeletal response of the subject / patient, for instance by introducing the force reducing effect of rotator cuff tears, or tendon transfers into the model (Magermans et al., 2004), it is expected that the neural network can be trained using output from the

adapted model as target. Simulation studies can be performed to explore this potential, by using existing datasets, adapting the musculoskeletal model and train neural networks on this adapted output, to see if the method is capable of learning these altered relations between kinematics, EMG and joint reaction forces. If the results from such simulation studies are successful, the method can be applied to predict joint loading in daily conditions for patients as well.

Although the initial preparations for the ambulatory measurements are not time consuming and neural network simulations have proven to be faster than real time, the calculation of musculoskeletal model output, and the concurrent training of neural networks takes several hours of processing. As soon as, in the near future, these last two procedures can be performed in a much shorter time frame, due to the continuous increase of processing power of computers, smart parallel processing, or the development of faster optimization procedures for the musculoskeletal model and the neural network training, the neural network method as a whole can be used as a real time feedback instrument. The instantaneous prediction of joint loading can then be used to instruct subjects or patients how they load their joints, and potentially aid in the avoidance of overloading behavior.

References

(In Citation order)

1. Winters, J. C. et al, (2008). NHG-standaard schouderklachten. pp. 555-565.
2. van Andel, C. J., Wolterbeek, N., Doorenbosch, C. A. M., Veeger, D. H. E. J., Harlaar, J., (2008). Complete 3D kinematics of upper extremity functional tasks. *Gait & Posture* 27, 120-127.
3. van der Helm, F. C. T., (1994a). Analysis of the Kinematic and Dynamic Behavior of the Shoulder Mechanism. *Journal of Biomechanics* 27, 527-550.
4. Torchia, M. E., Cofield, R. H., Settegren, C. R., (1997). Total shoulder arthroplasty with the Neer prosthesis: Long-term results. *Journal of Shoulder and Elbow Surgery* 6, 495-505.
5. Westerhoff, P., Graichen, F., Bender, A., Halder, A., Beier, A., Rohlmann, A., Bergmann, G., (2009a). In vivo measurement of shoulder joint loads during activities of daily living. *Journal of Biomechanics* 42, 1840-1849.
6. Anglin, C., Wyss, U. P., Pichora, D. R., (2000). Glenohumeral contact forces. *Proceedings of the Institution of Mechanical Engineers Part H- Journal of Engineering in Medicine* 214, 637-644.
7. Magermans, D. J., Chadwick, E. K. J., Veeger, H. E. J., van der Helm, F. C. T., (2005). Requirements for upper extremity motions during activities of daily living. *Clinical Biomechanics* 20, 591-599.
8. van der Helm, F. C. T., (1994b). A Finite-Element Musculoskeletal Model of the Shoulder Mechanism. *Journal of Biomechanics* 27, 551-569.
9. Bolsterlee, B., Veeger, D. H. E. J., Chadwick, E. K., (2013). Clinical applications of musculoskeletal modelling for the shoulder and upper limb. *Medical & Biological Engineering & Computing* 51, 953-963.

10. Magermans, D. J., Chadwick, E. K. J., Veeger, H. E. J., Rozing, P. M., van der Helm, F. C. T., (2004). Effectiveness of tendon transfers for massive rotator cuff tears: a simulation study. *Clinical Biomechanics* 19, 116-122.
11. Roetenberg, D., Luinge, H. J., Baten, C. T. M., Veltink, P. H., (2005). Compensation of magnetic disturbances improves inertial and magnetic sensing of human body segment orientation. *Ieee Transactions on Neural Systems and Rehabilitation Engineering* 13, 395-405.
12. Cutti, A. G., Giovanardi, A., Rocchi, L., Davalli, A., Sacchetti, R., (2008). Ambulatory measurement of shoulder and elbow kinematics through inertial and magnetic sensors. *Medical & Biological Engineering & Computing* 46, 169-178.
13. van den Noort, J. C., Ferrari, A., Cutti, A. G., Becher, J. G., Harlaar, J., (2013). Gait analysis in children with cerebral palsy via inertial and magnetic sensors. *Medical & Biological Engineering & Computing* 51, 377-386.
14. Picerno, P., Cereatti, A., Cappozzo, A., (2008). Joint kinematics estimate using wearable inertial and magnetic sensing modules. *Gait & Posture* 28, 588-595.
15. Wu, G., van der Helm, F. C. T., Veeger, H. E. J., Makhsous, M., Van Roy, P., Anglin, C., Nagels, J., Karduna, A. R., McQuade, K., Wang, X. G., Werner, F. W., Buchholz, B., (2005). ISB recommendation on definitions of joint coordinate systems of various joints for the reporting of human joint motion - Part II: shoulder, elbow, wrist and hand. *Journal of Biomechanics* 38, 981-992.
16. Luinge, H. J., Veltink, P. H., Baten, C. T. M., (2007). Ambulatory measurement of arm orientation. *Journal of Biomechanics* 40, 78-85.
17. Ochia, R. S., Cavanagh, P. R., (2007). Reliability of surface EMG measurements over 12 hours. *Journal of Electromyography and Kinesiology* 17, 365-371.

18. Song, R., Tong, K. Y., (2005). Using recurrent artificial neural network model to estimate voluntary elbow torque in dynamic situations. *Medical & Biological Engineering & Computing* 43, 473-480.
19. Liu, M. M., Herzog, W., Savelberg, H. H. C. M., (1999). Dynamic muscle force predictions from EMG: an artificial neural network approach. *Journal of Electromyography and Kinesiology* 9, 391-400.
20. Schollhorn, W. I., (2004). Applications of artificial neural nets in clinical biomechanics. *Clinical Biomechanics* 19, 876-898.
21. Nyan, M. N., Tay, F. E. H., Tan, A. W. Y., Seah, K. H. W., (2006). Distinguishing fall activities from normal activities by angular rate characteristics and high-speed camera characterization. *Medical Engineering & Physics* 28, 842-849.
22. De Vries, S. I., Bakker, I., Hopman-Rock, M., Hirasing, R. A., Van Mechelen, W., (2006). Clinimetric review of motion sensors in children and adolescents. *Journal of Clinical Epidemiology* 59, 670-680.
23. Mokkink, L. B., Terwee, C. B., van Lummel, R. C., de Witte, S. J., Wetzels, L., Bouter, L. M., De Vet, H. C. W., (2005). Construct validity of the DynaPort (R) KneeTest: a comparison with observations of physical therapists. *Osteoarthritis and Cartilage* 13, 738-743.
24. Coley, B., Jolles, B. M., Farron, A., Bourgeois, A., Nussbaumer, F., Pichonnaz, C., Aminian, K., (2007). Outcome evaluation in shoulder surgery using 3D kinematics sensors. *Gait & Posture* 25, 523-532.
25. Zijlstra, W., Bisseling, R., (2004). Estimation of hip abduction moment based on body fixed sensors. *Clinical Biomechanics* 19, 819-827.
26. Bachmann, E. R., Xiaoping, Y., Peterson, C. W., (2004). An investigation of the effects of magnetic variations on inertial magnetic sensors. pp. 1115-1122.
27. Meskers, C. G. M., Fraterman, H., van der Helm, F. C. T., Vermeulen, H. M., Rozing, P. M., (1999). Calibration of the "Flock of Birds"

- electromagnetic tracking device and its application in shoulder motion studies. *Journal of Biomechanics* 32, 629-633.
28. Spoor, C. W., Veldpaus, F. E., (1980). Rigid Body Motion Calculated from Spatial Coordinates of Markers. *Journal of Biomechanics* 13, 391-393.
29. Brodie, M., Walmsley, A., Page, W., (2008). Fusion motion capture: Can technology be used to optimise alpine ski racing technique. pp. 825-831.
30. Coley, B., Jolles, B. M., Farron, A., Aminian, K., (2008). Arm position during daily activity. *Gait & Posture* 28, 581-587.
31. Janssen, W. G. M., Bussmann, J. B. J., Horemans, H. L. D., Stam, H. J., (2008). Validity of accelerometry in assessing the duration of the sit-to-stand movement. *Medical & Biological Engineering & Computing* 46, 879-887.
32. Cappozzo, A., Catani, F., Della Croce, U., Leardini, A., (1995). Position and Orientation In-Space of Bones During Movement - Anatomical Frame Definition and Determination. *Clinical Biomechanics* 10, 171-178.
33. Kontaxis, A., Cutti, A. G., Johnson, G. R., Veeger, H. E. J., (2009). A framework for the definition of standardized protocols for measuring upper-extremity kinematics. *Clinical Biomechanics* 24, 246-253.
34. de Vries, W. H. K., Veeger, H. E. J., Baten, C. T. M., van der Helm, F. C. T., (2009). Magnetic distortion in motion labs, implications for validating inertial magnetic sensors. *Gait & Posture* 29, 535-541.
35. Stokdijk, M., Biegstraaten, M., Ormel, W., de Boer, Y. A., Veeger, H. E. J., Rozing, P. M., (2000). Determining the optimal flexion-extension axis of the elbow in vivo - a study of interobserver and intraobserver reliability. *Journal of Biomechanics* 33, 1139-1145.
36. Tay, S. C., van Riet, R., Kazunari, T., Koff, M. F., Amrami, K. K., An, K. N., Berger, R. A., (2008). A method for in-vivo kinematic analysis of the forearm. *Journal of Biomechanics* 41, 56-62.

37. Cutti, A. G., Cappello, A., Davalli, A., (2006). In vivo validation of a new technique that compensates for soft tissue artefact in the upper-arm: Preliminary results. *Clinical Biomechanics* 21, S13-S19.
38. Ericson, A., Arndt, A., Stark, A., Wretenberg, P., Lundberg, A., (2003). Variation in the position and orientation of the elbow flexion axis. *Journal of Bone and Joint Surgery-British Volume* 85B, 538-544.
39. van Andel, C., van Hutten, K., Eversdijk, M., Veeger, D., Harlaar, J., (2009). Recording scapular motion using an acromion marker cluster. *Gait & Posture* 29, 123-128.
40. Karduna, A. R., McClure, P. W., Michener, L. A., Sennett, B., (2001). Dynamic measurements of three-dimensional scapular kinematics: A validation study. *Journal of Biomechanical Engineering-Transactions of the Asme* 123, 184-190.
41. de Groot, J. H., Brand, R., (2001). A three-dimensional regression model of the shoulder rhythm. *Clinical Biomechanics* 16, 735-743.
42. de Vries, W. H. K., Veeger, H. E. J., Cutti, A. G., Baten, C., van der Helm, F. C. T., (2010). Functionally interpretable local coordinate systems for the upper extremity using inertial & magnetic measurement systems. *Journal of Biomechanics* 43, 1983-1988.
43. Cheron, H., Leurs, F., Bengoetxea, A., Draye, J. P., Destree, M., Dan, B., (2003). A dynamic recurrent neural network for multiple muscles electromyographic mapping to elevation angles of the lower limb in human locomotion. *Journal of Neuroscience Methods* 129, 95-104.
44. Shirao, N. A., Reddy, N. P., Kosuri, D. R., (2009). Neural network committees for finger joint angle estimation from surface EMG signals. *Biomedical Engineering Online* 8.
45. Hahn, M. E., (2007). Feasibility of estimating isokinetic knee torque using a neural network model. *Journal of Biomechanics* 40, 1107-1114.

46. de Vries, W. H. K., Veeger, H. E. J., Baten, C. T. M., van der Helm, F. C. T., (2014). Can Shoulder joint reaction forces be estimated by Neural Networks ?
47. Hermens, H. H., Freriks, B., (1997). Seniam 5, The state of the art on sensors and sensor placement procedure for surface electromyography: a proposal for sensor placement procedure. Roessingh Research & Development, enschede.
48. Kingma, I., Baten, C. T. M., Dolan, P., Toussaint, H. M., van Dieen, J. H., de Looze, M. P., Adams, M. A., (2001). Lumbar loading during lifting: a comparative study of three measurement techniques. *Journal of Electromyography and Kinesiology* 11, 337-345.
49. Luh, J. J., Chang, G. C., Cheng, C. K., Lai, J. S., Kuo, E. S., (1999). Isokinetic elbow joint torques estimation from surface EMG and joint kinematic data: using an artificial neural network model. *Journal of Electromyography and Kinesiology* 9, 173-183.
50. Olney, S. J., Winter, D. A., (1985). Predictions of Knee and Ankle Moments of Force in Walking from Emg and Kinematic Data. *Journal of Biomechanics* 18, 9-20.
51. Weir, J. P., (2005). Quantifying test-retest reliability using the intraclass correlation coefficient and the SEM. *Journal of Strength and Conditioning Research* 19, 231-240.
52. Nikooyan, A. A., Veeger, H. E. J., Westerhoff, P., Graichen, F., Bergmann, G., van der Helm, F. C. T., (2010). Validation of the Delft Shoulder and Elbow Model using in-vivo glenohumeral joint contact forces. *Journal of Biomechanics* 43, 3007-3014.
53. de Monsabert, B. G., Visser, J. M. A., Vigouroux, L., van der Helm, F. C. T., Veeger, H. E. J., (2014). Comparison of three local frame definitions for the kinematic analysis of the fingers and the wrist. *Journal of Biomechanics* 47, 2590-2597.

54. Praagman, M., Stokdijk, M., Veeger, H. E. J., Visser, B., (2000). Predicting mechanical load of the glenohumeral joint, using net joint moments. *Clinical Biomechanics* 15, 315-321.
55. van Drongelen, S., van der Woude, L. H. V., Veeger, H. E. J., (2011). Load on the shoulder complex during wheelchair propulsion and weight relief lifting. *Clinical Biomechanics* 26, 452-457.
56. Steenbrink, F., de Groot, J. H., Veeger, H. E. J., van der Helm, F. C. T., Rozing, P. M., (2009). Glenohumeral stability in simulated rotator cuff tears. *Journal of Biomechanics* 42, 1740-1745.
57. van Drongelen, S., Schlüssel, M., Arnet, U., Veeger, D., (2013). The influence of simulated rotator cuff tears on the risk for impingement in handbike and handrim wheelchair propulsion. *Clinical Biomechanics* 28, 495-501.
58. Parsons, I. M., Apreleva, M., Fu, F. H., Woo, S. L. Y., (2002). The effect of rotator cuff tears on reaction forces at the glenohumeral joint. *Journal of Orthopaedic Research* 20, 439-446.
59. Langenderfer, J., LaScalza, S., Mell, A., Carpenter, J. E., Kuhn, J. E., Hughes, R. E., (2005). An EMG-driven model of the upper extremity and estimation of long head biceps force. *Computers in Biology and Medicine* 35, 25-39.
60. Laursen, B., Jensen, B. R., Nemeth, G., Sjogaard, G., (1998). A model predicting individual shoulder muscle forces based on relationship between electromyographic and 3D external forces in static position. *Journal of Biomechanics* 31, 731-739.
61. Nikooyan, A. A., Veeger, H. E. J., Westerhoff, P., Bolsterlee, B., Graichen, F., Bergmann, G., van der Helm, F. C. T., (2012). An EMG-driven musculoskeletal model of the shoulder. *Human Movement Science* 31, 429-447.
62. Bergmann, G., Graichen, F., Bender, A., Kaab, M., Rohlmann, A., Westerhoff, P., (2007). In vivo glenohumeral contact forces -

- Measurements in the first patient 7 months postoperatively. *Journal of Biomechanics* 40, 2139-2149.
63. Westerhoff, P., Graichen, F., Bender, A., Rohlmann, A., Bergmann, G., (2009b). An instrumented implant for in vivo measurement of contact forces and contact moments in the shoulder joint. *Medical Engineering & Physics* 31, 207-213.
64. Bolsterlee, B., Zadpoor, A. A., (2014). Transformation methods for estimation of subject-specific scapular muscle attachment sites. *Computer Methods in Biomechanics and Biomedical Engineering* (17), 13, 1492–1501.

Summary

To gain more insight in the development of joint wear and the gradual degradation of the shoulder and shoulder endo-prostheses over time, it is desirable to obtain an overview of the exposure to forces of these joints in the body, in daily conditions. A method to estimate such a mechanical load profile of the shoulder joint in daily conditions has not been established yet. Existing laboratory based methods for the estimation of shoulder joint reaction forces require upper extremity kinematics and external force as input. These existing methods cannot be applied directly to daily conditions, since one of the variables needed as input for these methods, external force by the hand, cannot be measured continuously outside the laboratory, or only with great difficulty.

Inertial Magnetic Measurement Systems (IMU's) have shown to enable the ambulatory measurement of upper extremity kinematics. IMU's use accelerometers, gyroscopes and magnetometers to estimate sensor orientation by a fusion algorithm which integrates angular velocity (gyroscopes), within the frame of reference composed by gravity (accelerometers) and magnetic north (magnetometers). Using such measurements as input for a long term detailed biomechanical analysis requires additional insight in two topics. First, the assumptions in, and threats to the minimization of integration drift in long term estimation of sensor orientation should be very clear. Second, an adequate sensor to segment calibration should be available, to obtain segment orientations which can be used to drive detailed musculoskeletal biomechanical models.

IMU's and associated orientation estimating algorithms make use of the earth magnetic field to minimize integration drift of gyroscope, under the assumption of a homogeneous field. Ferro magnetic materials cause a distortion of the earth

magnetic field, is a widespread building material (construction steel), and holds a potential threat for indoor measurements with IMU's. As shown in chapter 2, distortion of the earth magnetic field is depending on construction materials used in the building, and should be taken into account for calibration, alignment to a reference system, and further measurements. The behavior of the used orientation estimating algorithm is examined in the laboratory used for the measurements of this thesis, in terms of *temporal* and *spatial* sensitivity for the magnetic distortion. Mapping the measurement volume to define *safe* and *unsafe* areas in advance of planned experiments can aid in the collection of a usable data set. If such a pre-measurement-mapping is not possible before long term measurements take place, close inspection of the collected dataset in general, and especially the norm of the earth magnetic field can reveal distortion of the magnetic field. These measurement stages should be labeled as unsafe, and discarded from the collected data. If a too large portion of the collected dataset is labeled as unsafe, another measurement method should be considered.

Taking into account the potential threats to a stable orientation estimation, IMU's enable long term, accurate measurement of sensor orientation. With a proper calibration procedure these sensor orientations can be converted into segment motion in terms of joint angles. The standard procedure for the definition of segmental orientation in the laboratory is based on the measurement of positions of bony landmarks (BLM). However, IMU's do not deliver position information. An alternative method to establish IMU's based, anatomically understandable segment orientations is proposed in chapter 3. For five subjects, IMU's recordings were collected in a standard anatomical position for definition of static axes, and during a series of standardized motions for the estimation of kinematic axes of rotation. For all axes, the intra- and inter individual dispersion was estimated. Subsequently, local coordinate systems (LCS) were constructed on the basis of

the combination of IMU's axes with the lowest dispersion and compared with BLM based LCS. The repeatability of the method appeared to be high; for every segment at least two axes could be determined with a dispersion of at most 3.8°. Comparison of IMU's based with BLM based LCS yielded compatible results for the thorax, but less compatible results for the humerus, forearm and hand, where differences in orientation rose to 17.2°. Although different from the 'gold standard' BLM based LCS, IMU's based LCS can be constructed repeatable, enabling the estimation of segment orientations outside the laboratory. The procedure for the definition of local reference frames using IMU's is described.

Standard musculoskeletal models estimate joint load using upper extremity kinematics and external force. Although kinematics can be measured ambulatory for longer duration by means of IMU's, external force by the hands cannot be measured continuously in ambulatory settings, hampering the use of these standard biomechanical models. An alternative method has been sought for. When exerting force by the hands, the musculoskeletal response of upper extremity muscles is reflected in EMG, which can easily be measured ambulatory for longer duration. Besides that, Neural Networks (NN) have been shown to be capable of learning complex relationships in general, and more specifically, the fusion of distinct variables like kinematics and EMG into measures of joint loading for repetitive and closed chain movements. Chapter 4 describes a method for the estimation of joint reaction forces at the glenohumeral joint, in daily conditions, by training a Neural Network (NN) using kinematics and EMG as inputs. A relatively small data set of specified movements with known external force is used in two ways. First, a standard musculoskeletal model calculates several variables of joint load, and a set of Generalized Forces and Net Moments (GFNM) around the models degrees of freedom, using kinematics and known external force as input. Second, using kinematics and EMG, a NN is trained to

predict these GFNM from corresponding trials. These GFNM can concurrently be used as input for the model, resulting in full model output independent of external force. The method is validated with an independent trial not used in the training of the NN. The NN could predict GFNM within 10% relative RMS, compared to output of the model. The NN–model combination estimated joint reaction forces with relative RMS values of 7 to 17 % when compared to original musculoskeletal model output, enabling the estimation of a detailed load profile of the shoulder in daily conditions.

In chapter 5 a study is presented in which a neural network is trained for the direct prediction of glenohumeral joint reaction forces, based upon arm kinematics and shoulder muscle EMG. In this study several setups for NN training were examined in more detail, with varying combinations of type of input, type of motion, and handled range of weights. When joint reaction forces are predicted directly by a trained NN, for motion data independent of the training data, results show a high intraclass correlation (ICC between 0.83 and 0.98) and relative SEM ranging from 3% to 21% for the different setups, when compared to similar output of a musculoskeletal model. A convenient setup in which kinematics and only one channel of EMG were used as input for the NN's showed comparable predictive power as more complex setups. These results are promising and enable long term estimation of shoulder joint reaction forces outside the motion lab, based on ambulatory obtainable variables like upper extremity kinematics and EMG.

Is this the way to go? Within certain constraints it is possible to measure the musculoskeletal response with wearable equipment like IMU's and EMG for longer duration, and predict a complex variable like joint reaction force in daily conditions. With the developed method, the collection of a long-term joint load

profile comes closer at hand. By determining such a load-profile over time, over subjects, more insight can be gained in the nature, magnitude and variation of the forces acting on the joints of the shoulder girdle, and possibly shed more light on the damaging effects of these forces. Increased insight in the 'play of forces' around the shoulder can also aid in the development of future endo-prostheses; such prostheses can then be designed to better withstand the forces they will be exposed to in the body, in daily conditions.

Samenvatting

Om meer zicht te krijgen op de ontwikkeling van gewrichtsslijtage en de degeneratie van de schouder en schouder endoprothesen is het wenselijk om een overzicht te krijgen van het krachtenspel waaraan deze gewrichten dagelijks in het lichaam worden blootgesteld. Bestaande methoden voor de schatting van gewrichtreactiekracht in de schouder zijn gebaseerd op laboratorium onderzoek en apparatuur, en gebruiken kinematica van de romp en bovenste extremiteit, en uitgeoefende handkracht als input voor rekenmodellen. Deze bestaande methoden kunnen niet zonder meer worden toegepast op metingen in de dagelijkse praktijk omdat het tot nog toe onmogelijk is om de uitgeoefende handkracht onder dagelijkse omstandigheden continue te meten. Een methode om het beoogde mechanisch belastingprofiel van de schouder onder dagelijkse omstandigheden te schatten is nog niet ontwikkeld.

Inertiële Magnetische Meet Systemen (IMU's, inertiaele sensoren) hebben in de loop van de tijd hun waarde bewezen in het meten van 3D kinematica van de bovenste extremiteit. IMU's maken gebruik van 3 typen sensoren, accelerometers, gyroscopen en magnetometers om de sensor oriëntatie te schatten. Hierbij wordt een Kalmanfilter gebruikt om de hoeksnelheid (gemeten met gyroscopen) te integreren binnen een referentie systeem gebaseerd op de zwaartekracht (accelerometers) en het magnetisch noorden (magnetometers). Wanneer een dergelijk meetsysteem wordt gebruikt om input te genereren voor een gedetailleerde biomechanische analyse dienen er twee belangrijke onderwerpen goed uitgewerkt te zijn.

Ten eerste, bij de schatting van sensor oriëntatie uit langdurige metingen speelt de minimalisatie en compensatie van integratie drift een belangrijke rol. De aannames op basis waarvan deze minimalisatie en compensatie plaatsvinden, en

ook de bedreigingen voor een juiste sensor oriëntatie schatting moeten helder in kaart gebracht zijn. Ten tweede is er een goede en bruikbare calibratie methode nodig om de sensor oriëntatie te kunnen transformeren naar lichaamssegment oriëntatie, een van de benodigde typen input parameters voor de spierskeletmodellen waarmee gewrichtreactiekracht kan worden geschat.

IMU's en de bijbehorende Kalmanfilter waarmee de sensor oriëntatie geschat wordt maken gebruik van de magnetometer data om de integratiedrift van de gyroscoop data te minimaliseren, onder de aanname van een homogeen aardmagnetisch veld. Ferro-magnetische materialen veroorzaken een verstoring van dit aardmagnetisch veld, e.a. afhankelijk van de massa van en afstand tot het materiaal. Bekende ferro-magnetische materialen zoals ijzer en constructie staal worden wijdverbreid gebruikt als bouwmaterialen, en vormen daarmee een bedreiging voor de beoogde metingen met de IMU's binnenshuis. Hoofdstuk 2 beschrijft het versturende effect van constructie staal op het aardmagnetisch veld in het door ons gebruikte bewegingslaboratorium, en laat zien dat hier terdege rekening mee gehouden moet worden bij de calibratie van het IMU's systeem, de gebruikte referentie assenstelsels, en tijdens de verdere metingen. Het gedrag van het Kalmanfilter werd onderzocht in termen van spatiële en temporele gevoeligheid voor de magnetische verstoring. Het in kaart brengen van veilige (homogeen magneetveld) en onveilige (verstoord magneetveld) gebieden van het meetvolume vóór de uitvoering van de beoogde experimenten kan aanzienlijk bijdragen aan de collectie van een bruikbare dataset. Als een dergelijke verkenning niet mogelijk is, bijvoorbeeld bij lange termijn metingen onder dagelijkse omstandigheden, waarbij het meetvolume van te voren niet bekend is, dan dient de verkregen dataset nauwkeurig beoordeeld te worden op eventuele verstoringen van het magneet veld, bijvoorbeeld op basis van de norm van het gemeten magneetveld. De meetperiodes die als ernstig verstoord aangemerkt

worden kunnen beter niet gebruikt worden. Is een te groot deel van de verzamelde dataset als verstoord aangemerkt, dan moet er wellicht aan een andere meetmethode gedacht worden.

Mits de potentiële bedreigingen van een stabiele oriëntatie schatting in acht genomen worden, kunnen IMU's in principe langdurig en nauwkeurig de sensor oriëntatie meten. Met de juiste calibratie procedure kunnen deze sensor oriëntaties vertaald worden naar segment oriëntaties en gewrichtshoeken. De standaard methode voor de bepaling van segment assenstelsels en oriëntatie is gebaseerd op het meten van posities van Bony Land Marks (BLM). IMU's meten geen posities in 3D, alleen oriëntaties. In hoofdstuk 3 wordt een alternatieve methode beschreven om met behulp van IMU's anatomisch interpreteerbare segment oriëntaties te bepalen. Bij 5 gezonde proefpersonen werden metingen verricht met IMU's in een aantal standaard houdingen voor de bepaling van statische assen, en tijdens een aantal gestandaardiseerde bewegingen om functionele bewegingsassen te kunnen bepalen. Voor alle individueel te bepalen assen werden de intra- en inter individuele dispersie (variatie) berekend. Vervolgens werden per segment lokale assenstelsels bepaald op basis van de statische en functionele bewegingsassen met de laagste dispersie. Deze IMU's lokale segment assenstelsels werden vervolgens weer vergeleken met de standaard BLM assenstelsels. De IMU's methode bleek zeer herhaalbaar; voor elk segment konden minstens twee assen bepaald worden met een dispersie van maximaal 3.8°. Vergelijking van IMU's en BLM gebaseerde segment assenstelsels leverde vrijwel geen verschil op voor het thorax assenstelsel, maar wel oplopende verschillen voor humerus, onderarm en hand, waarbij deze laatste een oriëntatie verschil van 17.2° liet zien. Ondanks dit verschil met de "gouden standaard" methode op basis van BLM gebaseerde assenstelsels, kunnen IMU's gebaseerde assenstelsels zeer herhaalbaar bepaald worden, waarmee het meten van segment

oriëntaties buiten het laboratorium mogelijk wordt. De gehele procedure voor de definitie van IMU's gebaseerde lokale assenstelsels wordt beschreven in een appendix van het hoofdstuk.

Met standaard spierskeletmodellen wordt gewrichtsreactiekracht in de schouder geschat met behulp van kinematica van de bovenste extremiteit en uitgeoefende handkracht. Zoals hierboven beschreven kan de kinematica van de bovenste extremiteit met behulp van IMU's langdurig gemeten worden onder dagelijkse omstandigheden. De uitgeoefende handkracht kan echter niet continu gemeten worden in de dagelijkse praktijk, waardoor de standaard spierskeletmodellen niet zonder meer gebruikt kunnen worden. Er zal een alternatieve methode gezocht moeten worden om de activiteit van het spierskelet systeem te vertalen naar gewrichtsreactiekracht. Wanneer de handen kracht uitoefenen in het manipuleren van objecten, dan is de activiteit van het spierskelet systeem meetbaar in het EMG van de armspieren. Bovendien is EMG met de huidige generatie meetapparatuur goed langdurig en ambulant te meten. Daarnaast staan Neurale Netwerken al jaren in de belangstelling wat betreft het algemene vermogen om complexe relaties te leren, en meer in het bijzonder, de fusie van verschillende datatypen zoals kinematica en EMG in het voorspellen van gewrichtsbelasting bij repeterende en gesloten keten bewegingen. Hoofdstuk 4 beschrijft een methode om de gewrichtskrachten in het gleno-humerale gewricht te schatten, onder dagelijkse omstandigheden, door Neurale Netwerken te trainen met kinematica en EMG van de bovenste extremiteit als input. Hiervoor was slechts een relatief kleine initiële dataset van specifieke bewegingen en bekende krachten nodig. Voor deze initiële dataset kon de uitgeoefende handkracht namelijk berekend worden door de proefpersoon bewegingen uit te laten voeren met een bekend gewicht in de hand. Met behulp van de gemeten kinematica kon de handkracht eenvoudig uitgerekend worden ($F = m \times a$). De initiële dataset werd op twee manieren geanalyseerd. Ten

eerste werd op basis van gemeten kinematica en uitgeoefende handkracht met een spierskeletmodel verschillende variabelen van gewrichtsbelasting uitgerekend, en een set Generalized Forces and Net Moments (GFNM) rond de vrijheidsgraden van het model. Ten tweede werd op basis van gemeten kinematica en EMG een Neuraal Netwerk getraind om deze GFNM te voorspellen. De voorspelde GFNM van langdurige ambulante metingen werden vervolgens gebruikt als input voor het spierskeletmodel, zodat volledige model output berekend kon worden op basis van de ambulante gemeten variabelen kinematica en EMG. De methode werd gevalideerd met metingen die niet gebruikt werden voor de training van het Neuraal Netwerk. De Neurale Netwerken voorspelden de GFNM met een afwijking van 10% relatieve RMS, vergeleken met de GFNM die door het spierskeletmodel werden berekend. De combinatie van Neuraal Netwerk – spierskeletmodel voorspelden gewrichtsreactiekracht die 7 tot 17% relatieve RMS afweken van de originele model output. Met deze resultaten is de weg geopend naar het schatten van een mechanisch belastingprofiel van de schouder onder dagelijkse omstandigheden.

In hoofdstuk 5 wordt een methode beschreven waarin Neurale Netwerken getraind werden om direct reactiekrachten in het glenohumerale gewricht te voorspellen op basis van kinematica en EMG gemeten aan de thorax, schoudergordel en bovenste extremiteit. In deze studie werden verschillende configuraties voor het vergaren van de initiële dataset en het trainen van Neurale Netwerken in meer detail bestudeerd, met diverse combinaties van type input, type beweging, en range van gebruikte gewichten. De door de Neurale Netwerken voorspelde gewrichtsreactiekracht lieten een hoge Intra Class Correlation zien (ICC van 0.83 tot 0.98) met de gewrichtsreactiekracht die berekend was met het spierskeletmodel, voor een onafhankelijke dataset (niet gebruikt in de training van NN). De gebruikte foutmaat, relatieve Standaard Error of Measurement (relSEM)

varieerde van 3% tot 21% voor de verschillende configuraties. De configuratie met de laagste relSEM werd beschouwd als de meest succesvolle; het best haalbare resultaat van de methode. Een zeer praktisch toepasbare configuratie waarbij kinematica en slechts één kanaal EMG gebruikt werd als input voor de Neurale Netwerken liet een gelijke voorspellende kracht zien als meer complexe configuraties. Deze veelbelovende resultaten tonen aan dat het mogelijk is om gewrichtskrachten in de schouder vast te stellen buiten het bewegingslaboratorium, op basis van langdurige ambulant te meten variabelen als segment kinematica en EMG.

Is de ingeslagen weg de juiste? Binnen zekere randvoorwaarden is het mogelijk om de spierskelet respons langdurig te meten met draagbare meetapparatuur zoals IMU's en EMG, en een complexe variabele zoals de gewrichtsreactiekracht van het glenohumerale gewricht te voorspellen onder dagelijkse omstandigheden. Met de ontwikkelde methode komt het gewenste lange termijn mechanische belastingprofiel van de schouder binnen handbereik. Door het vaststellen van een dergelijk belastingprofiel over langere tijd, bij meerdere personen, kan er meer inzicht verkregen worden in de orde van grootte en variatie van deze krachten in de gewrichten van de schoudergordel, en hopelijk ook meer informatie opleveren over het beschadigende effect van deze krachten. Verhoogd inzicht in het krachtenspel rond de schouder kan ook bij dragen aan de ontwikkeling van toekomstige schouder endoprothesen; dergelijke prothesen kunnen dan ontworpen worden om het krachtenspel waaraan ze in het lichaam onder dagelijkse omstandigheden worden blootgesteld beter te weerstaan.

Curriculum Vitae

- 16-08-1968 Born in Apeldoorn, The Netherlands
- 1980 – 1986 VWO, Bisschoppelijk College St. Jozef, Sittard
- 1986 – 1987 Technische Natuurkunde, TUDelft
- 1987 – 1989 Fysiotherapy, Hogeschool van Amsterdam
- 1989 – 1998 Human Movement Science (parttime), Vrije Universiteit, Amsterdam. A master research internship focused on the validation of a data-glove during manual wheelchair propulsion, supervised by Prof. dr. H.E.J. Veeger and Prof. dr. L.H.V. van der Woude. A literature review on “The role of force feedback in the coordination of human movement” was supervised by Prof. dr. M. Bobbert
- 1998 – 2002 Participation in several research projects at Coronel Institute (AMC, Amsterdam, The Netherlands) and ERGOcare (VU, FBW, Amsterdam, The Netherlands), collaborating with Paul Kuijer (measuring physical and mechanical load of garbage collectors) en Erik Mol (measuring physical load of the police officers in active duty)
- 2002 - 2006 Project Exozorg, ambulatory estimation of joint load, Roessingh Research & Development, Enschede
- 2006 – 2010 PhD at TUDelft, Faculty of Biomechanical Engineering, in collaboration with Roessingh Research & Development, Enschede: Estimation of the mechanical loading of the shoulder joint in daily conditions.
- 2010 - 2015 Lab Coordinator at Roessingh Research & Development (2010 – 2014), Product & Innovation Manager at Hankamp Rehab (2014 – 2015), finishing dissertation in spare time.
- Further info: <https://nl.linkedin.com/in/whkdevries>

Publications by W.H.K. de Vries

Shoulder joint reaction forces can be estimated by Neural Networks. W.H.K. de Vries, H.E.J. Veeger, C. Baten, F.C.T. van der Helm. Submitted.

Neural Networks can predict input for a biomechanical model of the shoulder based on ambulatory obtainable variables. W.H.K. de Vries, H.E.J. Veeger, C. Baten, F.C.T. van der Helm. *Human Movement Science*, 31 (2012) 419-428/2012.

Effects of an implantable two channel peroneal nerve stimulator versus conventional walking device on spatiotemporal parameters and kinematics of hemiparetic gait. Anke I. R. Kottink, Martin J. B. Tenniglo, Wiebe H. K. de Vries, Hermie J. Hermens, Jaap H. Buurke. *Journal of Rehabilitation Medicine*, 2012; 44: 51-57

Functionally interpretable local coordinate systems for the upper extremity using inertial & magnetic measurement systems. W.H.K. de Vries, H.E.J. Veeger, A.G. Cutti, C. Baten, F.C.T. van der Helm. *Journal of Biomechanics* (2010), 43, 1983–1988.

Magnetic distortion in motion labs, implications for validating inertial magnetic sensors. W.H.K. de Vries, H.E.J. Veeger, C. Baten, F.C.T. van der Helm. *Gait & Posture* (2009), 29, 535-541

Effect of lifting height and load mass on low back loading. Hoozemans, Marco J. M., Kingma, Idsart, de Vries, Wiebe H.K. and van Dieën, Jaap H. *Ergonomics*, (2008) 51:7, 1053 - 1063

Upper extremity Load Spectrum in daily situations: System Accuracy and Soft Tissue Artefacts. W.H.K. de Vries, H.E.J. Veeger, C.B.T.M. Baten and F.C.T. van der Helm. *Journal of Biomechanics* (2007), 40, S2 S424

Spinal force estimation from Non-Normalized EMG. J.M.A. Visser, W.H.K. de Vries, C.T.M. Baten, J.H. van Dieën. *Journal of Biomechanics* (2006), 39, S1, S493

Effect of job rotation on work demands, workload, and recovery of refuse truck drivers and collectors. Kuijer PP, de Vries WH, van der Beek AJ, van Dieën JH, Visser B, Frings-Dresen MH. *Hum Factors*. 2004 Fall;46(3):437-48.

Mechanical loading of the low back and shoulders during pushing and pulling activities. Hoozemans MJ, Kuijer PP, Kingma I, van Dieen JH, de Vries WH, van der Woude LH, Veeger DJ, van der Beek AJ, Frings-Dresen MH. *Ergonomics*. 2004 Jan 15;47(1):1-18.

Effect of a redesigned two-wheeled container for refuse collecting on mechanical loading of low back and shoulders. Kuijer PP, Hoozemans MJ, Kingma I, Van Dieen JH, De Vries WH, Veeger DJ, Van der Beek AJ, Visser B, Frings-Dresen MH. *Ergonomics*. 2003 May 15;46(6):543-60.

Conferences

Gait analysis during a marathon: Objectifying the influence of fatigue. SMALLL 2013, Antwerpen, Poster Presentation.

Neural Networks can predict shoulder joint load. ISG 2010, Minneapolis, Oral presentation.

Functionally interpretable local coordinate systems using inertial & magnetic measurement systems. ISB 2009 CapeTown, Oral Presentation.

Estimation of functional interpretable local frames of reference using inertial sensors. BME 2009, Egmond, Oral Presentation.

Magnetic distortion in motion labs, implications for validating inertial magnetic sensors. 3DMA 2008, Santpoort, Oral Presentation.

Determining functional axes of rotation of upper extremity. ISG 2008 Bologna, Oral Presentation.

Ambulatory estimation of Upper Extremity Load. ISB 2007 Taipei, Oral Presentation.

Dankwoord

Het is zover! De definitieve versie van mijn proefschrift gaat naar de drukker. Ondanks de verwachte vliegende start werd het een uitgebreid proces met vele vertakkingen, tegenslagen, opstoppingen, parallel trajecten, maar ook diverse successen, voldoende publicaties (en citaties!) en uiteindelijk de voldoening van de afronding.

Een promotie traject doorloop je niet in je eentje, en er zijn vele mensen die op hun eigen manier een rol hebben gespeeld in dit proces. Ik wil jullie allemaal integraal bedanken voor jullie samenwerking, steun, vragen, discussie, kritiek, wandelgang gesprekken, lol en arbeidsvitaminen.

Een aantal hoofdpersonen rondom het traject wil ik graag wat gericht bedanken:

Beste Frans, jou doelgerichtheid, gedrevenheid, kritisch en relativerend vermogen, zonder ook maar één detail uit het oog te verliezen, hebben mijn visie op het opzetten en uitvoeren van wetenschappelijk onderzoek enorm verruimd. Ondanks je overvolle agenda altijd de rust zelve, en aandacht voor de persoon. Ontzettend bedankt voor je inzet.

Beste DirkJan, scherpzinnig, heerlijk direct in de communicatie en eventuele kritiek altijd in de opbouwende vorm. Tactisch, zakelijk en humor op het juiste moment. Op die punten dat ik door de bomen het bos niet meer zag, wist jij met een paar gerichte vragen het geheel tot overzichtelijke proporties terug te snoeien. Messcherpe inhoudelijke discussies voerden naar de kern van het probleem, en wanneer in de loop van de tijd mijn aandacht verslaptte, wist je me op de een of andere manier toch te inspireren om weer door te gaan, en het verhaal af te ronden. Je weet niet half hoeveel ik van je heb geleerd.

Anouk en Dineke, ook in tijden van tegenslag was er jullie luisterend oor, zodat ik een en ander weer in de juiste proporties kon zien. Dank.

Daarnaast wil ik de diverse collega PhD's en postdocs (Alfred, David, Erwin, Jasper, John, Otto, Sander) in Delft bedanken, ook al was ik maar één dag in de week in Delft, er was altijd genoeg aansluiting en ruimte voor inhoudelijke discussie en meer.

Het promotie traject vond plaats binnen een samenwerkingsverband van onder andere TUDelft en Roessingh Research & Development. Aan RRD zijde wil ik Bart Freriks bedanken voor zijn inspanningen om deze dubbele aanstelling

mogelijk te maken en daarnaast ook Hans Rietman voor de geboden ruimte om het traject af te ronden.

Beste Chris, als penvoerder van de projecten Freemotion en Fusion heb jij het framework opgezet waarbinnen dit promotie onderzoek plaats kon vinden. Je bent een echte initiator, creatief, altijd op zoek naar verbinding en verbetering, met de bijbehorende creatieve sprongen. Juist doordat we het lang niet altijd met elkaar eens waren over de te volgen route ben ik steeds zelfstandiger het overleg ingestapt en meer en meer mijn eigen afwegingen en keuzes gaan maken. Gezien de overlap in onze interesse en expertise op het gebied van de ambulante bewegingsanalyse komen wij elkaar ongetwijfeld weer tegen; ik kijk er naar uit!

Aan diezelfde RRD zijde van het project waren Ruben en Jan Hindrik mijn “sparring partners” van het eerste uur. Al hadden we elkaar door diverse job-hops wat uit het oog verloren, ik ben blij dat we elkaar weer weten te vinden.

In de 2e helft van het traject zat ik voornamelijk bij RRD te werken aan de analyses en artikelen. Mijn trouwe kamergenote Jacqueline, wat heb je me met je aardse benadering van zaken regelmatig weer met beide benen op de grond gekregen. Top.

En dan al die andere collega's bij RRD, ik zou jullie allemaal wel op willen noemen hier, maar die lijst wordt gewoon te lang. In de 12 jaar en de verschillende rollen bij RRD heb ik altijd met heel veel plezier met jullie samengewerkt, gediscussieerd en in een goede mix met de maandelijkse Laatste-Donderdag-van-de-Maand-Borrel, voortgebouwd aan de brug tussen onderzoek en klinische praktijk. Ik kijk terug op een hecht team, en een zeer prettige werkomgeving. We houden contact.

Wil, Jos en Leendert. Na afloop van mijn project aandeel in Fusion bleef er nog een stukje promotie werk over. Door in de rol van labbeheerder te mogen kruipen bleef ik verbonden met de wetenschappelijke omgeving van RRD en kon ik zodoende het proefschrift in eigen tijd afronden. Daarnaast voelde ik me bij jullie op de kamer al snel als een van de vier spinnen in het web van ICT & Labbeheer. Wat een diversiteit aan vaardigheden is er nodig om de ‘technische ruggengraat’ van wetenschappelijk onderzoek in stand te houden, aan te passen, te verbeteren of te vernieuwen, en ook weer inzichtelijk over te dragen aan de wetenschappelijke gebruiker. 'n Zeer dynamische en leerzame werkplek. Daarnaast was de werksfeer met jullie ongekend open, direct, stimulerend en intens. Dank!

XSense was als industriële partij betrokken in de project consortia en ik wil Daniel, Henk en ook Martin bedanken voor hun betrokkenheid, het delen van informatie en de nodige kritische vragen rondom mijn thema.

Beste Sabine, feitelijk stond mijn traject bij jou los van het promotie traject, maar heeft het indirect wel degelijk fors bijgedragen aan de uiteindelijke afronding. Nogmaals dank.

Beste Peke, de basis voor dit proefschrift is reeds lang geleden gelegd, door jou eigen nieuwsgierige aard als voorbeeld, maar ook in de opleidingsmogelijkheden waar jij als vader, en soms ook in de rol van projectmanager, de randvoorwaarden creëerde. Dank je wel voor deze levenslange steun en interesse.

En dan tot slot, mijn eigen kleine kring, Marianne, Pepijn, en Floris.

Mijn promotie traject was de afgelopen periode alom aanwezig, wat betreft afweging van tijdsbesteding (proefschrift versus bijwonen van honkbal wedstrijden of klussen), maar ook in de vorm van een stevige mentale achtergrondruis. Daarnaast hebben we als gezin diverse hobbels moeten overwinnen, en overwonnen. Ik ben nog steeds dagelijks blij met jullie steun, begrip, relativiseringsvermogen, veerkracht, humor en eigenzinnigheid, en ik ben supertrots op jullie alle drie.

Lieve Marianne, dank voor de diverse inhoudelijke bijdragen wat betreft statistiek, of juist die handige en logische alternatieve benadering die ik zelf niet zag. Daarnaast heb je een ongelooflijke portie geduld gehad, en me daarmee de ruimte gegeven om een en ander op mijn eigen eigenwijze wijze op te lossen. Met je nuchtere kijk op de wereld heb je me regelmatig uit een “closed loop” weten te halen, en daar waar nodig, je vertrouwen op een goede afloop op mij over kunnen brengen. Hiermee ben je een enorme ‘mentale steunpilaar’ geweest in het gehele proces. Super! Ik heb je lief.

Wiebe

